

Prevention of Micromotion-Related Periprosthetic Bone Loss using Local Release of Bisphosphonate: Theoretical Developments and Experimental Validations

THÈSE N°4157 (2008)

PRÉSENTÉE LE 30 JUILLET 2008

À LA FACULTE SCIENCES DE BASE

LABORATOIRE DE BIOMÉCANIQUE EN ORTHOPÉDIE EPFL-HOSR

PROGRAMME DOCTORAL EN BIOTECHNOLOGIE ET GÉNIE BIOLOGIQUE

ÉCOLE POLYTECHNIQUE FÉDÉRALE DE LAUSANNE

POUR L'OBTENTION DU GRADE DE DOCTEUR ÈS SCIENCES

PAR

Vincent STADELMANN

ingénieur physicien diplômé EPF
de nationalité suisse et originaire de Escholzmatt (LU)

acceptée sur proposition du jury:

Prof. N. Stergiopulos, président du jury

Prof. D. Pioletti, directeur de thèse

Dr J. Gasser, rapporteur

Prof. B. Jolles-Haeberli, rapporteur

Prof. N. Verdonchot, rapporteur



ÉCOLE POLYTECHNIQUE
FÉDÉRALE DE LAUSANNE

Suisse
2008

Summary

Total joint replacements are highly successful in relieving pain and restoring movement of damaged joints. However, the lifespan of the implants is limited. The implant's long-term stability depends largely on the preservation of periprosthetic bone. Debris-wear particulates were first identified as the factor inducing periprosthetic bone loss. However, it was shown later that the resorption process starts before the particulates reach the periprosthetic bone. Thus a mechanical factor, interface micromotions, has been suspected to be the initiator of early bone loss.

In the first part of this thesis, we investigated the response of bone cells to micromotions. Using an *ex vivo* setup, we applied micromotions on fresh human bone cores and showed that micromotions could indirectly activate osteoclasts after only 1 hour. Thus micromotion-related osteoclastic activity could be the initiator of periprosthetic bone loss. Local release of bisphosphonate seemed therefore to be an ideal solution to prevent early bone loss, as the target is a local process.

The few previous studies assessing local release of bisphosphonate *in vivo* reported increased periprosthetic bone stock and/or strengthen implant fixation. But these studies only concerned rats and were designed empirically. In the second part of the thesis, to overcome the limitation resulting from the sole usage of rats, we performed a study of local zoledronate release in sheep trabecular bone. We measured that, at 4 weeks post-operatively, periprosthetic bone was 50% denser with zoledronate than without.

To further analyze these experimental results, a theoretical model of bone adaptation with bisphosphonate was developed. This new model updated an existing mechanically-driven bone adaptation model by adding an equation of drug-driven bone adaptation. The identification of the model parameters was carried-out with the existing experimental data.

Based on the new model, the dose of zoledronate that would maximize the periprosthetic bone density was calculated; this dose was then tested *in vivo* and the results validated the model's prediction with a good accuracy.

The fundamental assumption in the theoretical model was that the mechanical stimulus and the drug stimulus were independent. The last aim of the thesis was then to verify this assumption. We investigated potential interactions between mechanical effects and bisphosphonate on bone adaptation in a model of adaptation of the mouse tibia to axial compression, combined with systemic injections of zoledronate. We observed that the effects of each stimulus were independent in general, however in very high strain conditions, zoledronate seemed to reduce the bone response to mechanical stimulation.

On a clinical perspective, the major results of the thesis were, first, that local micromotions can initiate periprosthetic bone resorption rapidly and thus favor aseptic loosening on long-term. This new data provides a strong rationale for the local use of bisphosphonate rather than systemic. The second major result was the demonstration that local release of zoledronate increases periprosthetic bone stock in sheep. Finally, the new theoretical model is a convenient tool to plan clinical studies and compare experimental results.

Keywords:

Micromotions; periprosthetic bone loss; bisphosphonate; local delivery; orthopedic implants; *in vivo* mechanical loading; bone adaptation; theoretical model.

Résumé

Les arthroplasties totales réussissent avec succès à soulager la douleur et à rendre leur mobilité aux articulations endommagées, mais la durée de vie des implants est limitée. La stabilité à long terme des implants dépend surtout de la préservation de l'os périprosthétique. Les particules d'usure des composants prothétiques ont été les premiers facteurs identifiés comme induisant une perte osseuse. Cependant, la résorption peut survenir avant que des débris n'apparaissent dans la zone périprosthétique. On suppose donc que la résorption puisse être initiée par un facteur mécanique : les micromouvements à l'interface os-implant. Dans la première partie de cette thèse, nous avons étudié la réponse des cellules osseuses aux micromouvements. Dans un système *ex-vivo*, nous avons appliqué des micromouvements sur des échantillons d'os humains fraîchement disséqués et nous avons observé que les micromouvements peuvent indirectement activer les ostéoclastes en seulement 1 heure. L'activité des ostéoclastes liée micromouvements pourrait donc être à l'origine de la perte osseuse périprosthétique. La libération locale de bisphosphonate semble alors être une solution idéale pour prévenir l'ostéolyse périprosthétique, qui est un processus local. Les études précédentes évaluant l'usage local de bisphosphonate ont rapporté une densité osseuse accrue et/ou un renforcement de la fixation des implants dans l'os. Mais ces études ne concernaient que des rats et avaient été conçues de manière plutôt empirique. Dans la deuxième partie de la thèse, pour surmonter la limitation résultante du seul usage des rats, nous avons réalisé une étude de libération locale de zoledronate chez le mouton. Nous avons mesuré que, après 4 semaines, l'os trabéculaire périprosthétique était 50% plus dense avec zoledronate que sans.

Pour mieux interpréter les données expérimentales, un modèle théorique de l'adaptation osseuse en présence de bisphosphonate a été développé en se basant sur un modèle mécanique

d'adaptation auquel on a ajouté une équation de l'effet du bisphosphonate. Les paramètres numériques ont été identifiés à partir des données expérimentales. La dose de zoledronate qui maximiserait la densité osseuse périprothétique a été calculée et une expérience *in vivo* a validé le résultat du modèle avec une bonne précision.

L'hypothèse fondamentale du modèle était que le stimulus mécanique et le stimulus du bisphosphonate étaient indépendants. Le dernier but de la thèse consistait à vérifier cette hypothèse. Pour cela, nous avons étudié les interactions entre les effets mécaniques et l'effet du bisphosphonate sur l'adaptation osseuse dans un modèle *in vivo* de compression axiale du tibia de souris, combiné avec des injections systémiques de zoledronate. Nous avons observé qu'en général les effets étaient indépendants, mais qu'en conditions de contraintes élevées, le zoledronate semble diminuer la réponse osseuse aux stimulations mécaniques.

D'un point de vue clinique, les principaux résultats de la thèse sont, premièrement, que les micromouvements locaux induisent rapidement une résorption osseuse et favorisent ainsi le descellement aseptique, ce qui justifie l'usage local de bisphosphonate plutôt que systémique. Deuxièmement, la libération locale de zoledronate induit une augmentation de la densité osseuse chez le mouton. Finalement, le nouveau modèle théorique est un outil pratique pour planifier des études cliniques et comparer les résultats expérimentaux.

Mots-clés:

Micromouvements; Perte osseuse périprothétique; bisphosphonate; libération locale; implants orthopédiques; stimulation mécanique *in vivo*; adaptation osseuse

Acknowledgements

First of all, I would like to thank Prof Dominique Pioletti for trusting me with the lead of this project. I also thank my labmates at the Laboratory of Biomechanical Orthopedics: your support motivated me to achieve this thesis on time!

I thank also all the people with whom I collaborated: Marc Jeanneret for his technical expertise during the design of experimental devices; Pierre Latin for his demonstrations with animal handling; Olivier Gauthier for the animal surgery. None of the experimental work could have been performed without the precious help of these collaborators.

During a four years thesis, everyone encounters difficult moments. I had the chance to have kind friends who supported me: Ana, Claire, Elise, Eduardo, Tyler, Philippe, Pierre-Jean, Hicham, Tom, Francesco... their presence in the lab helped me a lot. A particular thanks goes to Tyler who spent a hell of a time editing my English.

I would like to thank my family for their support during these long years of student status. They allowed me to follow my own way and helped me along this path.

Finally, I want to express my immeasurable gratitude to Salima for her love, her understanding and her patience. Salima gave me the strength I needed to achieve my goals.

Table of content

SUMMARY	2
RÉSUMÉ	4
ACKNOWLEDGEMENTS	6
INTRODUCTION	9
1 EPIDEMIOLOGY OF ORTHOPEDIC IMPLANTS	9
1.1 <i>The success story of total joint replacement</i>	9
1.2 <i>Complications after total joints replacements</i>	11
1.3 <i>Preview of paper 1: Microstimulation at the bone-implant interface upregulates osteoclast activation pathways</i>	19
1.4 <i>Osteoclasts, a target to reduce periprosthetic bone loss?</i>	19
2 BONE MECHANOBIOLOGY	20
2.1 <i>The skeleton</i>	20
2.2 <i>Cortical and trabecular bone</i>	21
2.3 <i>Composition of bone</i>	22
2.4 <i>Bone renewal and adaptation</i>	24
3 PREVENTION OF PERIPROSTHETIC BONE LOSS WITH LOCAL DELIVERY OF BISPHOSPHONATE	32
3.1 <i>Bisphosphonates</i>	32
3.2 <i>Effects of bisphosphonates on periprosthetic bone</i>	34
3.3 <i>Preview of paper 2: Development and validation of a theoretical framework to predict the bone density around orthopedic implants delivering bisphosphonate locally</i>	38
3.4 <i>Preview of paper 3: Implants delivering bisphosphonate locally increase periprosthetic bone density in an osteoporotic sheep model</i>	39
3.5 <i>Interactions between bisphosphonate and mechanical stimulations on bone adaptation</i>	40
3.6 <i>Preview of paper 4: 3D strain map of axially loaded mouse tibia: a numerical analysis validated by experimental measurements</i>	41

3.7	<i>Preview of paper 5: Combined effects of zoledronate and mechanical stimulation on bone remodeling in an axially loaded mouse tibia</i>	42
PAPERS		43
4	PAPER 1: MICROSTIMULATION AT THE BONE-IMPLANT INTERFACE UPREGULATES OSTEOCLAST ACTIVATION PATHWAYS	44
5	PAPER 2: DEVELOPMENT AND VALIDATION OF A THEORETICAL FRAMEWORK TO PREDICT THE BONE DENSITY AROUND ORTHOPEDIC IMPLANTS DELIVERING BISPHOSPHONATE LOCALLY	64
6	PAPER 3: IMPLANTS DELIVERING BISPHOSPHONATE LOCALLY INCREASE PERIPROSTHETIC BONE DENSITY IN AN OSTEOPOROTIC SHEEP MODEL. PILOT STUDY	85
7	PAPER 4: 3D STRAIN MAP OF AXIALLY LOADED MOUSE TIBIA: A NUMERICAL ANALYSIS VALIDATED BY EXPERIMENTAL MEASUREMENTS	106
8	PAPER 5: COMBINED EFFECTS OF ZOLEDRONATE AND MECHANICAL STIMULATION ON BONE ADAPTATION IN AN AXIALLY LOADED MOUSE TIBIA: A PRELIMINARY STUDY	123
	CONCLUSION AND PERSPECTIVES	141
	REFERENCES	145
	CURRICULUM VITAE	158

Introduction

1 Epidemiology of orthopedic implants

1.1 The success story of total joint replacement

Total joint replacement is an effective treatment for relieving pain and restoring function for patients with damaged joints. According to the American Academy of Orthopedic Surgeons (AAOS)¹:

“Total joint replacement is a success story, enabling hundreds of thousands of people to live fuller, more active lives. Using metal alloys, high-grade plastics, and polymeric materials, orthopedic surgeons can replace a painful, dysfunctional joint with a highly functional, long-lasting prosthesis.”

Orthopedic prostheses have been designed to replace damaged joints, such as hips, knees, shoulders (Figure 1), elbows, ankles, wrists, etc. Over the past half-century, there have been many advances in the design, construction, and surgical implantation of total joint replacement, resulting in a high percentage of successful outcomes. For the majority of patients, initial results following surgery are excellent. Therefore, joints replacements are considered nowadays amongst the most successful surgical procedures.

¹ www.aaos.org

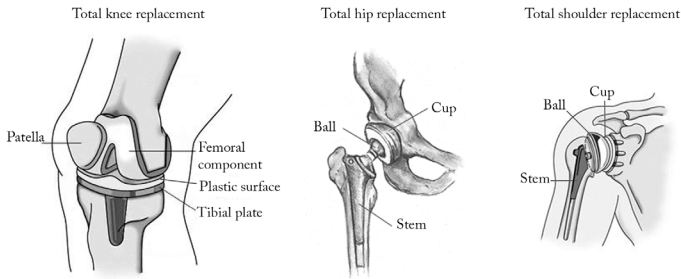


Figure 1 - Schemes of knee, hip and shoulder total replacements (source AAOS).

In the AAOS statistics, total knee replacements and total hips replacements were respectively ranked 1st and 3rd in the top five primary procedures for musculoskeletal-related hospitalizations. The costs of hospitalization related to joints replacements account for billions of dollars each year in the USA only. In 2005, 534'000 total knees, 235'000 total hips, 234'000 partial hips and 15'000 total shoulders replacements have been performed in the USA. These numbers keep increasing each year, as the population continues to age and as the indications for joints replacements extend to younger patients (Figure 2) [1].

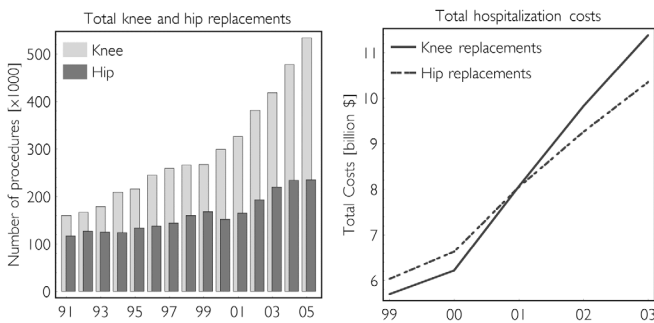


Figure 2 - Number of joints replacements in USA between 1991 and 2005 and associated costs between 1999 and 2003. (Adapted from AAOS)

1.2 Complications after total joints replacements

Implants have limited life span. Numerous revisions are performed.

Despite the very high rate of successful surgery, joint replacements cannot be expected to last for the patient's lifetime. In reality, they last 10 to 15 years on average. At ten years post-operatively 15% to 20% of replaced hips have already been revised [1].

The past years have seen the growing number of joint replacements be followed by a growing number of revisions and increasing associated hospitalization costs. In 2005, 35'000 hip replacements revisions and 37'000 knee replacements revisions were performed in the USA. The total hospitalization costs for these revisions exceeded 3 billions of dollars (Figure 3). As younger people are likely to place more demands on their artificial joints as they generally live more active lives, the younger a person is at the time of surgery, the more likely is that surgery will have to be repeated later in life. The indication of total joint replacement extends more and more to young patients and, as a result, the number of revisions will certainly keep growing in the future.

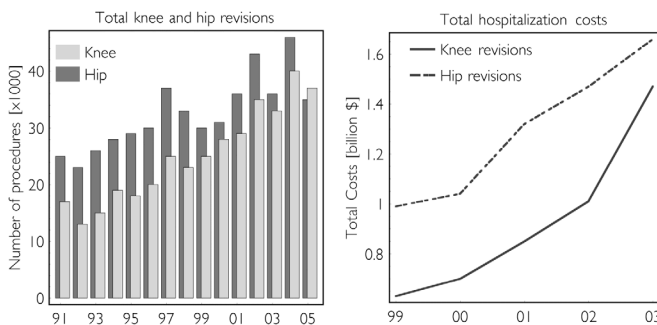


Figure 3 - Number of joints implants revisions between 1991 and 2005 and associated costs between 1999 and 2003. (Adapted from AAOS)

Revisions are dangerous

Revision surgery is difficult to perform and expensive. Clinical outcomes after joint replacements revision surgery are less predictable and generally inferior to the outcome after primary joint replacements [1]. With each revision surgery, the lifespan of an implant decreases. This is one reason why physicians often delay joint replacement surgery as long as possible.

For example, revision of the conventional hip prostheses involves technical difficulties and complications such as femoral fractures and postoperative dislocations: Witjes *et al.* have reported that hip revision procedures are associated with a high rate of complications within 2 years of implantation [2]. In their study, Chen *et al.* have reported 51% of poor satisfaction in a patient survey and that 12% of the hip prosthesis needed revision within 7 years post-operatively [3].

Reasons for revisions

There are several major complications of total joint arthroplasties. The most important complications are loosening, infections and dislocations. These three reasons account for almost 90% of the diagnoses (Figure 4) [1].

Surgical or long-term infections are the most feared of all the complications in total joint arthroplasties. Fortunately, the incidence of infection is quite low. The rate of infection is less than 0.4 % of joint replacement surgeries. The causes for infection are generally contamination during the surgical procedure. These infections can be prevented mostly by good surgical practice [1, 2].

Dislocation is the shifting of the replaced joint out of the replaced socket. Dislocations occur in 2 to 5% of patients undergoing total hip replacement. It is generally a consequence of high stresses on the joints generated by undesired postures or excessive physical activities [1, 2].

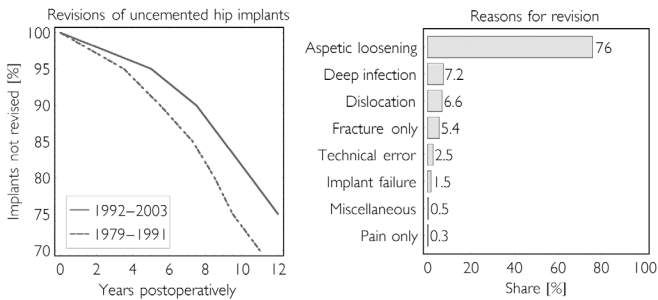


Figure 4 - Uncemented hip implants survival and reasons for hip arthroplasty revisions.

(Adapted from the Swedish Total Hip Replacement Register²)

1.2.1 Loosening

Loosening is the major problem facing the long-term success of total joint replacements.

The components of a joint arthroplasty may become loose over time. The patient denotes increased pain in his replaced joint. On the x-rays, areas of loosening are identified by radiolucent zones revealing the replacement of bone mineralized tissue by a soft fibrous tissue that does not provide the necessary mechanical support. Once a component becomes loose, it generally does not regain fixation in the future. For this reason, patients are followed on a regular basis with repeated radiographies to identify loosening risks.

Theories of implant loosening and debate about debris particles and micromotions

The exact processes that provoke the replacement of periprosthetic bone by a layer of soft fibrous tissue are still under debate. Two hypotheses are generally used to explain the etiology of periprosthetic bone resorption. The most supported theory focuses on a biological reaction

² jru.orthop.gu.se/

to sub-micron size wear particles. Numerous studies have shown that the debris after implant wear induces inflammatory reactions in the tissues surrounding the implant [4-6]. The second hypothesis suggests that mechanical factors also contribute to osteolysis. In particular, micromotions at the bone-implant interface are suspected to play a key role in tissue differentiation [7].

1.2.1.1 Role of wear debris particles in aseptic loosening

Wear at the articulating bearing surfaces can be defined as the removal of particles that occurs as a result of the relative motion between two opposing surfaces under load [8]. Total joint arthroplasty components are made of artificial materials. Over time, as these parts move back and forth relative to each other, this will result in wear of the components. Using radiostereometry, a very accurate measuring technique, Önsten *et al.* found a mean annual wear rate of hip components of 0.09 mm/year during a follow-up of 5 years [9].

Once removed from the implant material, the wear debris remains within the tissue and fluid surrounding the total joint arthroplasty. In tissue retrieved from hip revisions of 15 patients, Korovessis and Repanti found granules or larger cement particles, polyethylene fibers and metal deposits [6].

Previous studies have shown that these large amounts of wear particles of polyethylene, cement, metal, or ceramics set into motion a cascade of cellular events in the periprosthetic bone [4]. The particles activate macrophages, which in turn trigger osteoclasts activity via pro-inflammatory factors [10]. The resulting imbalance in local bone metabolism leads to a progressive and massive bone loss.

1.2.1.2 Role of mechanical factors in aseptic loosening

Stress shielding

Stress shielding has been reported for many implants designs. This is the consequence of the reduction of mechanical loading in the bone by the presence of an implant resulting in bone loss. Stress-shielding can be interpreted as the normal adaptation of bone to disuse [11].

Micromotions

The presence of an interface between two materials of different mechanical properties in a mechanically loaded structure induces a slip at the interface. In a joint arthroplasty, the slip between the metallic component and the bone is generally referred to as micromotions because of its magnitude: in hip replacements for example, relative displacements up to about 200µm were measured at the bone implant interface during normal gait cycles [12, 13].

Micromotion of the implant components relative to the adjacent bone in patients undergoing total joint arthroplasty are thought to contribute to aseptic loosening. In a dog model, Jasty *et al.* found that micromotions lower than 40µm favor bone formation, while micromotions of higher magnitude lead to the creation of a fibrous tissue [14]. In a post-mortem study, Engh *et al.* found that cementless implants which showed signs of bony ingrowth had maximum relative micromotion of 40 µm, and implants which had failed bony ingrowth had relative micromotion of 150 µm [15]. Therefore it is believed that micromotions may facilitate osteolysis by enlarging the so-called effective joint space [16] and hence allow access of debris particles to wider areas of the bone-prosthetic interfaces.

1.2.2 Early resorption, an initiator of aseptic loosening?

The origins of aseptic loosening are still unclear. However, although aseptic loosening is generally a long-term outcome, some studies suggest that it is initiated in the early post-operative period.

Early migration predicts loosening

Rapid early migrations have been detected by roentgen stereophotogrammetry in many asymptotic hips, often as early as 4 months postoperatively [17, 18]. Similarly, in knee replacements, Petersen *et al.* measured migrations of the component of 0.7 mm already after 6 weeks (Figure 5) [19]. These early migrations of the components have been found to predict an increased risk of clinical loosening [17, 20].

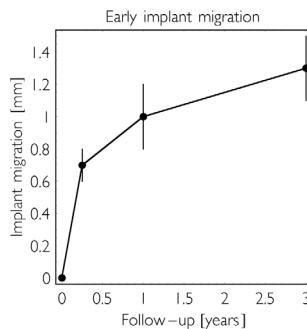
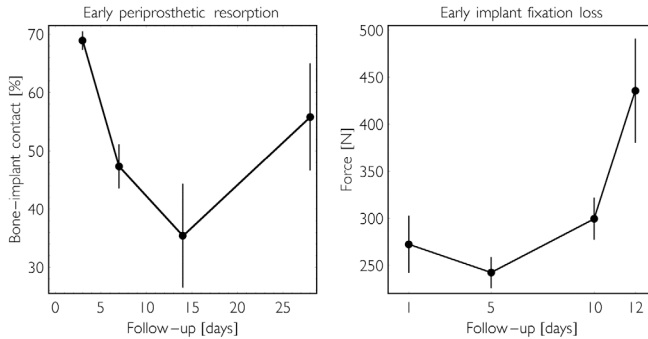


Figure 5 - Clinical follow-up of total knee replacement migration. Most of the migration occurs within months post-operatively (adapted from [19])

Early migration is related to early periprosthetic bone loss

Using a rabbit model, Dhert *et al.* demonstrated that immediately after implantation, a sequence of hematoma formation, bone resorption, and bone formation is initiated. As a result of this sequence bone-implant contact is temporary reduced (Figure 6) [21]. Moreover, in an

in vivo study of screw fixation in a rabbit model performed in collaboration with Stryker, we observed a small decrease of 10% of the screw pullout force at 5 days post-operatively; the decrease was compensated after 10 days and then the pullout force increased significantly at 12 days (Figure 6) [22]. The reported decrease in bone-implant contact and pullout-force certainly reflects an early osteoclastic activity.



*Figure 6 - Early bone-implant contact loss and fixation loss in rabbit studies
(adapted from [21] and [22]).*

Furthermore, a clinical study showed that up to 14% periprosthetic bone is lost during the first three months after total hip arthroplasties [23]. And it was found that the early migration amplitude was correlated to the gravity of periprosthetic bone loss [19].

Finally, it is interesting to note that Korovessis and Repanti, in their retrieved tissues study of non-loosened cases, had the opportunity to study the progressive development of the fibrous membrane and the first appearance of the cement debris. The first signs of the fibrous membrane appeared 2.5 months postoperatively, whereas the first cement debris were observed only seven months after the implantation of the prosthesis [6].

To sum up, these results indicate that the fate of an orthopedic implant is mainly determined at an early stage, probably before any wear particles are produced and can reach the periprosthetic bone. Therefore this suggests that early bone loss is related to other factors, for example mechanical factors. Micromotions at the bone-implant interface are then ideal candidates to explain the initiation of periprosthetic resorption. But the exact chronology of the early stage events that finally lead to critical bone loss is unknown. In my first paper, the role of micromotions is further investigated.

1.3 Preview of paper 1: Microstimulation at the bone-implant interface upregulates osteoclast activation pathways.

So far no data existed that quantified the effect of micromotions directly on human bone. We hypothesized that micromotions at the bone implant interface may activate bone resorption around the implant through bone cell signaling. We tested this hypothesis with an *ex vivo* loading system developed to stimulate human bone cores with micromotions. We observed significant up-regulation of the activation pathways of the bone resorbing cells. This suggested that the micromotions at the bone-implant interface have the potential to induce bone resorption after only one hour. (Full paper on page 44)

1.4 Osteoclasts, a target to reduce periprosthetic bone loss?

Based on the early resorption data and the results of the first paper [24], it seems clear that the efforts to treat aseptic loosening should be concentrated at the prevention of early periprosthetic bone loss. As this process seems to be initiated by micromotions which activate the osteoclasts almost immediately, it was proposed recently that blocking the osteoclastic resorption with bisphosphonate treatments might prevent the periprosthetic bone loss at short term, and thus limit the risk of aseptic loosening [25].

This solution is discussed in chapter 3. Some elements of bone mechanobiology are introduced in chapter 2. These elements are necessary for the understanding of chapters 3.

2 Bone mechanobiology

Bones purposes are the mechanical support of the body mass (load bearing support, momentum transfer), the protection of vital organs, the housing of hematopoietic bone marrow and the stock of calcium and phosphate for the calcium homeostasis. To ensure these functions bones are modeled and renewed continually through the processes called *bone modeling* and *bone remodeling*. These processes ensure that bones shape and microstructure are adapted to the actual mechanical demand. Remodeling is also essential for maintenance of the calcium balance. Bone modeling and remodeling rely on the actions of the different bone cells that constantly ‘sense’ the mechanical demand, and adapt to this demand by resorbing old bone or synthesizing new bone.

2.1 The skeleton

The skeleton is the hard framework of the body. It is made of 206 bones of different shapes (long load-bearing bones, flat bone, mandible, vertebrae, etc.). Some bones have highly specialized functions, for example bones of the ear transmit sounds. Most long bones contain a dense outer shell made of cortical bone while the inside is made of trabecular bone, a fine network of connected bone trabeculae. The junction between the two types of bone is continuous. The relative proportion of cortical and trabecular bone varies in function of the anatomical location (Figure 7). The ends of the bones that form joints are covered with cartilage [26, 27].

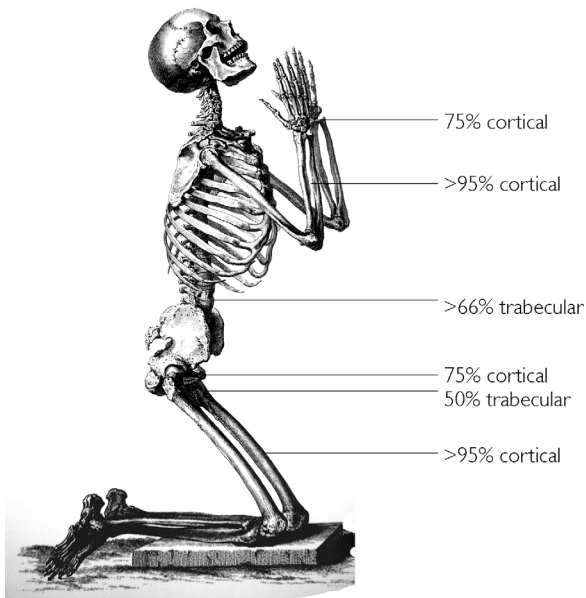


Figure 7 - The skeleton is made of 206 bones of different shapes and sizes with various relative proportions of cortical and trabecular bone (source: cabinetmag³).

2.2 Cortical and trabecular bone

Cortical bone represents nearly 80% of the skeletal mass. It has a slow turnover rate and a high resistance to bending and torsion. It provides strength to resist bending at the middle of long bones. At microscopic level the cortical bone matrix is organized in lamellae of 3 to 7 μm thickness, composed of collagenous fibers. The orientation of the fibers alternate, which gives compact bone its strength.

³ Cabinet Magazine, a quarterly of art and culture, issue 28, www.cabinetmagazine.org/

Trabecular bone, also known as cancellous or spongy bone, represents only 20% of the skeletal mass but 80% of the bone surface. Trabecular bone is less dense, more elastic and has a higher bone turnover rate than cortical bone. Trabecular bone forms the interior scaffolding, which helps bone resist to compressive forces. Trabecular bone consists of a network of interconnected bone trabeculae with spaces filled with bone marrow. The trabeculae are of two types, rods and plates. Their size is less than about 0.2 mm (Figure 8) [26].

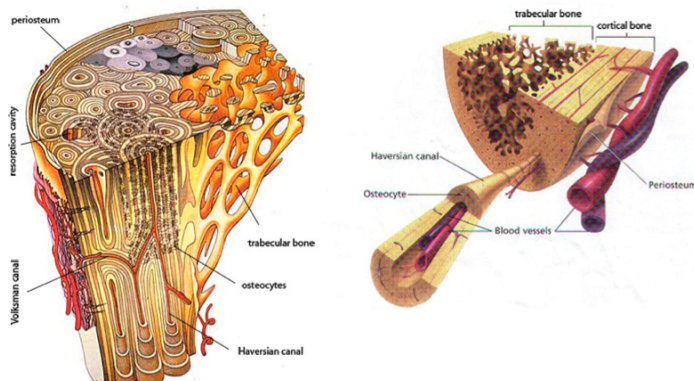


Figure 8 - Details of the microstructure of cortical bone and the junction with trabecular bone. (source: www.mednote.co.kr)

2.3 Composition of bone

The composition of bone varies with age, anatomical location and metabolism. Bone mineral accounts for 50% to 70% of adult bone, the organic matrix for about 20% to 40%, water for 5% to 10 % and lipids for 1% to 5 %. About 90% of bone organic matrix is composed of type I collagen. Bone mineral is mostly composed of hydroxyapatite (HA), which provides rigidity and strength for mechanical functions of the skeleton (Figure 9) [28, 29].

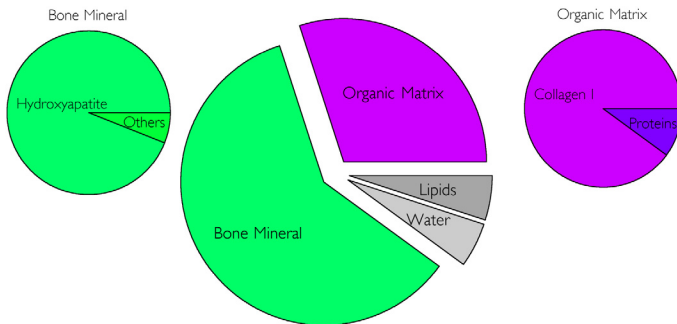


Figure 9: The two main components of bone are hydroxyapatite and type I collagen.

It is worth noting that its composition makes bone opaque, and thus optical microscopy techniques cannot be used to study bone structure or metabolism in situ. However, the high mineralization of the bone matrix allows the use of backscattered scanning electron microscopy (SEM) and x-ray microcomputed tomography (μ CT) to image bone microstructure and density [30-34]. These are the core experimental observation techniques in papers 2 to 5.

2.3.1 Bone quality

The health of a bone is generally defined by its strength and stiffness. But these measures are not directly related to the risk of fracture. Bone mass density (BMD) is highly correlated with strength and stiffness but there is a less clear relation between BMD and the risk of fracture, because structural and geometric adaptation can compensate a decreased BMD. Another important parameter to define bone quality is its degree of fatigue. Cyclic loading, even at low strains, causes fatigue: a gradual reduction of strength and stiffness over time. In bone, the reduction in mechanical properties is attributed to the formation of microcracks [26, 35].

2.4 Bone renewal and adaptation

In adults, ten per cent of the bone mass is replaced every year. This constant renewal, called *bone remodeling*, prevents the accumulation of microcracks and therefore allows bone to carry out its functions. Remodeling repairs bone defects that result from mechanical stresses, and maintains the optimal levels of calcium in the blood. Remodeling requires cells that resorb old bone, the *osteoclasts*, and cells that form new bone, the *osteoblasts*.

The ability of bone to adapt to mechanical loads also relies on bone resorption and bone formation by bone cells. In the adaptation process, called *bone modeling*, resorption and formation occur at different locations and the bone morphology is changed. To adapt to mechanical demands, bone modeling requires cells that sense the mechanical stimuli, the *osteocytes*.

2.4.1 Bone cells

Four major types of cells participate actively in bone remodeling and modeling: osteoclasts, osteoblasts, osteocytes and bone lining cells.

2.4.1.1 Osteoclasts

Osteoclasts are the bone resorbing cells. These giants multinucleated cells containing 4 to 20 nuclei, measure 20 to 100 μm diameter. They originate from hematopoietic stem cells into osteoclasts progenitors, then to pre-osteoclasts which fusion into mature osteoclasts. The maturation of osteoclasts is activated by osteoblasts' cytokines [36, 37]. Mature osteoclasts attach to the bone tissue matrix and form a ruffled border at the bone/osteoclast interface that is completely surrounded by a “sealing” zone. This creates an isolated microenvironment in which the osteoclast secretes acids to dissolve the organic and inorganic matrices of the bone (Vaananen et al, 2000).

2.4.1.2 Osteoblasts

Osteoblasts are the bone forming cells: they mineralize the bone matrix. These spherical, mononucleated cells, of 10 to 20 μm of diameter, originate from mesenchymal stem cells and differentiate into mature osteoblasts under the influence of local growth factors. Osteoblasts are highly enriched in alkaline phosphatase and secrete type I collagen and specialized bone matrix proteins as unmineralized osteoid at their bone-forming front. In a second time, the matrix is mineralized externally. During the process of bone matrix formation, some osteoblasts become embedded in their own matrix production and differentiate into osteocytes. The remaining osteoblasts synthesize bone until they eventually transform to lining cells that cover the newly formed bone surface [38, 39].

2.4.1.3 Osteocytes

Osteocytes are the bone mechanosensory cells. There are numerous evidences that osteocytes are the mechanical sensors that signal to osteoblasts and osteoclasts where bone needs to be formed or resorbed [40, 41]. Osteocytes communicate with each other via cell processes extending through network of canaliculi [42-44].

2.4.1.4 Lining cells

Lining cells are thin elongated cells that cover the quiescent bone surfaces. Lining cells are highly interconnected with the osteocytes in the bone matrix via the canaliculi network (Lian & Stein, 2001). The bone lining cells are thought to be inactive osteoblasts, which can be activated to produce bone matrix for bone, modeling. Lining cells can retract prior to osteoclastic bone resorption [45, 46].

2.4.2 Bone remodeling and bone modeling

Bone modeling and remodeling are not very different at the cell level, as they fundamentally rely on bone resorption and bone formation, but their final effect on the bony structure is very different.

2.4.2.1 Bone remodeling

Bone remodeling begins at a quiescent bone surface with the retraction of lining cells and the appearance of osteoclasts. There, osteoclasts acidify and dissolve the bone matrix. In a second time, osteoblasts appear at the same site, deposit osteoids and mineralize them, to form new bone. In bone remodeling, osteoclasts and osteoblasts closely collaborate in a Basic Multicellular Unit (BMU). The tip of a BMU is made of osteoclasts, which resorb bone, followed by several thousands of osteoblasts that fill the tunnel (in cortical bone) or the canal (on trabeculae surfaces) (Figure 10a). BMU gradually burrows through the bone with a speed of 20-40 $\mu\text{m/day}$ [47, 48].

2.4.2.2 Bone modeling

In bone modeling, formation and resorption of bone are not balanced and bone formation is not necessarily preceded by resorption (Figure 10b). Lining cells at the bone surface can differentiate back to osteoblasts and form new bone on top of old bone, while osteoclasts can resorb bone where lining cells have retired without forming a BMU. Modeling can result in changes of the bone micro-architecture, the bone mass and the shape of the bones [49, 50].

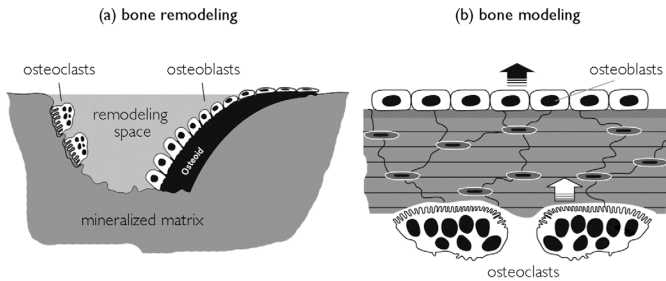


Figure 10 - (a) in bone remodeling osteoclasts precede osteoblasts. (b) In bone modeling resorption and formation can occur at different locations (source: Surgeon General⁴).

2.4.2.3 Biological regulation of bone adaptation

Local regulation

Osteoblasts produce several cytokines that regulate the osteoclasts formation and activity. In a BMU for example, the coordination between bone resorption and formation relies on this local regulation. Osteoblasts produce the *macrophage colony-stimulating factor* (m-CSF). M-CSF, which binds to its receptor on preosteoclastic cells, is necessary for osteoclast development [51]. But the most interesting regulatory system is RANKL/OPG [52]: osteoblasts produce the *receptor activator of nuclear kappa B ligand* (RANKL) that resides on their outer cell membrane [53, 54]. RANKL can bind to its receptor (RANK) on osteoclast precursors and stimulate their differentiation. So, when an osteoclast precursor encounters an osteoblast, the resulting interaction between RANK and RANKL stimulates the osteoclast precursor to mature into a fully differentiated, bone-resorbing cell [53, 54]. But osteoblastic cells also secrete *osteoprotegerin* (OPG), the soluble decoy receptor of RANKL, which can bind to RANK and disable it and therefore inhibiting osteoclastic differentiation

⁴ www.surgeongeneral.gov

and activation by RANKL (Figure 11) [55]. So, the balance between RANKL and OPG regulates the number and activity of osteoclasts and thus the rate at which bone is resorbed [56, 57].

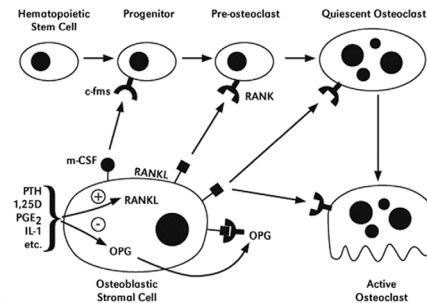


Figure 11 - Local regulation of osteoclasts differentiation and activation by RANKL/OPG. (source: Surgeon General⁵).

Hormonal regulation

Bone cells have receptors for sex steroids and other hormones [58]. Estrogen, parathyroid hormone (PTH) or factors such as 1,25 dihydroxy D (vitaminD) can alter the osteoblasts RANKL/OPG production ratio and therefore modulate the action of bone cells [59]. For example, hormonal control allows calcium to be released from bone when it is needed elsewhere in the metabolism by increasing the bone resorption rate [59, 60].

⁵ www.surgeongeneral.gov

2.4.2.4 Regulation of bone adaptation by mechanical factors

It is obvious that mechanical factors have a major influence on bone adaptation, since their effects on bone morphology have been observed for more than a century. Adaptations of bone to specific mechanical situations have been reported in numerous studies. In intense physical activities, bone adapts to the specific loading. For example, the lumbar spine of professional weight lifters have 13% higher bone mineral content (BMC) than controls [61]. The loaded humerus and radius of professional female racquet-sports players are up to 28% stronger than the unloaded ones [62]. Lower limbs of soccer players exhibit 10% higher BMC than age-matched controls [63]. On the other hand, when the mechanical demand is reduced, bone adapts by decreasing its mass and mechanical properties to the required levels. For example, when elite athletes reduce their training as their careers end, they generally lose their “extra” bone rapidly [63]. In the same manner, during long periods of disuse, such as in space flights, bone loss can be as fast as 7% of BMC after 4 weeks flights [64].

The current understanding of the mechanical regulation of bone adaptation is that bone is regulated locally. This idea originates from Roux (1881), who proposed that bone adaptation is self-organized. More recently, Frost captured these assumptions in his ‘mechanostat’ theory [65-68]. In this theory, local strains regulate bone mass: if strain levels exceed a formation threshold, bone is formed, but in contrary, when strain levels are below a resorption threshold, bone is removed (Figure 12). This qualitative approach is the basis for numerous mathematical and computational models that were developed to study bone adaptation to specific mechanical situations [11, 69-73].

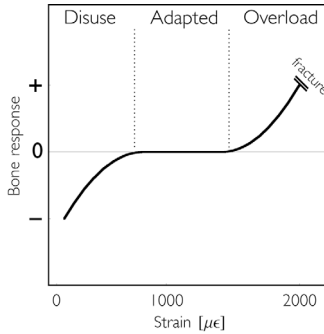


Figure 12 - Graphical interpretation of Frost's mechanostat (adapted from [68]). Typical strain magnitude in human bone range from 0 to about 2000 $\mu\epsilon$ [74].

2.4.2.5 Mechanosensation and mechanotransduction

Frost's mechanostat is a qualitative theory and it does not concern the underlying cellular mechanisms. Bone adaptation necessarily involves the perception of mechanical loading signal or *mechanosensation* and the translation of this signal into an action or *mechanotransduction*.

The precise biological pathways by which mechanical loads stimulate bone formation and suppress resorption, whereas unloading has the opposite effect, is still an unresolved issue in bone mechanobiology. The most accepted hypothesis states that osteocytes have a primary function in the transduction of mechanical signals. Several studies revealed that these cells respond to mechanical stimulation such as strains or fluid flow by the mean of their surface receptors, but it is not clear if the dendritic processes, the cell body or cilia are the mechanosensors [75-77]. Moreover, osteocytes are mutually connected by a network of canalicular channels (Figure 13). It is hypothesized that the intra-canalicular fluid-flow driven by mechanical loadings imposes a shear stress on osteocytes, and therefore acts as strain amplifier [78].

Cells in this network apparently communicate together through dendritic processes and gap junctions [79]. At the bone surface, this network also connects with the lining cells. Thus, osteocytes and lining cells form a functional syncytium, which is ideally located and is well suited for signal transduction [80, 81]. Mechanically stimulated osteocytes may then transfer signals through the canaliculi network to the bone surface to control osteoclast and osteoblast activity [42]. But this theory has not yet been formally proven.

There is still a debate about the fundamental nature of the signal that is perceived by the osteocytes. Beside the fluid-flow theory, others define this signal as the result of microcracks on the osteocytes network and the consequential osteocytes death [44, 82], while other studies identified this signal as purely mechanical properties, such as the surface strain energy [11, 73].

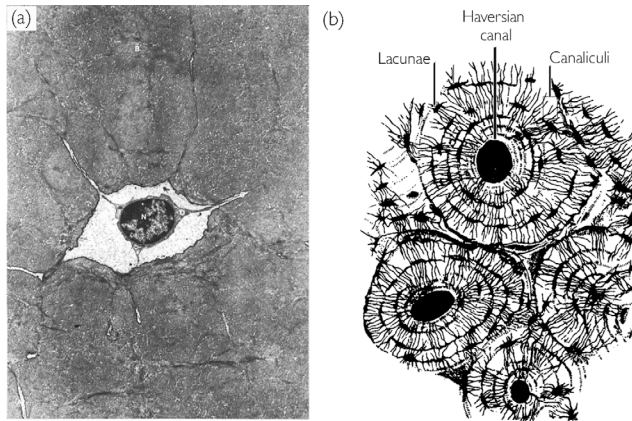


Figure 13 - (a) An osteocyte with its dendritic process entering the canaliculi network.

(b) Osteocytes form a network, which is ideally featured for signal transduction ⁶

⁶ source: (a) www.visualhistology.com, (b) www.cornell.edu/BioG

3 Prevention of periprosthetic bone loss

with local delivery of bisphosphonate

As suggested in section 1.2.2, the fate of orthopedic implants seems to be principally determined at an early stage. The lack of initial fixation promotes a positive feedback with bone-implant micromotions appearance, debris particulate formation and osteoclastic resorption that can finally lead to critical bone loss [20, 83, 84]. In contrary, when primary stability is achieved, the long-term survival of the implant is significantly improved [17, 18]. Based on these observations, Horowitz and Gonzales proposed to improve the implant fixation by preventing the early post-operative resorption through the action of drugs that inhibit osteoclastic activity, namely, *bisphosphonates* [25].

3.1 Bisphosphonates

Bisphosphonates are synthetic molecules characterized by a P–C–P group. They have been used in industry since the late 19th century. Bisphosphonates inhibit the precipitation of calcium phosphate and also slow down the dissolution of these crystals. In 1968, Fleisch *et al* demonstrated that bisphosphonates have a potentially interesting biological effect: *in vivo*, bisphosphonates inhibit bone resorption [85]. Hence, bisphosphonate were rapidly used in medicine to prevent bone resorption in diseases like osteoporosis and Paget's disease⁷ [86].

⁷ Osteoporosis is the low bone mass disease. It is characterized by the progressive thinning of bone tissue and loss of bone density over time. Paget's disease is a metabolic bone disease that involves bone destruction and regrowth, which results in deformities and pain.

Eight bisphosphonates are commercially available today and more are in development (Figure 14).

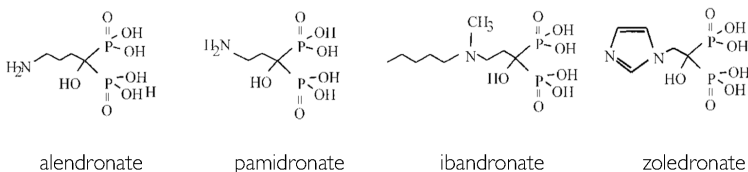


Figure 14 - Chemical structure of four famous bisphosphonates available on the market.

From left to right: alendronate, pamidronate, ibandronate and zoledronate [91].

The commercially available bisphosphonates are administered orally or injected. All bisphosphonates have low and variable bioavailability independently of the administration route [87]. With high water solubility and high ionization, they penetrate biological membranes of the gastrointestinal tract poorly and thus the bioavailability is as low as 2% of the oral dose and can be lower if absorbed together with food [88]. The determination of the drug level in the bone metabolism *in vivo* is inaccurate [87].

Systemic administration of bisphosphonate presents several adverse effects like fever, ulcers and, in patients with metastases, osteonecrosis of the jaw [89, 90].

3.1.1 Bisphosphonates' mechanisms of action

Bisphosphonates have a high affinity for hydroxyapatite, and therefore localize onto bone mineral surfaces. In particular, bisphosphonates appear to localize to sites of osteoclast activity rather than at sites of bone formation [92]. Bisphosphonates are released from the bone matrix during its resorption and are internalized by osteoclasts. There, the molecules inhibit key metabolic enzymes, and interfere with a variety of cellular functions essential for

the activity and survival of osteoclasts [93, 94], sometimes ending by the programmed cell death, or *apoptosis* [95].

Yet, recent studies have demonstrated that some bisphosphonates such as alendronate, risendronate and zoledronate, beside their role as inhibitors of osteoclastic activity, are also promoters of osteoblast proliferation and maturation [96, 97].

3.1.2 Skeletal effects of bisphosphonates

Numerous clinical studies have analyzed the skeletal effects of bisphosphonate in postmenopausal women⁸. Bisphosphonates therapies generally suppressed biochemical indices of bone resorption to about 50% of baseline after one month, while bone mineral density (BMD) increased slowly (2–6%) during the first year of treatment [98, 99]. From a traumatology point of view, the most striking effect of bisphosphonate therapies is the durable reduction of vertebral and hip fractures in patients with osteoporosis, therefore increasing considerably the comfort of these persons [100, 101], as fractures are the primary cause of morbidity in patients with osteoporosis [102, 103].

3.2 Effects of bisphosphonates on periprosthetic bone

Recent studies have shown that bisphosphonates can preserve periprosthetic bone stock in animal studies and clinical trials. These therapeutic approaches of periprosthetic bone resorption can be classified in three categories with respect to the delivery route: systemic, topical and local. In general, these approaches have all been shown to reduce periprosthetic resorption.

⁸ After menopause women face a significant risk of having osteoporosis

3.2.1 Systemic bisphosphonate treatments

Previous studies have demonstrated that systemic administration of bisphosphonates enhances the quality of the bone-implant interface. In dogs, alendronate increased bone ongrowth, bone density and shear strength of the bone implant interface by 24%, 60% and 10% respectively [104]. In rats, ibandronate reduced the implant osseointegration delay by 52% [105]. Finally, recent clinical data showed that post-operative treatment with systemic administration of clodronate prevents knee prosthesis migration at short term and at 4-years follow up [106, 107].

Systemic bisphosphonate seems then to be an easy and efficient way to prevent periprosthetic bone loss and therefore enhance the long-term outcome of orthopedic implants. However, systemic bisphosphonate treatments induce risks of secondary effects such as described previously. It is probably not acceptable to expose patients to these morbid adverse effects when they do not have osteoporosis. Furthermore, given the very low bioavailability of bisphosphonates, the drug has reduced probabilities to reach the implant locations on time to prevent early resorption, and the dose that finally reaches this location is unpredictable.

3.2.2 Topical bisphosphonate applications

Because of the drawbacks associated with the systemic use of bisphosphonates, local treatments seem to be more suitable for the prevention of periprosthetic bone loss. Topical applications of bisphosphonate consist of rinsing the implant, the implant's cavity, or both, with a solution of bisphosphonate just before the implant is inserted. The efficiency of this technique was demonstrated in a few recent studies: in dogs, topical alendronate increased periprosthetic bone density by 85% and bone-to-implant contact by 89% [108, 109]. In a remarkable clinical study, topical application of clodronate decreased knee prosthesis migration by 28% [106].

There are several drawbacks associated with topical applications. First, this method adds an extra step in the surgical procedure; this induces additional costs and increases surgical risks, such as infections or technical errors. More importantly, the technique does not guarantee a precise distribution of the drug. It is likely that some of the rinsing solution ends up in undesired sites, such as the periost, the muscles or the cardiovascular system with unpredictable effects. Finally, it has to be noted that most of the drug in the rinsing solution is wasted during the rinsing process.

3.2.3 Local bisphosphonate release

The drawbacks associated with systemic and topical treatments can be avoided with the third technique: local bisphosphonate release or *drug delivery*. It consists of grafting the drug onto the implant surface, by the mean of a carrier material, for example a thin layer of hydroxyapatite. Once the implant is inserted, the drug is released from the carrier directly at the desired site, which in the present case is the periprosthetic bone. By varying the carrier material properties, it is then possible to release the drug at different rates, in function of the needs. Furthermore, if the drug release is controlled, the optimal dose is delivered and immediately active.

Local delivery avoids extra surgical procedures, as the bisphosphonate coating can be prepared in advance. This technique also ensures that the drug is restrained in the periprosthetic area and that the amount of drug is controlled and limited.

Recent studies assessed local bisphosphonate delivery from an implant: Roussiere *et al.* have shown that the loading and release of zoledronate on and from hydroxyapatite are controllable and that the released molecule is intact [110]. *In vivo*, in rats, cortical screws releasing ibandronate and pamidronate from multi-layers of fibrinogens increased the pullout force by two-folds at 8 weeks [111]. Furthermore, in rats and osteoporotic rats, implants releasing

zoledronate increased the pullout force by 30% and the peri-implant bone density by 50% [112].

In regard of these results, local delivery is a very promising technique. However, one limiting aspect of the technique is that, according to Peter *et al.*, the intensity of the effect is clearly non-proportional to the released bisphosphonate dose [112, 113]. Small doses of bisphosphonate have a beneficial impact on periprosthetic bone stock and implant fixation, while excessive doses suppress this beneficial effect (Figure 15a). Moreover, some bisphosphonates, such as zoledronate, have been shown to increase in vitro the proliferation of osteoblasts at reasonable concentrations, but also to reduce their activity and proliferation at excessively high concentrations (Figure 15b) [114].

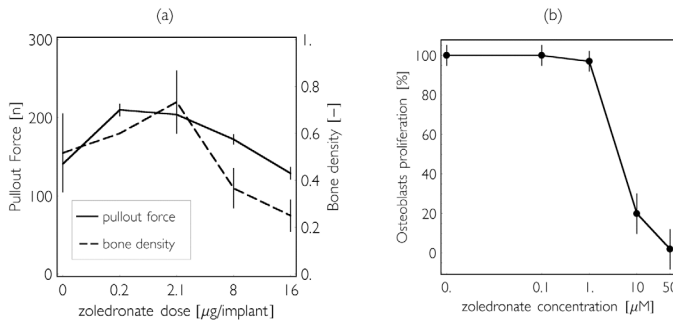


Figure 15 - (a) The non-linear relationship between zoledronate dose and periprosthetic bone density, and implant pullout force (adapted from [112]). (b) In vitro, high concentrations of zoledronate reduce osteoblasts proliferation (adapted from [114]).

For these reasons, drug-delivering implants are difficult to design: when developing an implant, it is essential to predict where the drug will diffuse and to produce designs that prevent the released bisphosphonate from accumulating excessively in periprosthetic bone. A biophysical model of the bone adaptation arising around drug-releasing implants would

certainly provide a powerful tool to further develop the technology. In paper 2, a theoretical model of periprosthetic bone adaptation with zoledronate delivery is developed and validated *in vivo*.

Finally, to validate the local release of bisphosphonate for a medical use, more data is needed. To date, studies were conducted only with rats, in which bone biology is slightly different from bone biology of humans. Therefore, efficiency evidences of the local delivery technique must be obtained in big animals prior to planning clinical studies. In paper 3, we show that local zoledronate delivery from an implant increases periprosthetic bone density in sheep.

3.3 Preview of paper 2: Development and validation of a theoretical framework to predict the bone density around orthopedic implants delivering bisphosphonate locally

The aims of the second paper were, first, to develop a model of bone adaptation around an implant delivering zoledronate based on our previously published results [112], second, to predict the dose that would induce the maximal periprosthetic bone density, and third to verify *in vivo* that periprosthetic bone density was maximal with the calculated dose.

In the mathematical model, the change in bone density is driven by a mechanical stimulus and a drug stimulus. The mechanical stimulus function was obtained from previous work [72, 73] and the drug stimulus function was identified numerically from experimental data. Implants with the calculated optimal dose of zoledronate were set in rats femurs and we measured that periprosthetic bone density was 4% greater with this dose compared to the dose previously described as the best one. (Full paper on page 64)

3.4 Preview of paper 3: Implants delivering bisphosphonate

locally increase periprosthetic bone density in an osteoporotic sheep model

The aim of the fourth paper was to verify the positive effect of local bisphosphonate delivery on the periprosthetic bone density of osteoporotic sheep. Implants coated with zoledronate and control implants were inserted in the femoral condyle of ovariectomized sheep for 4 weeks (Figure 16). The bone at the implant surface was 50% higher in the zoledronate-group compared to control group. The results of this trial study support the claim that local zoledronate could increase the fixation of an implant in weak bone. (Full paper on page 85)

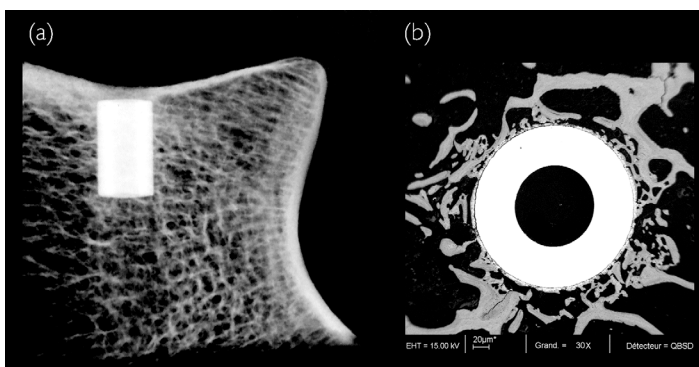


Figure 16 - In the study presented in paper 3, implants were implanted in sheep condyles. (a) μ CT view of an implant in the condyle. (b) SEM view of the periprosthetic bone structure.

3.5 Interactions between bisphosphonate and mechanical stimulations on bone adaptation

In the reference studies [112, 113] and the studies described in papers 2 and 3, the implants were not specifically loaded mechanically. In the clinical situation of load-bearing implants such as total joint replacements, the periprosthetic bone is exposed to intense mechanical stimulations [11], and in this case, the modulation of the bone response by bisphosphonate remains uncertain.

As described in section 2.4, bone adaptation is a process that relies on the communication between bone cells. Given that bisphosphonates reduce the activity of osteoclasts and may enhance the proliferation of osteoblasts, the communication between bone cells in response to mechanical stimulations might be altered. Moreover, bisphosphonate reduce the bone turnover rate, thus the bone matrix is less frequently renewed. The bone matrix gets more mineralized and therefore can get stiffer. In these conditions, the fluid flows that osteocytes sense when bone is exposed to mechanical loading might be accelerated because of the stiffer canalicular walls. This can induce higher shear stresses on the osteocytes receptors and thus artificially increase the mechanosensation.

Very few studies have been performed on the subject. In osteoporotic rats a possible positive synergistic effect between alendronate and exercise has been detected but not confirmed [115], while in humans the effect of strength training combined with bisphosphonate was not significantly different than training only [116, 117]. Nevertheless, in these studies, the strains induced by exercise training were much lower than strains that may exist proximally to a load bearing orthopedic implant. Therefore the question of bone response modulation by bisphosphonate in high strains conditions remains open.

The last two papers of the thesis concern an *in vivo* study of the effect of bisphosphonates plus intense strains on bone adaptation. First, theoretical aspects of the loading method are described in paper 4 and then the preliminary *in vivo* results are reported in paper 5.

3.6 Preview of paper 4: 3D strain map of axially loaded mouse

tibia: a numerical analysis validated by experimental

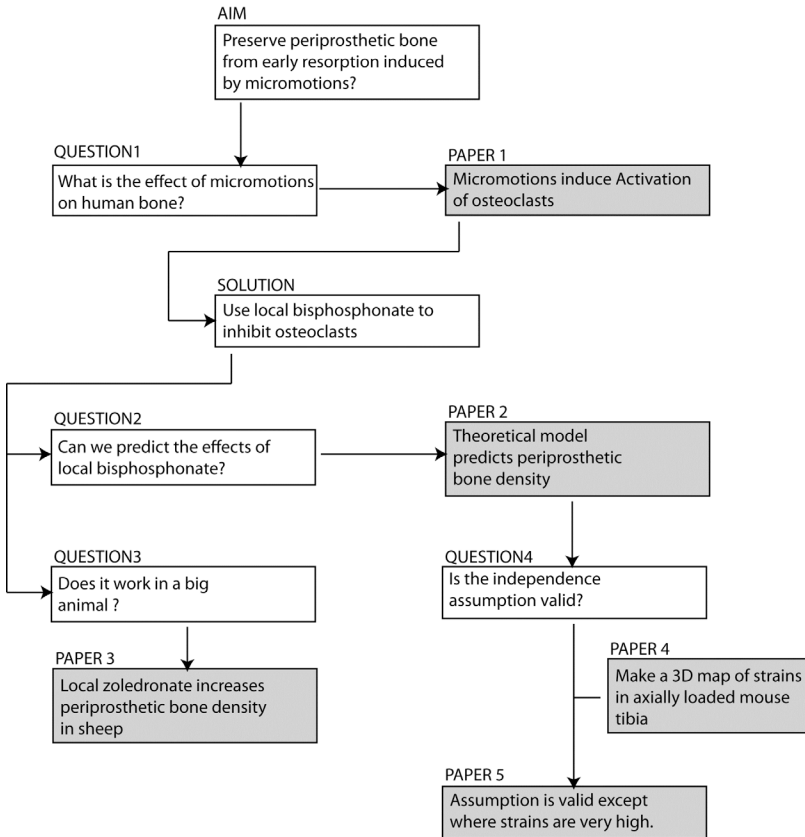
measurements

The aim of paper 4 was to calculate the 3D strains map of an axially loaded mouse tibia. A combined experimental/numerical study was performed to calculate the octahedral shear strain map. This study was motivated by the fact that, in this *in vivo* mouse model, the analysis of bone adaptation should be performed at the zone of highest mechanical stimulus to maximize the measured adaptations. It is concluded that quantification of bone remodeling should be performed at the tibial crest and at the distal diaphysis. The numerical model could also be used to furnish a more subtle analysis of the correlations between local strain and bone adaptation. (Full paper on page 106)

3.7 Preview of paper 5: Combined effects of zoledronate and mechanical stimulation on bone remodeling in an axially loaded mouse tibia.

The aim of the fifth paper was to assess the interactions between zoledronate and mechanical loading on bone adaptation in order to anticipate bone evolutions when using bisphosphonate in highly loaded bone structures such as periprosthetic bone. We combined an *in vivo* axial compression model of the mouse tibia and injections of zoledronate. Bone adaptation was assessed with *in vivo* μ CT and 3point-bending. Axial loading induced a localized increase of cortical thickness and bone area. Zoledronate increased cortical thickness, bone perimeter, and bone area. In highly loaded sites, the effect combined zoledronate and mechanical stimulation was significantly smaller than the sum of the effects, which suggested that an interaction might exist at high levels of strains. (Full paper on page 123)

Papers



4 Paper 1: Microstimulation at the bone-implant interface upregulates osteoclast activation pathways

Vincent A. Stadelmann, Alexandre Terrier, Dominique P. Pioletti*

Laboratory of Biomechanical Orthopedics EPFL-HOSR, Institute of Translational
Biomechanics, Ecole Polytechnique Fédérale de Lausanne, Switzerland

Bone. 2008 Feb; 42(2):358-64

*Corresponding author:

Dominique P. Pioletti, Ph.D.

Laboratory of Biomechanical Orthopedics EPFL-HOSR

Bat AI – Station 15

EPFL

1015 Lausanne

Switzerland

Tel: +41 21 693 83 41

Fax: +41 21 693 86 60

Email: dominique.pioletti@epfl.ch

Abstract

Peri-implant bone resorption after total joint arthroplasty is a key parameter in aseptic loosening. Implant wear debris and biomechanical aspects have both been demonstrated to be part of the bone resorption process. However, neither of these two parameters has been clearly identified as the primary initiator of peri-implant bone resorption. For the biomechanical parameters, micromotions up to $163\mu\text{m}$ were measured at the bone implant interface during normal gait cycles. The amplitude of the micromotions was shown to trigger differentiation of bone tissues. So far no data exists directly quantifying the effect of micromotions and compression on human bone. We hypothesize that micromotions and compression at the bone implant interface may induce direct activation of bone resorption around the implant through osteoblasts-osteoclasts cell signaling in human bone. This hypothesis was tested with an *ex vivo* loading system developed to stimulate trabecular bone cores and mimic the micromotions arising at the bone-implant interface. Gene expression of RANKL, OPG, TGFB2, IFNG and CSF-1 were analyzed after no mechanical stimulations (control), exposure to static compression or exposure to micromotions. We observed a 8-fold up-regulation of RANKL after exposure to micromotions, and down regulation of OPG, IFNG and TGFB2. The RANK:OPG ratio was up regulated 24 fold after micromotions. This suggests that the micromotions arising at the bone-implant interface during normal gait cycles induce a bone resorption response after only one hour, which occurs before any wear debris particles enter the system.

Keywords

Bone resorption; Orthopedic implant; Mechanical stimulation; Gene expression; Micromotions

Introduction

After total joint arthroplasty, a radiolucent zone is frequently observed at the interface of bone and implant [4, 29]. This radiolucent zone is associated with a progressive peri-implant bone resorption. The implant fixation is affected, therefore inducing a risk of aseptic loosening. This becomes a serious problem as aseptic loosening accounts for more than two-third of hip revisions in Sweden, country where an extensive implant register has been set up since many years [16].

Two hypotheses are generally used to explain peri-implant bone resorption. The first hypothesis focuses on a biological reaction to wear particles. Numerous studies have shown that the debris after implant wear induces inflammatory reactions in the tissues surrounding the implant [2, 7]. Bone formation may also be impaired by the presence of particles, such as titanium debris which were shown to induce apoptosis to osteoblasts culture *in vitro* [24]. In all cases, particulate debris accumulates in the tissue surrounding the implant. Upon accumulation, a chain of cellular events is triggered within the tissue leading to periprosthetic osteolysis and implant loosening [15]. The second hypothesis used to explain peri-implant bone resorption is based on biomechanical considerations. A stiff metallic implant in a load bearing bone considerably changes the mechanical state of the bone. Based on a numerical approach, Huiskes and Nunamaker showed that bone resorption around the implant is associated with high peak stresses immediately post-operatively [8]. The bone structure is affected by the new stress patterns around an implant. Numerical models also predict bone loss around the implant based only on these modified mechanical patterns [33].

Mechanical effects play certainly also a crucial role at the bone-implant interface. The pumping action of the implant during gait cycle causes load fluctuation within the hip joint fluid. Using a numerical model, the interfacial compressive stress involved was found to be between 2×10^{-3} and 0.1MPa [27]. Beside compressive stress, micromotions at the interface have been suspected to play a key role in tissue differentiation around the implant. It has been calculated that micromotions between 5 and $100\mu\text{m}$ occur at the bone-hip implant interface during normal gait cycles [27]. Mandell *et al.* analyzed the case of conical-collared intramedullary hip stem and reported micromotions up to $163\mu\text{m}$ in the worst design [17]. From an experimental point of

view, Baleani *et al.* quantified bone-implant micromotions under torsional load with position transducers in a hip implant model. A maximum of 56 μ m was measured in uncemented stems [1]. Finally, with *in vivo* models, Jasty *et al.* found that micromotions lower than 40 μ m favor bone formation in dog, while micromotions higher than 100 μ m lead to the creation of a fibrous tissue [10].

Based on clinical observations, numerical and experimental biomechanical analysis and *in vivo* experiments, there is strong evidence to support the theory that micromotions and compressive stress at the bone-implant interface play an important role in the process of peri-implant bone resorption. However, thus far no data exists quantifying directly the effect of micromotions and compression on human bone. Therefore we hypothesize that micromotions and pressure at the bone implant interface may induce direct activation of bone resorption around the implant through osteoblasts-osteoclasts cells signaling in human bone. This hypothesis is tested with an *ex vivo* loading system using human bone samples.

Materials and methods

Bone samples preparation

Twenty-five human femoral heads were obtained from the Hôpital Orthopédique de la Suisse Romande following total hip prosthesis procedures (Ethical Protocol 51/01, University of Lausanne). In the next 4 hours following the sample collection, each femoral head was fixed axially in a custom fixation device and at the central section a 6 mm thick slice was extracted with a surgical saw. Then, 4 to 16 trabecular bone cores of radius 3 mm and height 6 mm were extracted from the slice with a biopsy puncher (Shoney Scientific, Pondicherry, India) at 15mm from the cortical bone layer (see Figure 1 A-D). The bone cores were then incubated overnight in DMEM (Sigma, Buchs, Switzerland) containing 10% of fetal bovine serum (Sigma), and 1% of PSF (100X, 10'000 U/ml Penicillin, 10'000 μ g/ml Strepzin, 25 μ g/ml Fungizone) (GibcoBRL, New York, USA) at 37°C, 5%CO₂, 90%H₂O.

Initial Gene Expression Level

Nine samples were used to control the initial gene expression level after sample preparation. Three samples were collected immediately after punching, three samples 24hours after punching and three samples 48h after punching. These nine samples were not mechanically stimulated but placed in 1ml Trizol (Invitrogen AG, Switzerland) and stored at -80°C for later RNA extraction.

Bone samples stimulation

A device was developed to apply combined compression and micromotions regimen on the surface of trabecular bone samples simulating then the mechanical situation arising at the bone-implant interface [23]. Briefly, the device consists of a bottom fixed and top moving plates with bone core placed in between (Figure 1 F). A 0.5MPa static compression was applied from top and sinusoidal micromotions of 100 μ m at a frequency of 1Hz were applied on the top bone surface.

A Finite Element Analysis was performed to evaluate the mechanical stimulation in the bone core corresponding to the experimental boundary conditions. Because of the relative low frequency and high porosity, the inertial and fluid effects were omitted in this numerical study. The bone sample was assumed elastic, homogeneous and isotropic, and the contact was assumed to follow a Coulomb friction law. The elastic modulus was 250MPa [19] and the bone-metal friction coefficient was 0.2 [14, 28]. For the compression case, the volume average of the octahedral normal and shear strains were respectively 286 and 1190 microstrains. When micromotions were added to compression, normal stains were not affected, but shear strains increased by 7% (Figure 2).

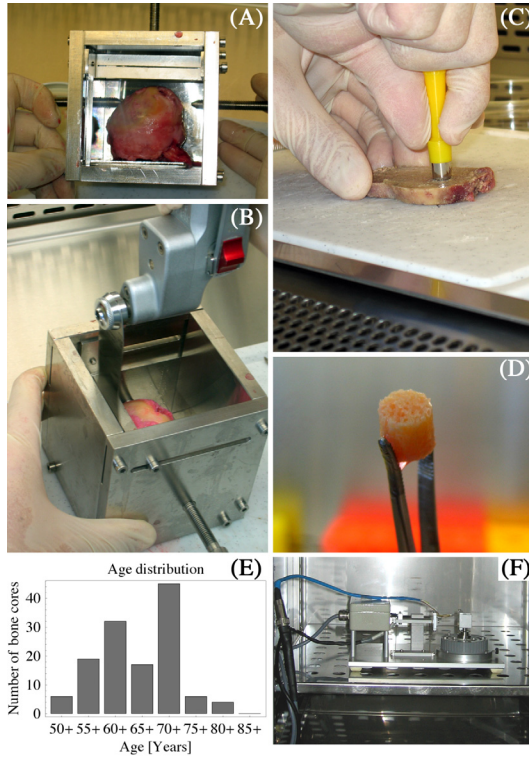


Figure 1 - Bone core extraction procedure: each femoral head was fixed axially with two screws in a custom fixation device (A). Using a surgical saw a 6mm thick slice was extracted from the central section of the femoral head (B). Each bone core was extracted manually from the slice with a biopsy puncher (C). The bone core was extracted manually from the biopsy puncher and rinsed (D). Histogram distribution of patient age from whom femoral head has been collected to process the cylindrical bone cores. No significant correlation was observed between age or sex and genetic expression following mechanical stimulation (E). The bone core was inserted in the microstimulation device, which was placed in a dedicated incubator during the mechanical stimulations. The upper part applies a 0.5MPa static compression and 100 μ m micromotions on the top of the bone core. The device is controlled with a computer (F).

The bone cores were separated randomly into three groups: control, compression and micromotions. Bone cores from the control group were incubated for one hour at rest in 1 ml culture medium (control). Bone cores from the compression group were incubated in 1 ml culture medium and a static compression of 0.5MPa was applied vertically on the sample in a special chirurgical steel chamber during 1 hour (compression). Bone cores from the micromotions group were incubated in 1ml culture medium. A 0.5MPa static compression was applied from top and sinusoidal micromotions of $100\mu\text{m}$ at a frequency of 1Hz were applied on the top surface during 1 h (micromotions). The parameters of the sample stimulations were chosen according to the results of previous numerical studies performed in our laboratory [27] and corresponded to a normal load during gait cycles.

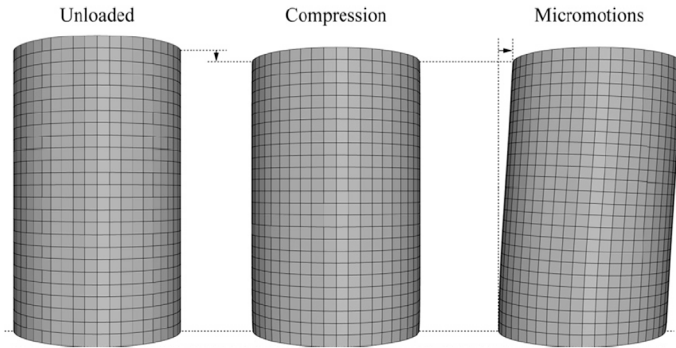


Figure 2 - A finite element analysis provided an estimation of the octahedral normal and shear strains, for the compression and micromotions cases. When micromotions were added to compression, normal strains did not changed, but shear strains increased by 7%. For illustration purpose, the deformation of the finite element mesh is magnified by 20.

RNA extraction

Immediately after the stimulations, each sample was placed in individual tube containing 1ml Trizol and stored at -80°C . The bone samples were mixed with a stainless steel bead (QIAGEN GmbH, Germany) deposited in each tube by shaking the tubes three times in the MM300 Mixer

Mill (Retsch GmbH & Co, Hann, Germany) at 30Hz during 30s. Then, 0.2ml of chloroform (Sigma-Aldrich, Switzerland) was added to the homogenate. The tubes were shaken manually, and after phase separation, 0.5ml of the upper phase was transferred in new tubes where 0.5ml of ice-cold isopropanol (Sigma-Aldrich) was added. Tubes were vortexed, and stored overnight at -80°C. RNA was isolated and purified with NucleoSpin columns (Macherey-Nagel, Düren, Germany) according to the protocol furnished by the manufacturer. The concentration and quality of the extracted RNA was measured with a biophotometer (Eppendorf AG, Germany), RNA integrity was verified by optical density (OD) absorption ratio $A_{260/280}$ nm. OD between 1.7 and 2.2 was chosen as a criterion on quality for inclusion (adapted from Cambridge Systems Biology Centre, Cambridge, UK). RNA was eluted in 40 μ l of RNase-free water and stored at -80°C until further processing.

First strand synthesis

The isolated RNA was reverse-transcribed to cDNA with the StratScript enzyme (Stratagene, San Diego, CA). For each sample, 5 μ l of total RNA was reverse-transcribed using the Taqman Universal polymerase chain reaction (PCR) reagents with random hexamers (Applied Biosystems, Foster City, CA). Reaction volumes were fixed at 50 μ l according to the protocol provided by the supplier. The thermal cycler PCT-0100 (MJ Research, Waltham, MA) was programmed as following: 25°C 10 min, 48°C 30 min, and 95°C 5 min.

qPCR

The following gene expressions were quantified: RANK ligand (RANKL), Osteoprotegerin (OPG), Interferon-gamma (IFNG), Colony Stimulating Factor 1 (CSF-1) and Transforming Growth Factor beta2 (TGFB2) as target genes, and glyceraldehyde-3-phosphate dehydrogenase (GAPDH) as non-regulated reference gene (housekeeping gene).

Specific primers for each gene were designed with the Primer Express® software (Applied Biosystems) and purchased from Integrated DNA Technologies (Coralville, IA). An additional sequence of 18bp was added to the 5' end of every forward primer to use the Amplifluor Universal Detection System (Intergen Discovery Products, Purchase, NY). PCR reactions were

performed in 25 μ l: 5 μ l of first strand, 12.5 μ l of TaqMan Universal PCR Master Mix (Applied Biosystems), and 7.5 μ l of the primers working solution. Thermal cycle conditions were 50°C 2 min, 95°C 10 min, then 50 cycles at 95°C 15s, 60°C 1 min. Amplifications were monitored with the ABI Prism 7700 (Applied Biosystems). Measurements were performed in duplicates.

Gene expression analysis and statistics

The threshold cycle C_T was measured for each gene and each sample from the PCR amplification curve with a standard routine. C_T table was analyzed for each gene in each experiment: if duplicates from one cDNA presented a difference larger than 3 cycles (due to experimental artifacts such as limited pipetting precision, presence of bubble in the well, etc.), the measure was dismissed; otherwise C_T was calculated as the duplicate mean. If C_T was greater than 35 cycles, the measure was dismissed.

Relative gene expressions were calculated with the $2^{-\Delta\Delta C_T}$ method [22] with GAPDH as housekeeping gene. As the level of GAPDH expression may be influenced by the mechanical stimulation and consequently would render invalid its use as reference gene, in a pilot study we normalized the GAPDH expression by the level of 18S expression. No effect of mechanical stimulation was observed on GAPDH expression (data not shown). Unless 18S is similarly regulated as GAPDH through mechanical stimulation, which seems to be unlikely, GAPDH gene expression can be used as a stable reference gene in this experiment. We used a randomization of the differences and one-way ANOVA to compare the gene expressions of the different groups [6]. All values were then normalized to the expression of the control group. All mathematical operations and statistical analysis were performed using Mathematica® (Wolfram Research, Inc. USA). A p-value lower than 0.05 was considered significant while p-value lower than 0.1 was considered as a strong trend.

Results

In the following results, we report normalized gene expressions as $\text{MEAN} \pm \text{SEM}$.

Sample collection

The bone core samples were obtained from femoral heads of male and female patient between 50 and 80 years old (Figure 1 E). No significant correlation was observed between age or sex and genetic expression following the experiments. Table 1 summarizes the number of cylindrical cores in each group. One hundred and twelve samples were used in the main experiment. Fifty-four samples passed the quality criteria (A260/A280) and were used for normalized gene expression analysis comparison between control, static compression and micromotions regimen.

# of bone cores	Control	Compression	Micromotion
112	62	20	30

Table 1 - Number of bone cores used for each condition

Initial gene expression level

As the process of bone core extraction may affect the gene expression of the sample, nine samples were used to evaluate the initial and 24h gene expressions level after samples preparation and compare it to the value obtained 48h after sample preparation. Immediately after sample punching, gene expressions were the following: RANKL 0.68 ± 0.25 , OPG 1.5 ± 0.7 , TGF β 3.2 ± 0.7 compared to the 48h values. After 24h, the expressions were: RANKL 0.5 ± 0.2 , OPG 0.6 ± 0.2 , TGF β 0.9 ± 0.2 compared to the 48h values. Finally, after 48h, when we compare the values between each sample, the expressions became: RANKL 1.4 ± 0.5 , OPG 0.77 ± 0.12 , TGF β 1.0 ± 0.2 (Figure 3). None of the expressions at 48h were significantly different from one, meaning that the gene expression of all core samples was similar. None of the expression levels at 24h were significantly different from those at 48h. The variances of the expression

levels were significantly different than those at t0. These results suggest that, after one or two days of incubation, the pool of bone samples is in a homogenous state of genetic expression at least for the tested genes. All the samples were then incubated 24h after extraction prior to the 1h mechanical test.

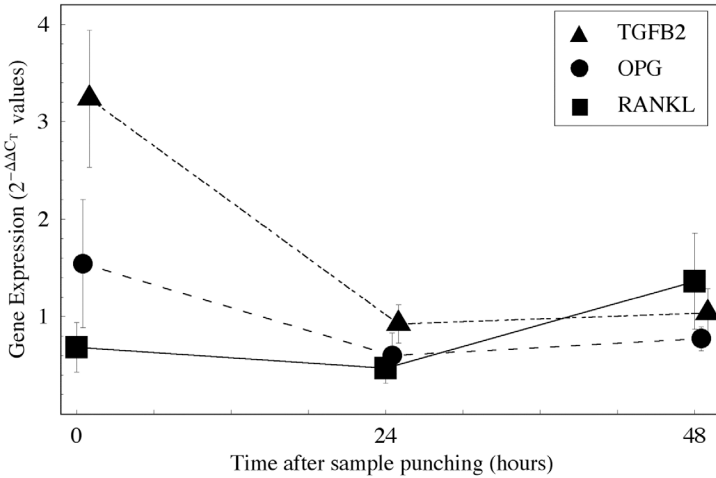


Figure 3 - Relative gene expression of TGFB2, OPG and RANKL quantified by RT-PCR after 0, 24 and 48 hours of incubation. The results are shown as $2^{-\Delta\Delta C_t}$ values and plotted as $MEAN \pm SEM$ of each individual experiment.

Gene expression according to the mechanical stimulus

The relative gene expression for the selected genes and mechanical stimulations are presented in Figure 4. RANKL was up-regulated in the compression and the micromotions groups. RANKL expression was up-regulated 2.8 ± 0.9 fold in the compression group and up-regulated 8 ± 2.8 fold in the micromotions group when compared to control. The difference between static compression and control, and the between micromotions and control were significant, whereas there was a strong trend suggesting that the expression level between micromotion and static

compression were different.

OPG expression was dramatically down-regulated 0.18 ± 0.02 fold in the compression group and down-regulated 0.34 ± 0.07 fold in the micromotions group when compared to control. The difference between static compression and control, micromotions and control, and micromotions and static compression were significant.

TGFB2 expression was down-regulated 0.3 ± 0.1 fold in the compression group and down-regulated 0.2 ± 0.08 fold in the micromotions group when compared to control. The difference between static compression and control and micromotions and control were not significant but the p-value ($p=0.08$) suggested a strong trend towards significant differences.

IFNG expression was not significantly changed in the static compression group (1.4 ± 0.4) and was down-regulated 0.29 ± 0.05 fold in the micromotions group when compared to control. The difference between micromotions and control and micromotions and static compression were significant

CSF-1 was not significantly affected in the static compression group (1 ± 0.5) nor in the micro-motion group (1 ± 0.5) when compared to the control group.

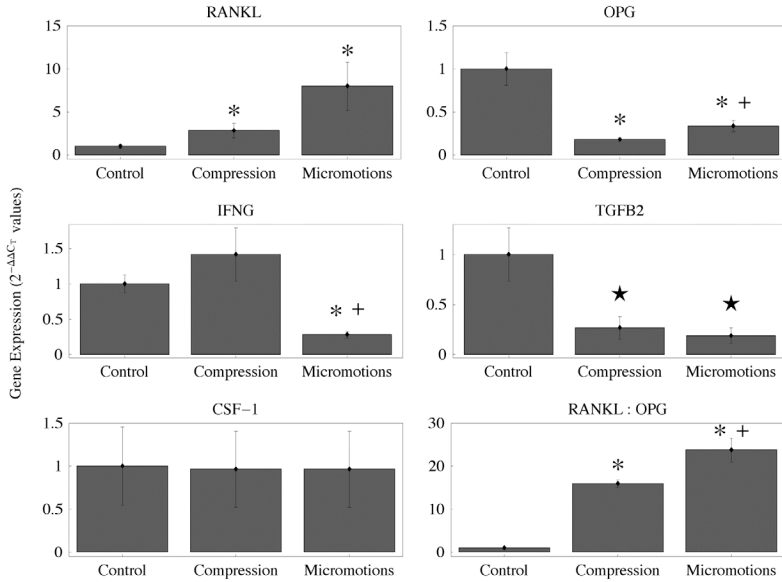


Figure 4 – Relative gene expression of RANKL, OPG, IFNG, TGFB2 and RANKL:OPG expression ratio quantified by RT-PCR after one hour of incubation (control), 0.5MPa static compression or 0.5MPa static compression + 100μm micromotions (micromotions). The results are shown as $2^{-\Delta\Delta CT}$ values and plotted as $MEAN \pm SEM$ of each individual experiment. Symbols: * ($p < 0.05$ vs control), + ($p < 0.05$ vs static compression), ★ (trend at $p < 0.1$ level vs control), † (trend at $p < 0.1$ level vs static compression).

Discussion

A clinical study showed that up to 14% bone loss arose during the first three months after total hip arthroplasties [34]. In parallel, rapid early migrations have been detected by roentgen stereophotogrammetry in many asymptotic hips, often as early as 4 months postoperatively [11, 18]. The migrations have been found to predict an increased risk of clinical loosening. The fate of an orthopedic implant seems then to occur at an early stage, probably before any wear particles are produced and is certainly related to mechanical factors. Micromotions at the bone-implant interface are then ideal candidates to “explain” peri-implant bone resorption and were identified as key players in animal studies.

However, no information thus far has confirmed these results for human bone, as the only information available are based on tissue retrieval obtained from failed implants, the last stage of the degeneration process [31]. Based on a unique *ex vivo* approach, the present study evaluates the micromotions effect on bone resorption for human samples and verifies if resorption could be initiated immediately after surgery, when no wear particles are part of the process.

We hypothesized that micromotions could induce an up-regulation of genes involved in osteoclastic bone resorption. Therefore, we analyzed the expression ratios of the RANKL/OPG signaling system, as well as the expression ratios of TGFB2, IFNG and CSF-1. We used a control group, a static compression group and a micromotions group, mimicking the situation arising around femoral stems of hip implants during gait cycles [27].

RANKL is a critical factor for late stage osteoclasts differentiation and activation. RANKL was shown to be expressed by osteoblasts after mechanical or hormonal stimulations [26]. OPG, the decoy receptor of RANKL produced by osteoblasts is a powerful inhibitor of osteoclasts formation *in vivo* and *in vitro* [30]. Our results show that micromotions and static compression dramatically increase RANKL expression suggesting that the number and the activity of osteoclasts at the implant surroundings are increased by micromotions and compression in normal gait conditions. We also observed a down-regulation of OPG expression after exposition to static compression alone or to micromotions suggesting that the balancing effect of RANKL by OPG is decreased.

Experimental and mathematical evidences have recently shown that OPG and RANKL

expressions are regulated inversely in osteoblasts, and that bone remodeling rate is probably determined by the RANKL:OPG ratio [3, 12, 13]. Our results are in concordance with these observations: RANKL and OPG are expressed inversely after exposition to static compression alone or after static compression and micromotions, as discussed previously. We observed that the RANKL:OPG ratio is significantly increased ten fold by static compression and significantly more than twenty fold by static compression and micromotions, suggesting that micromotions are potent activators of high bone turnover rate. Our observations on the regulation of RANKL/OPG by static compression and micromotions suggest that the number of osteoclasts is enhanced, and bone turnover rate is increased in the periprosthetic area with normal gait cycle conditions. This might be one of the causes of the observed bone resorption around orthopedic implants.

Osteoclasts and osteoblasts activities are strongly correlated *in vivo*, and an increased osteoclastic activity might induce an osteoblastic response. Similarly, micromotions may affect osteoblastic recruitment. Therefore we also analyzed the expression of bone formation signaling molecules such as TGF β 2 and IFNG. TGF β 2 is expressed by osteoblasts, and has contrasting effects on osteoblasts and osteoclasts. TGF β 2 is a bone formation promoting molecule operating through chemotactic attraction of osteoblasts and enhancement of osteoblasts proliferation at the early stages of differentiation [9]. In cell culture, IFNG was shown to inhibit osteoblastic cell function [5] and potentially inhibit osteoclasts formation. In bone explants, it inhibits osteoclasts differentiation [32]. We observed a down-regulation of TGF β 2 after exposure to static compression alone and after static compression plus micromotions, suggesting that micromotions at the implant interface do not increase recruitment of osteoblasts through TGF β 2 signaling. TGF β 2 was shown to be a promoter of osteoclasts formation by increasing the sensitivity of progenitors to RANKL (through up-regulation of RANK in preosteoclastic cells) [25, 35]. TGF β 2 can also inhibit osteoclasts formation through a down regulation of the RANKL:OPG ratio [35]. In our analysis, RANKL:OPG is increased while TGF β is decreased which is concordant. Our measures show that static compression and micromotions decrease IFNG expression by two thirds. The consequence is then difficult to interpret in the peri-implant situation, as the effect could be either a decrease of bone formation

through inhibition of osteoblastic function or a decrease of bone resorption through inhibition of osteoclastic differentiation. Further studies are needed to clarify the role of this molecule.

The aim of the experimental setup used here was to simulate the mechanical situation at bone-implant interfaces using *ex vivo* bone samples. The amplitude of the applied compression and micromotions were set to measured or calculated values. The drawbacks of this system are that the sample preparation procedures and *ex vivo* incubation certainly have biological consequences on bone cells functions despite we showed that at least there is an initial homogeneous level of gene expression between samples. We can then assume that we have a consistency of initial conditions in our experiment. However, certainly due to the inherent biological variability, we obtained variable quality of extracted RNA, which may affect the gene expression quantification. It has also to be mentioned that quantification of gene expression may only be part of the biological reaction to mechanical stimulus due to different post-transcriptional events. However, to our knowledge, no other experimental design allows one to study the effect of micromotions on the bone-implant interface with living human samples. These challenging technical difficulties were solved by *a posteriori* controls of RNA quality and variability of gene expression duplicates. More than 50% of the samples were discarded during these control procedures. It implied that paired-control statistical designs could not be use and that a large number of samples had to be processed to overcome the inter-specimen variations and to observe significant differences in the gene expressions.

To conclude, our results suggest that micromotions at the bone-implant interface during normal gait cycles induce a rapid bone resorption response after only one hour, which occurs before any wear debris particles enter the system. These results confirm our initial hypothesis.

Based on these results we proposed that blocking locally the osteoclastic resorption through the action of bisphosphonate might prevent the peri-implant osteolysis. The first results of our animal model of implants used as bisphosphonate delivery systems tend to confirm this idea [20, 21].

Acknowledgements

Project no. 04-P2 was supported by the AO Research Fund of the AO Foundation, Davos, Switzerland. We thank Marc-Olivier Montjovent and Sandra Jaccoud for technical assistance and Tyler Thacher for English editing.

References

1. Baleani, M., Cristofolini, L., and Toni, A. Initial stability of a new hybrid fixation hip stem: experimental measurement of implant-bone micromotion under torsional load in comparison with cemented and cementless stems. *J Biomed Mater Res* 50:605-615; 2000.
2. Clarke, I. C., Campbell, P., and Kossovsky, N. Debris-mediated osteolysis-A cascade phenomenon involving motion, wear, particulates, macrophage induction, and bone lysis. In: K. R. St. John (ed.), *Particulate debris from medical implants: mechanisms of formation and biological consequences*, ASTM STP 1144, pp. 7-26. Philadelphia: American Society for testing and materials; 1992.
3. Fazzalari, N. L., Kuliwaba, J. S., Atkins, G. J., Forwood, M. R., and Findlay, D. M. The ratio of messenger RNA levels of receptor activator of nuclear factor kappaB ligand to osteoprotegerin correlates with bone remodeling indices in normal human cancellous bone but not in osteoarthritis. *J Bone Miner Res* 16:1015-1027; 2001.
4. Freeman, M. A. R., Bradley, G. W., and Revell, P. A. Observations Upon the Interface between Bone and Polymethylmethacrylate Cement. *Journal of Bone and Joint Surgery-British Volume* 64:489-493; 1982.
5. Hirose, K., Hanazawa, S., Amano, S., Kikuchi, H., Takeshita, A., Murakami, Y., Hashimoto, H., Yokoyama, T., Suyama, R., and Kitano, S. Recombinant interferon-gamma is a potent inhibitor of osteoblastic cell functions. *Meikai Daigaku Shigaku Zasshi* 18:296-301; 1989.
6. Hooton, J. W. Randomization tests: statistics for experimenters. *Comput Methods Programs Biomed* 35:43-51; 1991.
7. Horikoshi, M., Macaulay, W., Booth, R. E., Crossett, L. S., and Rubash, H. E. Comparison of interface membranes obtained from failed cemented and cementless hip and knee prostheses. *Clin Orthop Relat Res*:69-87; 1994.

8. Huiskes, R., and Nunamaker, D. Local stresses and bone adaption around orthopedic implants. *Calcif Tissue Int* 36 Suppl 1:S110-117; 1984.
9. Janssens, K., ten Dijke, P., Janssens, S., and Van Hul, W. Transforming growth factor-beta1 to the bone. *Endocr Rev* 26:743-774; 2005.
10. Jasty, M., Bragdon, C., Burke, D., OConnor, D., Lowenstein, J., and Harris, W. H. In vivo skeletal responses to porous-surfaced implants subjected to small induced motions. *Journal of Bone and Joint Surgery-American Volume* 79A:707-714; 1997.
11. Karrholm, J., Borssen, B., Lowenhielm, G., and Snorrason, F. Does early micromotion of femoral stem prostheses matter? 4-7-year stereoradiographic follow-up of 84 cemented prostheses. *J Bone Joint Surg Br* 76:912-917; 1994.
12. Komarova, S. V. Mathematical model of paracrine interactions between osteoclasts and osteoblasts predicts anabolic action of parathyroid hormone on bone. *Endocrinology* 146:3589-3595; 2005.
13. Komarova, S. V., Smith, R. J., Dixon, S. J., Sims, S. M., and Wahl, L. M. Mathematical model predicts a critical role for osteoclast autocrine regulation in the control of bone remodeling. *Bone* 33:206-215; 2003.
14. Kuiper, J. H., and Huiskes, R. Friction and stem stiffness affect dynamic interface motion in total hip replacement. *J Orthop Res* 14:36-43; 1996.
15. Lerouge, S., Huk, O., Yahia, L., Witvoet, J., and Sedel, L. Ceramic-ceramic and metal-polyethylene total hip replacements: comparison of pseudomembranes after loosening. *J Bone Joint Surg Br* 79:135-139; 1997.
16. Malchau, H., Herberts, P., Eisler, T., Garellick, G., and Soderman, P. The Swedish total hip replacement register. *Journal of Bone and Joint Surgery-American Volume* 84A:2-20; 2002.
17. Mandell, J. A., Carter, D. R., Goodman, S. B., Schurman, D. J., and Beaupre, G. S. A conical-collared intramedullary stem can improve stress transfer and limit micromotion. *Clin Biomech (Bristol, Avon)* 19:695-703; 2004.
18. Mjoberg, B. The theory of early loosening of hip prostheses. *Orthopedics* 20:1169-1175; 1997.
19. Nazarian, A., Muller, J., Zurakowski, D., Muller, R., and Snyder, B. D. Densitometric, morphometric and mechanical distributions in the human proximal femur. *J Biomech* 40:2573-2579; 2007.
20. Peter, B., Gauthier, O., Laib, S., Bujoli, B., Guicheux, J., Janvier, P., van Lenthe, G. H., Muller, R., Zambelli, P. Y., Boulter, J. M., and Pioletti, D. P. Local delivery of

- bisphosphonate from coated orthopedic implants increases implants mechanical stability in osteoporotic rats. *J Biomed Mater Res A* 76:133-143; 2006.
21. Peter, B., Pioletti, D. P., Laib, S., Bujoli, B., Pilet, P., Janvier, P., Guicheux, J., Zambelli, P. Y., Bouler, J. M., and Gauthier, O. Calcium phosphate drug delivery system: influence of local zoledronate release on bone implant osteointegration. *Bone* 36:52-60; 2005.
 22. Pfaffl, M. W. A new mathematical model for relative quantification in real-time RT-PCR. *Nucleic Acids Res* 29:e45; 2001.
 23. Pioletti, D. P., Muller, J., Rakotomanana, L. R., Corbeil, J., and Wild, E. Effect of micromechanical stimulations on osteoblasts: development of a device simulating the mechanical situation at the bone-implant interface. *J Biomech* 36:131-135; 2003.
 24. Pioletti, D. P., Takei, H., Kwon, S. Y., Wood, D., and Sung, K. L. The cytotoxic effect of titanium particles phagocytosed by osteoblasts. *J Biomed Mater Res* 46:399-407; 1999.
 25. Quinn, J. M., Itoh, K., Udagawa, N., Hausler, K., Yasuda, H., Shima, N., Mizuno, A., Higashio, K., Takahashi, N., Suda, T., Martin, T. J., and Gillespie, M. T. Transforming growth factor beta affects osteoclast differentiation via direct and indirect actions. *J Bone Miner Res* 16:1787-1794; 2001.
 26. Quinn, J. M. W., and Gillespie, M. T. Modulation of osteoclast formation. *Biochemical and Biophysical Research Communications* 328:739-745; 2005.
 27. Ramaniraka, N. A., Rakotomanana, L. R., and Leyvraz, P. F. The fixation of the cemented femoral component. Effects of stem stiffness, cement thickness and roughness of the cement-bone surface. *J Bone Joint Surg Br* 82:297-303; 2000.
 28. Rancourt, D., Shirazi-Adl, A., Drouin, G., and Paiement, G. Friction properties of the interface between porous-surfaced metals and tibial cancellous bone. *J Biomed Mater Res* 24:1503-1519; 1990.
 29. Reckling, F. W., Asher, M. A., and Dillon, W. L. Longitudinal-Study of Radiolucent Line at Bone-Cement Interface Following Total Joint-Replacement Procedures. *Journal of Bone and Joint Surgery-American Volume* 59:355-358; 1977.
 30. Simonet, W. S., Lacey, D. L., Dunstan, C. R., Kelley, M., Chang, M. S., Luthy, R., Nguyen, H. Q., Wooden, S., Bennett, L., Boone, T., Shimamoto, G., DeRose, M., Elliott, R., Colombero, A., Tan, H. L., Trail, G., Sullivan, J., Davy, E., Bucay, N., Renshaw-Gegg, L., Hughes, T. M., Hill, D., Pattison, W., Campbell, P., Sander, S., Van, G., Tarpley, J., Derby, P., Lee, R., and Boyle, W. J. Osteoprotegerin: a novel

- secreted protein involved in the regulation of bone density. *Cell* 89:309-319; 1997.
31. Takagi, M., Santavirta, S., Ida, H., Ishii, M., Takei, I., Niissalo, S., Ogino, T., and Konttinen, Y. T. High-turnover periprosthetic bone remodeling and immature bone formation around loose cemented total hip joints. *J Bone Miner Res* 16:79-88; 2001.
 32. Takayanagi, H., Kim, S., and Taniguchi, T. Signaling crosstalk between RANKL and interferons in osteoclast differentiation. *Arthritis Res* 4 Suppl 3:S227-232; 2002.
 33. Terrier, A., Rakotomanana, R. L., Ramaniraka, A. N., and Leyvraz, P. F. Adaptation Models of Anisotropic Bone. *Comput Methods Biomech Biomed Engin* 1:47-59; 1997.
 34. Venesmaa, P. K., Kroger, H. P. J., Miettinen, H. J. A., Jurvelin, J. S., Suomalainen, O. T., and Alhava, E. M. Monitoring of periprosthetic BMD after uncemented total hip arthroplasty with dual-energy X-ray absorptiometry - a 3-year follow-up study. *Journal of Bone and Mineral Research* 16:1056-1061; 2001.
 35. Yan, T., Riggs, B. L., Boyle, W. J., and Khosla, S. Regulation of osteoclastogenesis and RANK expression by TGF-beta1. *J Cell Biochem* 83:320-325; 2001.

5 Paper 2: Development and validation of a theoretical framework to predict the bone density around orthopedic implants delivering bisphosphonate locally

Vincent A. Stadelmann¹, Alexandre Terrier¹, O. Gauthier², J.M. Boulter², Dominique Pioletti¹

¹Laboratory of Biomechanical Orthopaedics EPFL-DAL, IBI, Ecole Polytechnique Fédérale de Lausanne, Switzerland

²Laboratoire de Recherche sur les Matériaux d'Intérêt Biologique INSERM 99-03, Faculté de Chirurgie Dentaire, Nantes, France

Submitted to the Journal of Biomechanics

*Corresponding author:

Dominique P. Pioletti, Ph.D.

Laboratory of Biomechanical Orthopaedics EPFL-HOSR

Bat AI – Station 15 - EPFL

1015 Lausanne

Switzerland

Tel: +41 21 693 83 41

Fax: +41 21 693 86 60

Email: dominique.pioletti@epfl.ch

Abstract

The fixation of orthopedic implants depends strongly upon the initial stability of the implant. peri-implant bone resorbs shortly after the surgery. In a normal situation, this is shortly followed by new bone formation and implants fixation strengthening but if the initial stability is not reached, the resorption goes on and the implant fixation weakens, which leads to implant loosening. Studies with rats and dogs have shown that a solution to prevent peri-implant resorption is to use deliver bisphosphonate at the implant surface.

The present paper aims were, first, to develop a model of bone remodeling around an implant delivering bisphosphonate using our previously published results, second, to predict the bisphosphonate dose that would induce the maximal peri-implant bone density, and third to verify *in vivo* that peri-implant bone density is maximal with the calculated dose.

The mathematical model consists of a bone remodeling equation and a drug diffusion equation. The change in bone density is driven by a mechanical stimulus and a drug stimulus. The drug stimulus function and the other numerical parameters were calculated from experimental data. The model predicted that a dose of 0.3 μ g of zoledronate on the implant would induce a maximal bone density. Implants with 0.3 μ g of zoledronate were implanted in rats' femurs for 3, 6 and 9 weeks. We measured that peri-implant bone density was 4% greater with the calculated dose.

The approach presented in this paper could be used in the design and analysis processes of experiments in local delivery of bisphosphonate.

Introduction

The fate of orthopaedic implants seems to be principally determined at an early stage. Rapid early migrations of stems have been detected in many asymptotic hips, often as early as 4 months postoperatively (Karrholm, Borssen *et al.* 1994). These early migrations have been related to an increased risk of clinical loosening. It has been reported that peri-implant bone resorbs during a short period after the surgery, probably in response to the surgically-induced trauma, inducing a weakening of the fixation (Venesmaa, *et al.*, 2001). In normal healing conditions, the fixation strength increases after this initial weakening (Dhert, *et al.*, 1998), but in pathologic conditions, the lack of initial fixation promotes osteolysis via bone-implant micromotions production, debris particulate formation and osteoclastic resorption (Stadelmann, *et al.*, 2008). On the other hand, when a longer primary stability is achieved, the long-term survival of the implant is significantly improved (Karrholm, Borssen *et al.* 1994; Mjoberg 1997).

Based on current knowledge regarding early biological events at the implant interface, it has been proposed to use bisphosphonate to improve the early implant fixation by preventing the post-op osteoclastic resorption (Horowitz and Gonzales, 1996). A recent clinical study showed that post-surgical systemic administration of clodronate prevents knee prosthesis migration (Hilding and Aspenberg, 2006). Animal studies have shown that bisphosphonate increases peri-implant bone density and shear strength of the bone implant interface in dogs (Jensen, *et al.*, 2007) and in rats (Eberhardt, *et al.*, 2007).

Systemic administration of bisphosphonate presents several adverse effects, like fever, ulcers and osteonecrosis of the jaw (Dannemann, Gratz *et al.* 2007). Since bones are low-perfused organs, drugs diluted in blood stream have low probabilities to reach the required locations

with sufficient time or concentration to be effective. Therefore it seems ethically irresponsible to expose patients who have received orthopaedic implants to the risks induced by systemic administration of bisphosphonate, considering the benefits at the implant level are not ensured.

To ensure the availability of bisphosphonate at the peri-implant area, where it is needed most, and to reduce the risks related to systemic administration, methods for local delivery have recently been addressed: these methods consist of grafting the drug onto the implant surface, by the mean of a carrier material, such as hydroxyapatite coating or multi-layers of fibrinogens. This technique avoids extra steps in the surgical protocol that are necessary for topical application (Jakobsen, *et al.*, 2007), it ensures that bisphosphonate is restrained in the peri-prosthetic area, and allows a slower and more continuous release of the drug. The amount of drug applied can be delivered more efficiently and may be as low as 1/1000 of that used for an oral dose. The local delivery method proved its efficiency in different experimental situations. In rats, cortical screws releasing ibandronate and pamidronate increased the pullout force (Wermelin, *et al.*, 2007). In rats, implants releasing zoledronate also increased the pullout force and the peri-implant bone density (Peter, Pioletti *et al.* 2005; Peter, Gauthier *et al.* 2006). According to these studies, the effect of bisphosphonate released from implants is non-linearly dose dependent.

In order to calculate the optimal bisphosphonate dosage to obtain the best implant fixation, a biophysical theory of the events arising around an implant used for a local delivery of bisphosphonate is needed. Such a theory must relate bone remodeling to both the mechanical aspects of peri-implant situation and the effect of the bisphosphonate. Most of the existing models of bone remodeling are mechanically driven e.g. (Huiskes, 1997). They are widely

used, yet it is outside the scope of this article to review these models. Few attempts exist to address the effect of systemic bisphosphonate using a model of remodeling (Hernandez, Beaupre *et al.* 2001; Pioletti and Rakotomanana 2004). However these attempts did not take into account the spatial diffusion of bisphosphonate when released from a local source. Therefore, the goals of the present study were triple: first, to develop a mathematical model of bone remodeling including mechanical stimulus as well as the stimulus of bisphosphonate diffusing from an implant; second, to identify the numerical parameters of the model from published data; third to validate the model by verifying its prediction *in vivo*.

Materials and Methods

In this section, we first present the development of a theoretical model of bone remodeling coupled with bisphosphonate diffusing from an implant. In the second part, the model parameters are identified with published experimental data. Finally, we present *in vivo* experiments using rats that provided data for the model validation.

Theoretical developments

The following developments were based on an existing bone model of remodeling previously developed in our lab (Terrier, *et al.*, 2005). We extended the initial model by adding a new internal variable for the drug concentration. The bone density evolution law was adapted to include this new variable and finally we introduced a diffusion law for the drug.

The initial model of remodeling, the local bone density ϕ varies under the influence of a mechanical stimulus ψ . The choice for this stimulus was the plastic yield stress of Hill (Rakotomanana, *et al.*, 1992). According to this choice, it has been shown that the dependence of the stimulus in the density ϕ could be written in the form $\psi = Y/\phi^4$ (Terrier, *et*

al., 2005), where Y is a mechanical function that only depends on the stress, but may however depend on space and time through the stress. The bone density evolution law was characterized by three different regimes: resorption, equilibrium and densification, according to the stimulus level. In the present study, the extension of the initial model was limited to the densification regime. According to the evolution law (eq1), bone cells densify bone matrix when the stimulus exceeds a densification stimulus threshold ψ_d .

$$\partial_t \phi = v_d (\psi - \psi_d) \quad (\text{eq1})$$

The rate of densification is given by the constant v_d , which was determined from experiment in rats (Terrier, *et al.*, 2005).

The extension of the initial model consisted in adding the net effect of the drug as an imbalance of the remodeling process, resulting in a net gain in bone mass. This effect was introduced through a second stimulus, Φ_{drug} , called drug stimulus, which was defined as a function of a new internal variable, the local drug concentration κ . In a first step, the model was limited to the following hypothesis: (i) the drug stimulus depends only on the drug concentration (ii) the mechanical stimulus does not depend on the drug concentration, (iii) the bisphosphonate diffuses following Fick's law of diffusion.

The drug stimulus $\Phi_{drug}(\kappa)$ is expressed in [% change day⁻¹], and the drug concentration κ in [$\mu\text{g} / \text{mm}^3$]. The rate of densification (eq1) becomes

$$\partial_t \phi = v_d \left(\frac{Y}{\phi^4} - \psi_d \right) + \Phi_{drug}(\kappa) \quad (\text{eq2})$$

completed by drug diffusion

$$\partial_t \kappa = \nabla(D \nabla \kappa) \quad (\text{eq3})$$

where D is the effective coefficient of diffusion, which takes into account the diffusion of the drug into bone marrow, and the tortuosity of cancellous bone.

Identification of the model's parameters

The unknown parameters of the extended model are the diffusion coefficient D , the mechanical function $Y(x)$ and the drug stimulus function $\Phi_{drug}(\kappa)$.

First we estimated experimentally that $D \approx 800 \text{ } [\mu\text{m}^2/\text{day}]$ with an experimental setup using C14-zoledronate diffusing through trabecular bone sections (Peter, 2004).

To identify the other numerical parameters, we used previously published bone density profiles measured around drug-releasing implants (Peter, Pioletti *et al.* 2005). These profiles were obtained with five different doses of zoledronate (0, 0.2, 2.1, 8, 16 $\mu\text{g}/\text{implant}$) grafted onto the hydroxyapatite coating of cylindrical titanium implants in rat condyles at 3 weeks post-op. We simplified the system of equations (eq2 and eq3) with regards to this particular experimental setup, with the following assumptions: First, we reduced the system to a one-dimensional axisymmetric geometry where x is the distance from the coating. Second we idealized the boundary conditions by assuming that (i) the hydroxyapatite coating is an infinite source of bisphosphonate, i.e. $\kappa(x=0, t) = \kappa_0$, and (ii) at 2mm from the coating the drug concentration is null i.e. $\kappa(x=2000, t) = 0$ (Figure 1).

According to these assumptions we estimated the mechanical parameter, $Y(x)$, by solving the evolution equation (eq2) for the control group without drug stimulus. In the following calculations, we further assumed that $Y(x)$ is the same for all groups, which is reasonable since it only represents the stress state. Finally, we calculated the drug stimulus $\Phi_{drug}(\kappa)$ from the bone density at the coating surface, where drug concentrations can be assumed to be constant and equal to that of the coating, for the five different drug concentrations used in the *in vivo* data (Peter, Pioletti *et al.* 2005). The validity of these assumptions is discussed in the last section.

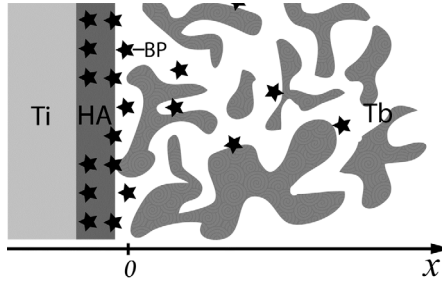


Figure 1. Simplified scheme of the experimental system: the titanium implant (Ti) is coated with a thin layer of hydroxyapatite (HA). Bisphosphonate molecules (stars) initially loaded in the hydroxyapatite coating are slowly released, diffuse in the peri-implant trabecular bone (Tb) and influence the remodeling locally. The bisphosphonate concentration and the bone density are functions of the distance x from the coating.

The bone density was then calculated from the model as a function of the distance from the coating and is represented in Figure 2. As seen in this figure, the theoretical density profiles calculated from the model are very similar to the experimental data. The error between data and model was estimated as the mean relative difference in bone density for $0 < x < 150\mu\text{m}$. The measured errors were smaller than 5% for each BP concentration. Computations were processed with custom-made routines of *Mathematica* (Wolfram Research, USA).

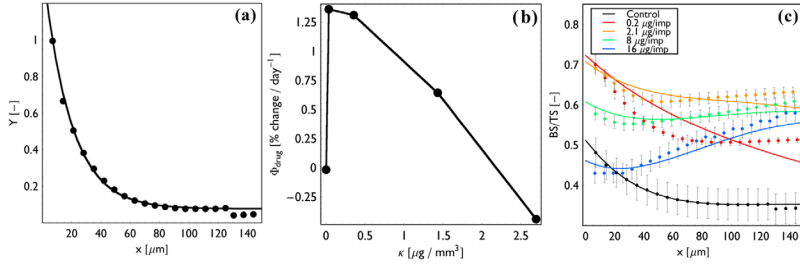


Figure. 2 - **(a)** Shows $Y(x)$ as a function of x as calculated from the data (points) and the continuous interpolation used for numerical computations (line). **(b)** Shows the drug stimulus as a function of drug concentration (points), and the continuous interpolation used for numerical computations (line). **(c)** Shows bone density (BS/TS) as a function of the distance from coating: experimental (points) and model (lines) for the different drug concentrations.

Validation of the model

The verification of the model was done in two steps. First, we evaluated the bisphosphonate dose, which theoretically induces the maximal peri-implant bone density. We refer to this dose as the “optimal dose” in the following pages. In the second step, we verified that this optimal dose induced *in vivo* the maximal peri-implant bone density in a rat model. The *in vivo* methods used in this part were adapted from (Peter, Pioletti *et al.* 2005).

Estimation of the optimal concentration

To calculate the optimal drug dose, we solved the theoretical model, with zoledronate concentration as the variable, to maximize the bone density over a thickness of $100\mu\text{m}$ from the coating:

$$\text{the coating: } \text{Max}_{\kappa} \int_0^{100\mu\text{m}} \phi(x, \kappa) dx, \text{ and we found that } \kappa_{\text{opt}} = 0.044 \mu\text{g}/\text{mm}^3 \text{ corresponding to}$$

$0.3\mu\text{g}/\text{implant}$. With this drug dose we calculated that the average bone density in the $100\mu\text{m}$

proximity of the implant would be BS/TS = 63%, i.e. 2% greater than the highest density measured so far with 2.1 µg/implant.

Implants

Twelve Titanium alloy cylinders (diameter 3 mm; length 5 mm) were plasma-coated with hydroxyapatite and then six implants were soaked in aqueous solutions of $3 \cdot 10^{-6}$ and six implants in $2.25 \cdot 10^{-5}$ mol L⁻¹ of zoledronate (Novartis Pharmaceuticals AG, Switzerland) for 48h. The amount of zoledronate loaded onto the implants was calculated to be respectively 0.3 µg and 2.1 µg.

Rats

Twelve female 6-month-old Wistar rats were used in this experiment. The animals had free access to normal diet. The animals were randomly separated into six different groups representing the two zoledronate doses: 0.3 and 2.1 µg/implant and three time points: 3, 6 and 9 weeks (Table 1). Each rat received one implant in a femoral condyle.

N animals	3w	6w	9w
0.3µg	2	2	2
2.1µg	2	2	2

Table 1 - Number of animal per group

Surgery

The local Ethical Committee for Animal studies of the National Veterinary School of Nantes approved the protocol for the animal experiment. Animals were kept at the Experimental

Surgery Laboratory of the Nantes University according to European Community guidelines for the care and use of laboratory animals (DE86/609/CEE).

Surgical procedures were conducted under general anaesthesia. The implantations were performed at the distal end of the femurs, at the epiphysometaphyseal junction. The lateral condyle was exposed and drilled perpendicularly to the long axis of the femur with two successive bits (2.2 and 2.8 mm in diameter) on a low-speed rotative dental handpiece and under sterile saline irrigation. The implant was then gently inserted into the cavity under digital pressure. Articular and cutaneous tissues were closed in two separate layers. After surgery, all the animals were allowed to move freely in their cages. Animals were killed 3, 6 or 9 weeks after implantation by intracardiac injection of overdosed sodium pentobarbital under general anaesthesia.

Preparation for Imaging

The femoral ends were then immediately dissected, fixed in glutaraldehyde solution, and stored in a 4% paraformaldehyde, 0.1% glutaraldehyde in 0.08 M cacodylate buffer. The sample was dehydrated in a series of alcohol solutions. For the impregnation, the sample was soaked in a mixture of 50% alcohol 1008 and 50% methyl methacrylate MMA (Fluka Chemika, Sigma Aldrich Chemie GmbH, Steinheim, Germany) during 24 h then in pure MMA during 24 h. For the inclusion, the sample was soaked during 2 h under vacuum in a solution containing 90% MMA, 10% dibutylphtalate and 1% benzoyl peroxide (Fluka Chemika), then soaked in the same solution but enhanced by a polymerization activator (N,N-dimethylp-toluidine) (Fluka Chemika). The polymerization took place at -20°C during 48 h. Three to four slices of 300µm thick perpendicular to the implant were cut from each sample, using a Microtome saw 1600 (Leica, Nussloch, Germany) diamond saw.

Scanning Electron Microscopy

The slices were carbon-coated. The samples were then observed in a JEOL JSM 6300 scanning electron microscope (JEOL, Tokyo, Japan) using the backscattered electron detector allowing distinguishing mineralized bone from soft tissue. Then, these images were used to measure the bone density as a function of the distance from the coating. The implant surface and trabecular bone regions were defined manually on each image. To distinguish bone from other tissues: pixels with graylevel between 0 and 62 were considered as calcified bone, while those with graylevel from 63 to 255 were considered as other tissues. We defined successive regions of interests inside the trabecular bone in the form of series of ten 20µm thick arcs co-centered with the implant. In each arc, the number of bone pixels was counted and the bone density was defined as bone pixels divided by total pixels in the arc (BS/TS), using custom algorithms developed with *ImageProcessing* for *Mathematica*.

Statistics

The number of slices per group was accounted for as repetition of the density measurement of the same group. Student-t test was used to determine the statistical significance of the results.

Results

In vivo verification of model's predictions

The model predicted that a drug dose of 0.3 µg/implant maximizes bone density within 100µm layer around the implant. To verify this prediction, bone density was measured *in vivo* with 0.3 µg/implant and 2.1 µg/implant zoledronate at 3, 6 and 9 weeks in rat condyles. These measures were compared to previous measures obtained by Peter *et al.* with 0, 0.2, 2.1, 8 and 16 µg zoledronate/implant from (Peter, Pioletti *et al.* 2005).

One rat in the 3 weeks - 2.1 μg zoledronate group and one rat in the 9weeks-0.3 μg -zoledronate group were excluded from further analysis, as, for unknown reasons, the implant was not integrated into bone. A total of thirty-three slices were analyzed (Table 2).

Number of slices	3w	6w	9w
0.3 μg	6	8	3
2.1 μg	3	6	6

Table 2 - Number of slices for imaging per group

At three weeks, the model's predictions were verified. The mean bone density of the group with optimal zoledronate dose was 4% greater than the highest bone density obtained so far in our previously published results (Figure 3a), however this difference of density with the 2.1 μg group was not significant ($p=0.09$). The mean bone density with 2.1 μg zoledronate / implant was in the range of our previous data. The difference in bone density between the 0.3 μg /implant group and the 2.1 μg /implant group observed at 3 weeks, was no longer observed at 6 and 9 weeks (Figure 3b).

Evolution of the integration of the implant

The SEM observations confirmed implant integration comparable to that previously described (Fig. 4a). The hydroxyapatite coating evolved at the different time points after implantation. At 3 weeks, the bone was in contact with the coating surface, but there were no signs of resorption in the coating and almost no bone entering the coating (Fig. 4b). At 6 weeks, the first signs of resorption appeared in the coating. Approximately half of the thickness of the coating had been resorbed and lacunae could be observed *in* the coating (Fig. 4c). At 9 weeks,

most of the coating had been resorbed and newly formed bone was in contact with the titanium surface. Lacunae were still present inside the coating and some speckles of bone grew directly from the implant surface (Fig. 4d).

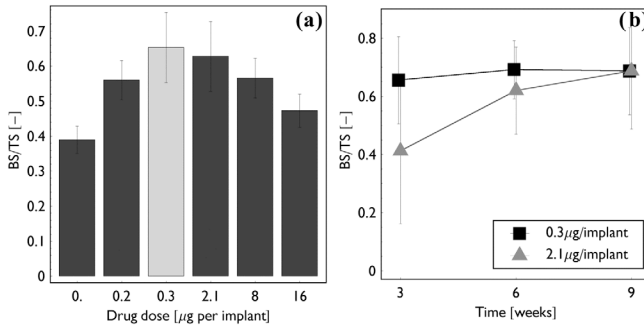


Figure 3 - (a) Mean peri-bone density (BS/TS) in the first 100 μm layer. The dark bars were adapted from (Peter et al.) the light bar represents the group with 0.3 μg /implant zoledronate. (b) Evolution of mean bone density (BS/TS) at 3 6 and 9 weeks post-op.

Discussion

The principal aims of this projects were first, to develop a theoretical framework of bone remodeling influenced by local release of bisphosphonate; second, to identify the numerical parameters of the model and third, to verify the model's predictions *in vivo*.

The development of the model consisted of adding the drug concentration as a new internal variable to an existing model of remodeling, completed by a function relating the drug concentration to the remodeling stimulus. The parameters appearing in this new model were identified from our previously published experimental data (Peter, et al., 2005). Next we solved this model to predict that a dose of 0.3 μg of zoledronate grafted on the implant coating

would maximize the peri-implant bone density. This prediction was finally confirmed experimentally: with this calculated dose, the bone density was maximal, compared to other doses, at 3, 6 and 9 weeks post-op.

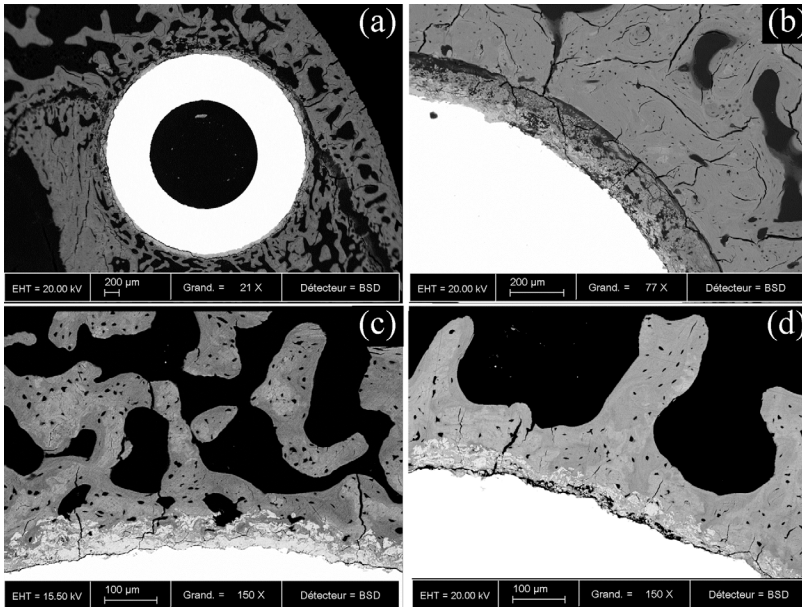


Figure 4 - SEM pictures of implanted condyles: panel (a) shows the bone structure of a condyle implanted with HA-coated implant containing 2.1µg zoledronate at 3 weeks. The implant integration is qualitatively similar to previously published results. Panel (b) shows a detail of the bone-coating interface at 3 weeks. Bone is not yet entering the coating. Panel (c) shows the interface at 6 weeks with the first signs of coating resorption, and panel (d) shows the interface at 9 weeks with more than 50% of the coating resorbed.

The intensity of the effect of bisphosphonate is dose dependent. The theoretical framework developed here shows that the interpretation of bone density profiles has to take into account the mechanical situation, the drug diffusion and the effect of drug on the remodeling balance, modeled here by the drug stimulus Φ_{drug} .

The drug stimulus function is the key point of the model. It can be interpreted as the signature of the drug in a particular animal model. The shape of this function reflects that the drug induces the imbalance of the remodeling process after the decrease of osteoclast activity. The shape of the function is concordant with what is observed *in vitro*: bisphosphonates, like most drugs, have a range of concentration with beneficial effects but can produce adverse effects at higher doses (Fleisch, 2002).

The model presented here is based on several hypotheses, which were consistent with the experimental situation addressed. We assumed that the model of a cylindrical implant could be reduced to a one-dimensional geometry. This assumption is relevant in our situation as we analyzed only the average density of a very thin layer of bone and we were not interested in histomorphometry aspects. Moreover the analyzed slices were not taken from the extremities of the implants, which are in the cortical regions of the condyles.

We identified from experimental data that the loading function $Y(x)$ increased significantly near the implant surface. This certainly reflects the mechanical stress following press-fit insertion and spring-back effect of bone (Kold, et al., 2003). With a different surgical protocol, the stress distribution would certainly be different, and $Y(x)$ would have to be re-calculated.

In the resolution of our model, we simplified the boundary conditions: we set the coating as an infinite source of drug at constant concentration. The relevance of this assumption for short-term studies was confirmed by the SEM observations: at three weeks, the coating was

indeed not significantly resorbed. It was probably still protected from osteoclastic resorption by its content in bisphosphonate. This is concordant with the very low release rate of zoledronate by hydroxyapatite (Roussiere, Montavon *et al.* 2005). However, this simplifying assumption cannot be used for long-term studies: we observed that the hydroxyapatite coating was partially degraded at 6 weeks, and this degradation continued at 9 weeks. The bisphosphonate concentration in the coating then certainly decreases significantly after 3 weeks. With the second boundary condition, we assumed that the drug concentration is negligible at 2mm from the implant surface, which corresponds to the growth plate and the bone marrow. Since these tissues are well perfused, the drug is certainly diluted into the blood volume.

The observed degradation of the coating at 6 and 9 weeks, and the lacunae in resorbed areas might reflect the presence of osteocytes in the newly formed bone-implant interface. This is a sign of good implant integration at mid- and long-term post-op with the optimal zoledronate concentration. However, more histology would be needed to confirm this observation.

Our results are certainly dependent on the choice of the drug and on the animal model. In the present study, we determined the drug stimulus function for zoledronate in rats. To extend the model predictions to other active molecules or other animals, the first step would be to determine the drug stimulus function, which we called the drug signature, with the specific drug using the specific animal model. To our knowledge, none of the required data for such identification with other animals or with different drugs has been published.

Only a limited number of animals were used in the experimental part of this project. The main objective of this project was to compare the theoretical model's outcomes to an *in vivo*

situation. The experiments were therefore designed to validate the model rather than to provide new statistically significant experimental results, which would have required a much larger number of animals.

The principal objective of coating implants with bisphosphonate for local delivery is to increase the fixation of the implant. The pullout force is somehow related to peri-implant bone density (Peter, *et al.*, 2005), but other factors, such as bone quality, also have an influence. A mathematical relationship between histomorphometry of bone and its mechanical capacity to resist pullout has yet to be determined (Jakobsen, *et al.*, 2006). Thus, the mathematical model presented here only predicts bone density. More work will be needed to link bone density to implant fixation strength.

One of the most important challenges associated to orthopaedic implants is to obtain sufficient early fixation to ensure long-term stability, for patients of variable age, daily activity level or bone quality. Although several studies have shown that implants delivering bisphosphonate improve this fixation, the bisphosphonate molecule, the dose, or the animal model have always been chosen empirically. The theoretical framework presented here could be of great interest to further analyze and compare the different experimental results.

Moreover such comparisons would be particularly helpful to design future animal or clinical studies. In the long term, mathematical framework could be necessary to design optimal orthopaedic implants.

Acknowledgements

Project no. 04-P2 was supported by the AO Research Fund of the AO Foundation, Davos, Switzerland.

We thank B. Bujoli for the preparation of the implants, Sophie Salice for her help with the sample preparation, Paul Pilet for the electronic microscopy and Tyler Thacher for English editing.

References

Dhert, W.J.A., Thomsen, P., Blomgren, A.K., Esposito, M., Ericson, L.E., Verbout, A.J., 1998. Integration of press-fit implants in cortical bone: A study on interface kinetics. *Journal of Biomedical Materials Research* 41, 574-583.

Eberhardt, C., Habermann, B., Muller, S., Schwarz, M., Bauss, F., Kurth, A.H., 2007. The bisphosphonate ibandronate accelerates osseointegration of hydroxyapatite-coated cementless implants in an animal model. *J Orthop Sci* 12, 61-66.

Fleisch, H., 2002. Development of bisphosphonates. *Breast Cancer Research* 4, 30-34.

Hilding, M., Aspenberg, P., 2006. Postoperative clodronate decreases prosthetic migration: 4-year follow-up of a randomized radiostereometric study of 50 total knee patients. *Acta Orthop* 77, 912-916.

Horowitz, S.M., Gonzales, J.B., 1996. Inflammatory response to implant particulates in a macrophage/osteoblast coculture model. *Calcified Tissue International* 59, 392-396.

Huiskes, R., 1997. Validation of Adaptive Bone-modeling Simulation Models. In: G., L., al., e. (Eds.), *Bone Research in Biomechanics*. IOS Press, pp. 33--48.

Jakobsen, T., Kold, S., Bechtold, J.E., Elmengaard, B., Soballe, K., 2006. Effect of topical alendronate treatment on fixation of implants inserted with bone compaction. *Clinical Orthopaedics and Related Research*, 229-234.

Jakobsen, T., Kold, S., Bechtold, J.E., Elmengaard, B., Soballe, K., 2007. Local alendronate increases fixation of implants inserted with bone compaction: 12-week canine study. *Journal of Orthopaedic Research* 25, 432-441.

Jensen, T.B., Bechtold, J.E., Chen, X.Q., Soballe, K., 2007. Systemic alendronate treatment improves fixation of press-fit implants: A canine study using nonloaded implants. *Journal of Orthopaedic Research* 25, 772-778.

Kold, S., Bechtold, J.E., Ding, M., Chareancholvanich, K., Rahbek, O., Soballe, K., 2003. Compacted cancellous bone has a spring-back effect. *Acta Orthop Scand* 74, 591-595.

Peter, B., 2004. Orthopedic implants used as drug delivery systems: numerical, in vitro and in vivo studies. *Ecole Polytechnique Fédérale de Lausanne, Lausanne*.

Peter, B., Pioletti, D.P., Laib, S., Bujoli, B., Pilet, P., Janvier, P., Guicheux, J., Zambelli, P.Y., Bouler, J.M., Gauthier, O., 2005. Calcium phosphate drug delivery system: influence of local zoledronate release on bone implant osteointegration. *Bone* 36, 52-60.

Rakotomanana, R.L., Leyvraz, P.F., Curnier, A., Heegaard, J.H., Rubin, P.J., 1992. A finite element model for evaluation of tibial prosthesis-bone interface in total knee replacement. *J Biomech* 25, 1413-1424.

Stadelmann, V.A., Terrier, A., Pioletti, D.P., 2007. Microstimulation at the bone-implant interface upregulates osteoclast activation pathways. *Bone*, 358--364.

Terrier, A., Miyagaki, J., Fujie, H., Hayashi, K., Rakotomanana, L., 2005. Delay of intracortical bone remodelling following a stress change: a theoretical and experimental study. Clin Biomech (Bristol, Avon) 20, 998-1006.

Venesmaa, P.K., Kroger, H.P.J., Miettinen, H.J.A., Jurvelin, J.S., Suomalainen, O.T., Alhava, E.M., 2001. Monitoring of periprosthetic BMD after uncemented total hip arthroplasty with dual-energy X-ray absorptiometry - a 3-year follow-up study. Journal of Bone and Mineral Research 16, 1056-1061.

Wermelin, K., Tengvall, P., Aspenberg, P., 2007. Surface-bound bisphosphonates enhance screw fixation in rats - increasing effect up to 8 weeks after insertion. Acta Orthopaedica 78, 385-392.

6 Paper 3: Implants delivering bisphosphonate locally increase periprosthetic bone density in an osteoporotic sheep model. Pilot Study

Vincent A. Stadelmann¹, O. Gauthier², Alexandre Terrier¹, J-M. Boulter², Dominique Pioletti^{1*}

¹Laboratory of Biomechanical Orthopedics EPFL-DAL, IBI, Ecole Polytechnique Fédérale de Lausanne, Switzerland

²Laboratoire de Recherche sur les Matériaux d'Intérêt Biologique INSERM 99-03, Faculté de Chirurgie Dentaire, Nantes, France

Accepted in European Cells & Materials Journal

*Corresponding author:

Dominique P. Pioletti, Ph.D.

Laboratory of Biomechanical Orthopedics EPFL-DAL

Bat AI – Station 15

EPFL

1015 Lausanne

Switzerland

Tel: +41 21 693 83 41

Fax: +41 21 693 86 60

Email: dominique.pioletti@epfl.ch

Abstract

It is a clinical challenge to obtain a sufficient orthopedic implant fixation in weak osteoporotic bone. When the primary implant fixation is poor, micromotions occur at the bone-implant interface, activating osteoclasts, which leads to implant loosening. Bisphosphonate can be used to prevent the osteoclastic response, but when administered systemically its bioavailability is low and the time it takes for the drug to reach the periprosthetic bone may be a limiting factor. Recent data has shown that delivering bisphosphonate locally from the implant surface could be an interesting solution. Local bisphosphonate delivery increased periprosthetic bone density, which leads to a stronger implant fixation, as demonstrated in rats by the increased implant pullout force. The aim of the present study was to verify the positive effect on periprosthetic bone remodeling of local bisphosphonate delivery in an osteoporotic sheep model. Four implants coated with zoledronate and two control implants were inserted in the femoral condyle of ovariectomized sheep for 4 weeks. The bone at the implant surface was 50% higher in the zoledronate-group compared to control group. This effect was significant up to a distance of 400µm from the implant surface. The presented results are similar to what was observed in the osteoporotic rat model, this suggests that the concept of releasing zoledronate locally from the implant to increase the implant fixation is not species specific. The results of this trial study support the claim that local zoledronate could increase the fixation of an implant in weak bone.

Introduction

A current clinical challenge in the field of Orthopedics is to obtain a stable implant fixation in weak osteoporotic bone. The fixation of orthopedic implants in bone relies strongly upon the initial stability of the implant. When the initial stability is not achieved, micromotions occur at the bone implant interface (Mandell *et al.*, 2004; Ramaniraka *et al.*, 2000). The micromotions then activate an osteoclastic response (Stadelmann *et al.*, 2008), which results in periprosthetic osteolysis and later implant migration and wear (Karrholm *et al.*, 1994). Both particulate formation from implant wear and implant migration have been shown to be associated with increased implant failure rate (Clarke *et al.*, 1992; Horikoshi *et al.*, 1994). In the case of osteoporotic patients, this early phase is particularly delicate as the bone is already weak at the time of surgery. In this case, the resorption of a small amount of bone near the implant may induce a dramatic decrease in early fixation, accelerating the failure process.

Bisphosphonate can be used to reduce periprosthetic osteolysis allowing orthopedic implants to achieve a stronger primary fixation (Hilding *et al.*, 2000). Bisphosphonate molecules inhibit osteoclastic activity, and therefore are widely used to treat patients with osteoporosis (Bone *et al.*, 2004; Fleisch, 2002). However, when administered orally, the bioavailability of bisphosphonate is generally very low, and its local delivery can be further delayed in regions of the skeleton with low blood perfusion, for example the femoral neck. Recent clinical studies have shown that systemic bisphosphonate treatment following prosthesis implantation reduced periprosthetic bone loss only after 3 months (Nehme *et al.*, 2003; Venesmaa *et al.*, 2001b), while significant bone loss arises during this initial period of 3 months (Venesmaa *et al.*, 2001a). A solution to accelerate the local availability of bisphosphonate at the implant location is to deliver the drug locally. This insures the immediate presence of drug molecules at the implant location regardless of the local blood perfusion.

Implants with local delivery of bisphosphonate have been studied previously in small animal models and the results are generally encouraging: In rats, hydroxyapatite coated implants releasing zoledronate increased periprosthetic bone density and the pullout force (Peter *et al.*, 2005); fibrin coated cortical screws releasing ibandronate and pamidronate increased the pullout force (Wermelin *et al.*, 2007). Moreover, in dog ulna, Tanzer et al. showed that local elution of zoledronate can cause substantial bone augmentation around and within porous tantalum implants (Tanzer *et al.*, 2005). Concerning the osteoporotic bone case, hydroxyapatite coated implants releasing zoledronate increased pullout force and periprosthetic bone density, compared to control implants in osteoporotic rats (Peter *et al.*, 2006).

Many differences, such as mineral density, healing capacity or the response to mechanical stimuli, exist in the bone metabolism of small animals when compared to that of humans (Egermann *et al.*, 2005; Holy *et al.*, 2000). Therefore it is questionable to extrapolate the *in vivo* results of small animals into the specific clinical situation of osteoporotic patients without pre-clinical tests in a large animal (Buma *et al.*, 2004). To our knowledge, no data exists concerning local delivery of bisphosphonate to increased fixation strength of an implant in a large osteoporotic animal model.

Therefore the aim of the present study was to verify the efficacy of local bisphosphonate delivery to increase the periprosthetic bone density in an osteoporotic sheep model (Turner, 2002).

Material and Methods

Implants

Six Titanium alloy (TA6V) cylinders (diameter 3 mm; length 5 mm) were plasma-coated with hydroxyapatite (thickness: 20 μm ; crystallinity index 62%). Two samples were used as controls, while the remaining 4 samples were soaked for 48h in 5ml ultrapure water solutions

of $2.25 \cdot 10^{-5} \text{ mol L}^{-1}$ of Zoledronate (1-hydroxy-2-[(1H-imidazole-1-yl)ethylidene] 1-bisphosphonic acid disodium salt) supplied by Novartis Pharmaceuticals AG, Switzerland. The amount of zoledronate loaded onto the implants was calculated to be 2.1 μg for each implant (Josse *et al.*, 2004).

Animals and surgical procedures

Animal handling and surgical procedures were conducted according to the European Community Guidelines for the care and use of laboratory animals (DE 86/609/CEE) and approved by the local ethical committee at the Nantes Veterinary School. Three adult female vendéen sheep with an average body weight of 55 kg were used in this study. Six months prior to the study, animals had been neutered by ovariectomy to induce osteoporosis. Subsequent bone changes were investigated on iliac crest bone biopsies. A control biopsy was harvested on the day of ovariectomy and was compared with a bone sample from the contralateral iliac crest harvested 6 months later on the day of implantation. Changes in the microarchitecture of iliac crest biopsies were investigated through 3D microtomography analysis.

The tested cylinders were implanted bilaterally for 4 weeks at the distal femoral end of the 3 mature female sheep. The first animal had two control implants. The second and third animals had two zoledronate coated implants. After 2 weeks of acclimatization, general anesthesia was induced using an intravenous injection of 4 mg/kg of propofol (Rapinovel[®], Shering-Plough, France) and 0.1 mg/kg of diazepam (Valium[®], Roche, France). Anesthesia was maintained for surgery with a gas mixture of isoflurane (1.5 %), and oxygen (98.5 %). A single dose of morphine (0.5 mg/kg) was injected subcutaneously at the beginning of the surgery as an analgesic. After shaving and disinfection (Vetidine[®], Vetoquinol, Lure,

France) of the knee, a stifle arthrotomy was performed to expose the distal lateral condyle of the femur.

A cylindrical osseous defect (3 mm in diameter and 6 mm length) was created on the distal femoral epiphysis using a motor-driven drill (Aesculap, Tuttlingen, Germany). After saline irrigation, the osseous cavity was carefully dried and filled with the coated cylinder.

The joint capsule was closed with non-absorbable sutures (Prolene® 2-0, Ethicon, France). The subcutaneous tissues and skin were closed in different layers using absorbable sutures (Polysorb® 2-0, TycoHealthcare, France). Finally, the surgical wound was covered with an adhesive bandage. Both hind limbs were operated, giving 2 tested implants per animal. At the end of surgery, animals received an injection of meloxicam to complete analgesia (Métacam Bovin®, Boehringer Ingelheim, Germany) but did not receive any postoperative antibiotics. The procedure was repeated on the contra lateral side.

After 4 weeks, general anesthesia was induced by a mixed injection of ketamine (Imalgène®1000, Merial, France) and xylazine (Rompun®, Bayer, France) and the animals were euthanized by intravenous injection of 20 ml of pentobarbital (Doléthol®, Vétoquinol S.A., France) through a catheter placed into the jugular vein. The femoral extremities were then dissected from the surrounding soft tissues and immediately placed in a 10 % neutral formol solution.

Preparation for imaging

The femoral distal ends were then immediately dissected, fixed in glutaraldehyde solution, and stored in a 4% paraformaldehyde, 0.1% glutaraldehyde in 0.08 M cacodylate buffer. Using a handsaw, the condyle was sawed off 1 cm above the implant. The sample was dehydrated in a series of alcohol solutions. The first impregnation step was to soak the sample in a mixture of 50% alcohol 1008 and 50% methyl methacrylate MMA (Fluka Chemika,

Sigma Aldrich Chemie GmbH, Steinheim, Germany) during 24 hours. The second impregnation step was to soak the sample in pure MMA during 24 hours. The first inclusion step was to soak the dehydrated sample during 2 hours under vacuum in a solution containing 90% MMA, 10% dibutylphthalate (Fluka Chemika) and 1% benzoyl peroxide (Fluka Chemika). The sample was then removed from the solution and soaked in the same solution but enhanced by a polymerization activator (N,N-dimethylp-toluidine) (Fluka Chemika). The polymerization took place at -20°C and was complete after 48 hours. Two to four slices of 300µm thick were cut from each sample, using a Microtome 1600 (Leica, Nussloch, Germany) diamond saw. The cutting plane was perpendicular to the implant.

Scanning Electron Microscopy

Slices were carbon-coated and observed using a JEOL JSM 6300 scanning electron microscope (SEM) (JEOL, Tokyo, Japan) using the backscattered electron detector, allowing mineralized bone to be distinguished from soft tissue.

Then, SEM images were used to measure the bone density as a function of the distance from the coating. The implant surface and trabecular bone regions were defined manually on each image. The implant center and radius were then calculated by least square fitting of a circle onto the implant surface. A threshold was applied to the image in order to distinct bone from other tissues: pixels with a graylevel between 0 and 62 were considered as calcified bone, while those with a graylevel from 63 to 255 were considered as other tissues. We defined successive regions of interests inside the trabecular bone in the form of series of ten 20µm thick arcs co-centered with the implant. In each arc, the number of bone pixels was counted and the bone surface fraction ($B.Ar/T.Ar$) was defined as bone pixels divided by total pixels in the arc, using custom algorithms developed with *Image Processing for Mathematica* (Figure 1).

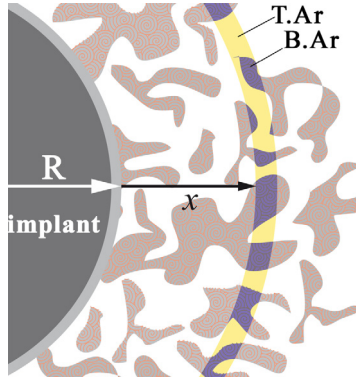


Figure 1: Schematic of the method used to determine the bone surface fraction profile. At a distance x from the coating surface, a region of interest (ROI) was defined as an annulus of $20\mu\text{m}$ thickness co-centered with the implant of radius $R+x$, where R is the implant radius. Then the number of bone pixels inside the ROI (blue pixels) was divided by the total number of pixels in the ROI (blue+yellow pixels). The distance x was incremented from 0 to 1mm in steps of $20\mu\text{m}$.

Statistics

The number of slices per group was accounted for as repetition of the density measurement of the same group. Student-t test was used to determine the statistical significance of the results. Wilcoxon test was used to identify the significant changes of microstructural properties in the iliac crest biopsies.

Results

A total of 19 slices (6 control, 13 zoledronate-loaded) were processed (Table 1).

	Control	Zoledronate
Sheep	1	2
Implants	2	4
Slices	6	13

Table 1: Number of animals, implants and slices per group

Osteoporosis induction

Significant microstructural evolutions were measured on the iliac crest biopsies (Figure 2). The bone volume fraction (BV/TV) decreased by 30% at six months post-ovariectomy. While trabecular thickness (Tb.Th), trabecular number (Tb.N) and trabecular separation (Tb.Sp) decreased by 11%, 19%, and increased by 14% respectively; the structural model index (SMI) was not significantly affected (Table 2).

Implant integration

The implant integration was verified qualitatively during backscattered electron microscopy imaging. We observed homogenous bone-implant contact as well as new bone formation along the coating surface. Lacunae were observed in the bone speckles growing from the coating. Different levels of mineralization were observed in the newly formed bone. The coating was partially resorbed, and new bone was observed in the resorption zones (Figure 3).

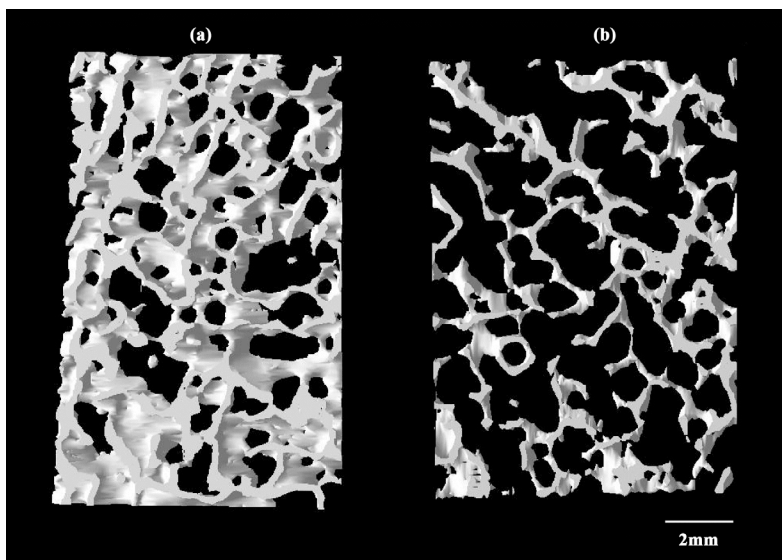


Figure 2: Three-dimensional microtomographic description of iliac crest biopsies microarchitecture (a) before ovariectomy and (b) 6 months after ovariectomy. The difference illustrates the induction of osteoporosis.

	<i>Control</i>	<i>OVX</i>	<i>Evolution (%)</i>
BV/TV (%)	19.0 ± 3.3	13,3 ± 1.3	-30
Tb.Th (μm)	144.1 ± 15.8	128,0 ± 11.1	-11
Tb.N (10 ⁻³ /μm)	1.32 ± 0.14	1,07 ± 0.15	-19
Tb.Sp (μm)	683 ± 56	783 ± 66	+14
SMI	0,86 ± 0.23	0,90 ± 0.18	

Table 2: Microstructure data of iliac crests biopsies obtained before ovariectomy (Control) and the day of implantation (OVX), data as Mean±SD. The evolution column shows significant changes ($p < 0.05$). The relative evolution of bone architecture parameters emphasise osteoporosis induction.

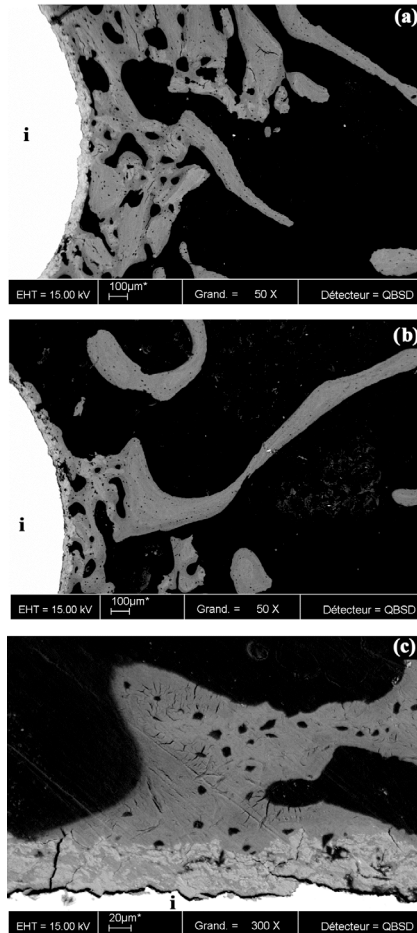


Figure 3: SEM pictures of three slices at magnifications of 50 \times (a, b) and 300 \times (b). (a) Local bone structure of a condyle implanted with an HA-coated implant (**i**) containing 2.1 μ g zoledronate. (b) Local bone structure of a condyle implanted with a control implant (**i**). (c) Details of the osseointegration of a zoledronate-implant (**i**) shows bone growth into resorbed spaces of the coating. Osseointegration in control implants was qualitatively similar.

Bone surface fraction

The bone surface fraction (B.Ar/T.Ar) in a 20 μ m-thick layer around the implant was 50% higher in the zoledronate group compared to the control group (B.Ar/T.Ar=0.45 \pm 0.08 for the zoledronate group, 0.30 \pm 0.07 for the control group, $p<0.05$). B.Ar/T.Ar of the zoledronate group decreased from 0.45 \pm 0.08 at the coating surface to 0.30 \pm 0.05 at 800 μ m from the coating, while the profile of the control group was almost constant (figure 4a). The difference between B.Ar/T.Ar of the zoledronate group and the control group was significant up to 400 μ m from the coating (figure 4b). The total bone area (B.Ar) in 400 μ m-thick layer around the implant was 10% greater in zoledronate group compared to control group ($p<0.05$) (figure 4c).

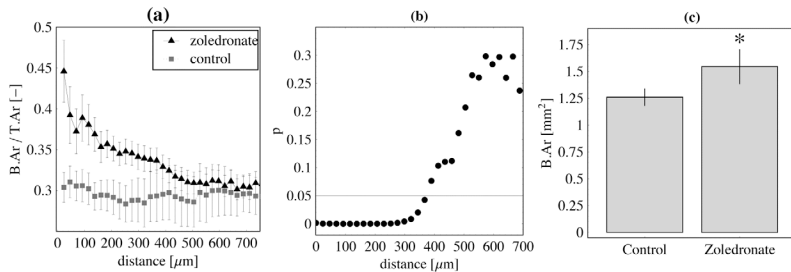


Figure 4: **(a)** Bone surface fraction (Mean \pm SEM) as a function of the distance from the implant coating. **(b)** Student test's p -value of B.Ar/T.Ar comparison between zoledronate-group and control-group as a function of the distance from the coating: the effect of local zoledronate is significant up to 400 μ m from the coating. **(c)** Total periprosthetic bone surface in a 400 μ m thick layer around the implant for zoledronate group and control group (Mean \pm SD, *: $P<0.05$ compared to control, SD were calculated from the number of slices per group which were accounted for as repetition of the density measurement of the same group).

Discussion

Implants locally delivering bisphosphonate have been shown to increase periprosthetic bone density and pullout forces in previous studies using rat models (Kajiwara *et al.*, 2005; Wermelin *et al.*, 2007). However the bone metabolism of healing and remodeling in rats is different than in humans (Buma *et al.*, 2004; Egermann *et al.*, 2005). Therefore a large animal study was necessary to validate these results for later applications to human patients with osteoporotic bone. In this study, our aim was to use the osteoporotic sheep model to verify the efficacy of locally delivering zoledronate from an orthopedic implant to increase the periprosthetic bone density.

Our results showed that B.Ar/T.Ar in a 20µm layer was increased by 50% in the locally delivered-zoledronate group compared to the control group in osteoporotic sheep. The effect of local delivery of zoledronate on B.Ar/T.Ar was significant up to 400µm distance from the implant. The mean B.Ar/T.Ar in the 400µm region around the implant was increased by 10% in the zoledronate-group compared to the control group.

The implant and dose of zoledronate used in the sheep condyles are identical to those implanted for three weeks in previous rat and OVX rat models (Peter *et al.*, 2006; Peter *et al.*, 2005). The experimental timeline for the sheep was chosen to be four weeks as to compensate for the possibility of a slower remodeling rate in larger animals. When the results of these different models were compared (Table 3), we observed: In non-osteoporotic rats, zoledronate coated implants induced an increase of 43% of B.Ar/T.Ar at the implant surface, while in osteoporotic rats the increase was 20% at 3 weeks post-surgery. In the present osteoporotic sheep model, at 4 weeks post-surgery, we observed an increase of 50%, which is significantly greater than the effect in rats. Moreover, the distance from the implant over which the effect of zoledronate is significant is five times greater in osteoporotic sheep than in osteoporotic rats.

	B.Ar/T.Ar Control	B.Ar/T.Ar Zoledronate	Relative Increase	Distance of the effect
Rats	0.48±0.04	0.69±0.03	43%	250µm
OVX rats	0.46±0.03	0.55±0.03	20%	70µm
OVX sheep	0.30±0.07	0.45±0.08	50%	400µm

Table 3: Comparison of the effect of 2.1µg zoledronate / implant versus control on periprosthetic B.Ar/T.Ar in a 20µm layer, and distance of the effect from the implant. Rats and osteoporotic rats data adapted from (Peter et al., 2005) and (Peter et al., 2006) respectively.

The observed difference cannot be explained simply with this data. It can be related to prolongation of one week in the post-surgery delay, to an enhanced reaction of sheep bone cells to zoledronate, or to the initial difference in bone density. Despite the questions that remain unanswered, these results show that a small dose of zoledronate delivered locally in osteoporotic sheep bone efficiently increases periprosthetic bone density in a way similar to what was previously observed in rats.

This result is concordant with the very recent study of Goodship et al., in which intravenous administration of zoledronate pre- peri- and postsurgery reduced periprosthetic cortical osteopenia in a sheep model of hip replacement (Goodship et al., 2008). Therefore, zoledronate treatments seem to have a benefic action on periprosthetic bone, cortical or trabecular.

The goal of local bisphosphonate release is to increase the implant fixation strength, but a complete pullout study would have required supplementary animals. Pullout force is mainly influenced by bone density in a thin layer of bone, extending 20µm radially from the implant (Peter et al., 2005). In osteoporotic rats an increase of 20% of bone volume fraction in the 20µm layer induced nearly a 100% increase in pullout force (175±70N with 2.1µg compared

to 90 ± 30 N for controls). However, the exact effect on pullout force in the sheep model cannot be calculated from rat models, as the scale of bone trabeculae and the bone density are very different in these species. But, with more than 2-fold increase in bone volume fraction in the 20 μ m layer, it is likely that an increase in pullout force would be observed as well in the present study.

Zoledronate, like other bisphosphonates, has been shown to limit bone loss in patients with osteoporosis (Glatt, 2001), while also inducing a beneficial impact on microarchitectural properties of trabecular bone (Poole *et al.*, 2007; Recker *et al.*, 2008). In the present study we did not assess other microarchitectural properties of periprosthetic bone than B.Ar/T.Ar. However some of these properties, such as the bone volume fraction are mathematically linked to B.Ar/T.Ar (Parfitt *et al.*, 1987; Revell, 1983).

Clinical relevance of the study

The clinical aim of coating orthopedic implants with zoledronate is to improve the fixation of orthopedic implants in patients with weak bone. Benefits of zoledronate local delivery were previously observed in osteoporotic rats. The present study further extended these results to a large animal model. The measured increase of periprosthetic bone density supported that local zoledronate delivery significantly improves the implant fixation in osteoporotic sheep.

To further validate the use of implants with local zoledronate delivery, the next set of experiments should be performed with full load bearing implants to quantify the combined effects of mechanical stimulus and zoledronate release to the response of periprosthetic bone.

Acknowledgements

Project no. 04-P2 was supported by the AO Research Fund of the AO Foundation, (Davos, Switzerland). We thank Novartis Pharma Research (Basel, Switzerland) for a generous gift of Zoledronate. We thank Bruno Bujoli, Sophie Salice and Paul Pilet for technical assistance and Tyler Thacher for English editing.

References

- Bone, H. G., D. Hosking, et al. (2004). "Ten years' experience with alendronate for osteoporosis in postmenopausal women." N Engl J Med **350**(12): 1189-99.
- Buma, P., W. Schreurs, et al. (2004). "Skeletal tissue engineering - from in vitro studies to large animal models." Biomaterials **25**(9): 1487-1495.
- Clarke, I. C., P. Campbell, et al. (1992). Debris-mediated osteolysis-A cascade phenomenon involving motion, wear, particulates, macrophage induction, and bone lysis. Particulate debris from medical implants: mechanisms of formation and biological consequences, ASTM STP 1144. K. R. St. John. Philadelphia, American Society for testing and materials: 7-26.
- Egermann, M., J. Goldhahn, et al. (2005). "Animal models for fracture treatment in osteoporosis." Osteoporos Int **16**: S129–S138.
- Fleisch, H. (2002). "Development of bisphosphonates." Breast Cancer Research **4**(1): 30-34.
- Glatt, M. (2001). "The bisphosphonate zoledronate prevents vertebral bone loss in mature estrogen-deficient rats as assessed by micro-computed tomography." Eur Cell Mater **1**: 18-26.
- Hilding, M., L. Ryd, et al. (2000). "Clodronate prevents prosthetic migration: a randomized radiostereometric study of 50 total knee patients." Acta Orthop Scand **71**(6): 553-7.
- Holy, C., J. Fialkov, et al. (2000). In vivo models for bone tissue-engineering constructs. Bone engineering. J. Davies. Toronto, em squared inc: 496-504.

Horikoshi, M., W. Macaulay, et al. (1994). "Comparison of interface membranes obtained from failed cemented and cementless hip and knee prostheses." Clin Orthop Relat Res(309): 69-87.

Josse, S., C. Fauchoux, et al. (2004). "Chemically modified calcium phosphates as novel materials for bisphosphonate delivery." Advanced Materials **16**(16): 1423-+.

Kajiwar, H., T. Yamaza, et al. (2005). "The bisphosphonate pamidronate on the surface of titanium stimulates bone formation around tibial implants in rats." Biomaterials **26**(6): 581-7.

Karrholm, J., B. Borssen, et al. (1994). "Does early micromotion of femoral stem prostheses matter? 4-7-year stereoradiographic follow-up of 84 cemented prostheses." J Bone Joint Surg Br **76**(6): 912-7.

Mandell, J. A., D. R. Carter, et al. (2004). "A conical-collared intramedullary stem can improve stress transfer and limit micromotion." Clin Biomech (Bristol, Avon) **19**(7): 695-703.

Nehme, A., G. Maalouf, et al. (2003). "Effect of alendronate on periprosthetic bone loss after cemented primary total hip arthroplasty: a prospective randomized study." Revue De Chirurgie Orthopedique Et Reparatrice De L Appareil Moteur **89**(7): 593-598.

Parfitt, A. M., M. K. Drezner, et al. (1987). "Bone histomorphometry: standardization of nomenclature, symbols, and units. Report of the ASBMR Histomorphometry Nomenclature Committee." J Bone Miner Res **2**(6): 595-610.

Peter, B., O. Gauthier, et al. (2006). "Local delivery of bisphosphonate from coated orthopedic implants increases implants mechanical stability in osteoporotic rats." J Biomed Mater Res A **76**(1): 133-43.

Peter, B., D. P. Pioletti, et al. (2005). "Calcium phosphate drug delivery system: influence of local zoledronate release on bone implant osteointegration." Bone **36**(1): 52-60.

Poole, K. E. S., N. Loveridge, et al. (2007). "The effects of zoledronate on iliac bone remodelling in stroke patients." Journal of Bone and Mineral Research **22**(7): 1138-1139.

Ramaniraka, N. A., L. R. Rakotomanana, et al. (2000). "The fixation of the cemented femoral component. Effects of stem stiffness, cement thickness and roughness of the cement-bone surface." J Bone Joint Surg Br **82**(2): 297-303.

Recker, R. R., P. D. Delmas, et al. (2008). "Effects of intravenous zoledronic acid once yearly on bone remodeling and bone structure." Journal of Bone and Mineral Research **23**(1): 6-16.

Revell, P. A. (1983). "Histomorphometry of Bone." Journal of Clinical Pathology **36**(12): 1323-1331.

Stadelmann, V. A., A. Terrier, et al. (2007). "Microstimulation at the bone-implant interface upregulates osteoclast activation pathways." Bone: 358--364.

Turner, A. S. (2002). "The sheep as a model for osteoporosis in humans." Vet J **163**(3): 232-9.

Venesmaa, P. K., H. P. J. Kroger, et al. (2001). "Alendronate reduces periprosthetic bone loss after uncemented primary total hip arthroplasty: A prospective randomized study." Journal of Bone and Mineral Research **16**(11): 2126-2131.

Venesmaa, P. K., H. P. J. Kroger, et al. (2001). "Monitoring of periprosthetic BMD after uncemented total hip arthroplasty with dual-energy X-ray absorptiometry - a 3-year follow-up study." Journal of Bone and Mineral Research **16**(6): 1056-1061.

Wermelin, K., P. Tengvall, et al. (2007). "Surface-bound bisphosphonates enhance screw fixation in rats - increasing effect up to 8 weeks after insertion." Acta Orthopaedica **78**(3): 385-392.

Discussion with reviewers

Reviewers: In the absence of extensive clinical data, the relative practical benefits of local versus systemic bisphosphonate delivery are still debatable. Whilst local delivery from a coated implant may reduce the risk of side effects, a patient requiring an implant is likely to have osteoporosis at other sites and would thus benefit from systemic drug exposure. Moreover, after a surgical intervention to implant a prosthesis, the surrounding bone is highly active and shows enhanced bisphosphonate uptake, calling into question the need for local delivery from coated implants.

Authors: Some patients requiring orthopedic implants are likely to have osteoporosis. Regarding these patients: in cases of undiagnosed and untreated disease, a zoledronate-coated implant would certainly offer benefits compared to uncoated implants, as indicated by the present pilot study. In cases of patients already treated with bisphosphonate, there is no experimental evidence that zoledronate-coating would provide a better fixation than a systemic administration. However, while zoledronate-coating provides an immediate release of a very small amount of drug at the desired location (which in this case is independent of the rate of activity of the surrounding bone), systemic treatment provides a continuous drug uptake on a long-term basis. Thus, the optimal implant fixation in patients with osteoporosis may be obtained by a combined approach of local and systemic treatment, rather than one or the other, taking advantages of both approaches. However this hypothesis has yet to be experimentally demonstrated.

Reviewers: This small paper suggests the possibility that local bisphosphonates can improve osseointegration of implants. Do authors have any estimate on the duration of such a positive effect?

Authors: Our objective was to obtain an increase of fixation at short-term. Indeed, clinical data suggests that a good short-term implant fixation is generally followed by a strong long-term fixation, when compared to implant with early loss of fixation. Based on these results, we believe that the benefit observed after 4 weeks should last for much longer.

But the duration of the beneficial effect depends on many factors such as the mechanical environment and the rate of elimination of the drug, thus the exact duration remains to be determined experimentally.

Reviewers: As bone loss in the ovine osteoporosis model can be influenced by breed, season, diet etc, the omission of any data to confirm the extent of the osteopenia/osteoporosis in these 3 animals is a concern. This could have been partially addressed by using each animal as its own control with a zoledronate coated implant in one femur and an uncoated control implant on the contralateral side – I doubt whether there would have been any systemic drug exposure from the coated implant.

Authors: Strictly speaking the condition of these animals is osteopenia (based on BV/TV standard deviations) but the severe bone loss of 30% detected in iliac crests biopsies suggests that this model is comparable to osteoporosis condition in some human bones.

Indeed, when planning the study, our concern was that the drug could influence the contralateral side bone density, that is why we didn't use each animal as its own control. At posteriori, the extent of the effect of the drug is very limited (400µm) and thus there would certainly be no systemic effect. This supports the own-control design in the future.

Reviewers: The reduced bone volume / trabecular volume is taken as an osteoporotic model of osteoporosis. Is this really a model of osteoporosis or osteopenia? Do the authors think that any sheep model is actually a realistic model of osteoporosis or more of osteopenia?

Authors: To be exact the presented data is a model of severe osteopenia. There are actually no animal models that realistically reflect the human condition of osteoporosis. However, to our knowledge the OVX sheep model is the best model available to study orthopedic applications in osteoporotic bone (see Turner 2002).

Reviewers: Long term bisphosphonates have been seen to increase cortical bone thickness in elderly osteoporotic patients, yet recently it has been observed that this new cortical bone is very brittle and if fractured, very difficult to repair. I assume this is because the natural remodeling is knocked out by the bisphosphonates and the osteoclasts no longer function. What effect would local bisphosphonates have on the quality of the osseointegrated bone formed?

Authors: In the case of patients not exposed systemically to bisphosphonate in parallel to the presented technique, we don't think the quality of the bone is an issue on a long term perspective: the coated dose is available in the bone only once and is slowly retrieved from the coating and from the surrounding bone with normal metabolic processes. Therefore the remodeling of the periprosthetic bone should be reactivated after some time, and the damaged bone renewed.

7 Paper 4: 3D strain map of axially loaded mouse tibia: a numerical analysis validated by experimental measurements

Vincent A. Stadelmann, Jean Hocké, Jensen Verhelle, Vincent Forster, Francesco Merlini,
Alexandre Terrier, Dominique P. Pioletti*

Laboratory of Biomechanical Orthopedics EPFL-HOSR, Institute of Translational
Biomechanics, Ecole Polytechnique Fédérale de Lausanne, Switzerland

Accepted in Computer Methods in Biomechanics and Biomedical Engineering, in press

*Corresponding author:

Dominique P. Pioletti, Ph.D.

Laboratory of Biomechanical Orthopedics EPFL-HOSR

Station 15

EPFL

1015 Lausanne

Switzerland

Tel: +41 21 693 83 41

Fax: +41 21 693 86 60

Email: dominique.pioletti@epfl.ch

Abstract

A combined experimental/numerical study was performed to calculate the 3D octahedral shear strain map in a mouse tibia loaded axially. This study is motivated by the fact that the bone remodeling analysis in this *in vivo* mouse model should be performed at the zone of highest mechanical stimulus to maximize the measured effects. Accordingly, it is proposed that quantification of bone remodeling should be performed at the tibial crest and at the distal diaphysis. The numerical model could also be used to furnish a more subtle analysis as a precise correlation between local strain and local biological response can be obtained with the experimentally validated numerical model.

Keywords:

mechanical loading, bone remodeling, strain quantification

Introduction

In vivo mechanical loading models have been developed to study mechano-transduction, which is the process of biological response to a mechanical stimulus. In particular for bone, the biological response to an applied external mechanical stimulus is generally quantified by morphological imaging (micro-computed tomography, scanning electron microscopy), histology or biomechanical tests (three or four point bending).

Rubin *et al.* were pioneers in this field showing that cortical bone mass and size of the turkey ulna was regulated by mechanical stimulations (Rubin et al. 1996, Rubin and Lanyon 1984). Since this work, different studies were performed confirming the responsiveness of bone to mechanical stimulus. For example, Chow *et al* showed that mechanical loading is a determinant for the physiological behavior of cancellous bone in a rat vertebrae model (Chambers et al. 1993, Chow et al. 1993). More recently, non-invasive models of mechanical loading were adapted to the challenging dimensions of mice bones. Cyclic four-point loading were applied on mouse tibia and the results highlighted the difference in response between different breeds of mice (Akhter et al. 1998). Tibial axial loading was used to study site-specific remodeling response to mechanical stimuli (De Souza et al. 2005, Fritton et al. 2005) and the loading effect on bone healing (Gardner et al. 2006).

In vivo loading experiments require a precise control of the mechanical stimulus to correctly interpret the measured changes of the bone structure. It is likely that the most relevant structural changes of the loaded bone will be observed at the maximally stimulated locations. Therefore, to optimize the significance of a study, the choice of the location where histological or histomorphological imaging is to be processed should be defined in function of the spatial distribution of the mechanical stimulus.

The most accessible measure of the mechanical stimulus is the strain. The strain variable has indeed been used in many different bone adaptation models (Carter 1987, Huiskes et al. 1987)

In this study, we want then to estimate the 3D strain map in an axial loading model of the mouse tibia.

The mouse tibia is neither homogenous nor axisymmetric. Therefore the maximum strain location is not known *a priori* when an external load is applied. In order to assess the spatial distribution and intensity of strain in an axially loaded mouse tibia, we designed a study based on three steps. The first step was to experimentally measure the strain occurring at three different locations on a mouse tibia under different axial loads. In the second step, a numerical biomechanical model of a mouse tibia was built and validated with the experimental data. In the third step, the numerical model was used to extrapolate the strain distribution over the whole tibial geometry and to determine the 3D octahedral shear strain map and the highest strain locations.

Materials and Methods

In this section we will first describe the experimental procedure of measuring the strain at three different locations on the mouse tibia, followed by a description of the numerical model developed to quantify the strain on the whole mouse tibia.

Animals

C57BL6 male mice were acclimated to our facility for three weeks. They were maintained under standard no barrier conditions and had access to mouse chow and water *ad libitum*. The local ethics committee on animal care approved all animal procedures (Protocol#1920).

Strain measures

Nine mice were sacrificed at the age of 15 ± 3 weeks, and the tibias were immediately extracted. Soft tissues were removed and the tibias were cleaned with acetone. The tibias were

separated randomly into three groups of six corresponding to three zones of tests on the tibia; zone 1: antero-proximal; zone 2: antero tibial crest; zone 3: postero-distal (Figure 1).

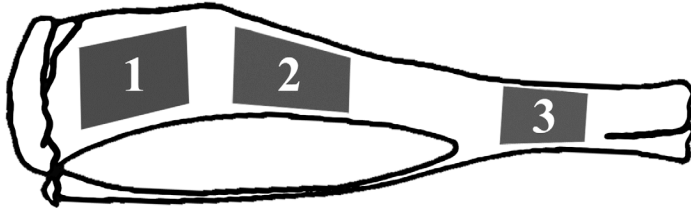


Figure 1: Definition of the regions of interest on the mouse tibia. Zone 1, proximal tibia, presents a flat and regular surface. It is the widest area of the tibia; therefore the easiest location to place a gage. Zone 2 begins at the tibial crest and ends 1mm before the junction with the fibula. This zone is relatively flat but narrower than zone 1, therefore the strain gage is harder to place. Zone 3, distal tibia, is narrow and curved. It is the hardest surface to fix a gage.

Each tibia received a single element foil strain gage (EA-06-015LA-120, Vishay Micro-Measurements, Raleigh, NC, USA) aligned with the long axis bond to the bone surface with cyanoacrylate (Rapid Mix 72771, Forbo CTU, Schönenwerd, Switzerland). The gage was connected to a tension amplifier and digital recorder (DAQ NI9215, National Instruments, Switzerland). To verify the linkage between the strain gage and the bone surface, two tibias were scanned by micro computed tomography (μ CT) at $9\mu\text{m}$ pixel size. The images showed that the gage location corresponded to the target and that no space was left between the gage and the bone surface (Figure 2).

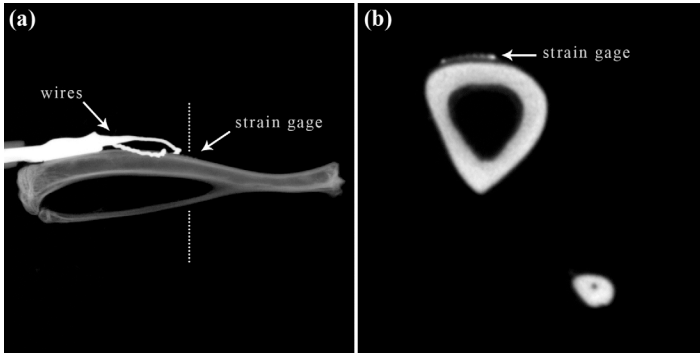


Figure 2: (a) Side-view of a μ CT scan of a tibia with a strain gage placed at Zone 2 and connecting wires. (b) Profile view along dotted line showing the strain gage linkage to the bone follows the contour of bone surface.

Calibration of the setup

A strain gage was placed at the center of an aluminum beam of dimensions $3 \times 10 \times 350$ mm and connected to the electronics. One end of the beam was fixed and controlled while loads were applied on the opposite end. The resulting tension was recorded for each load. To obtain the deformation-tension relationship, the beam deformation theory was applied to calculate to exact deformation at the center of the beam for each load.

Mechanical loading

A compression machine was developed to apply controlled compression cycles on mouse tibias, based on a previously published work (De Souza, Matsuura, Eckstein, Rawlinson, Lanyon and Pitsillides 2005, Fritton, Myers, Wright and van der Meulen 2005). Custom molded pads were placed on the axes to apply the compression on the bone ends. The tibia was then placed on the stimulation machine between the moving pad on the proximal-side and the fixed pad on the distal-side (Figure 3).

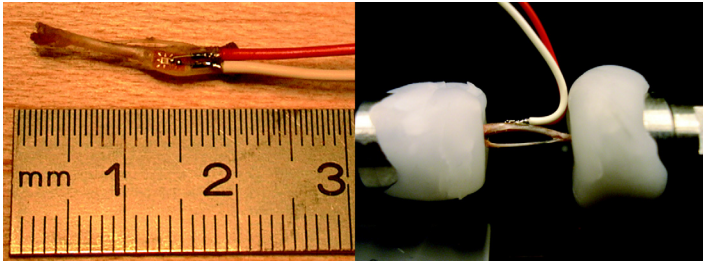


Figure 3: (a) Tibia with strain gage fixed in zone 2. (b) Tibia placed in the loading machine with strain gage in zone 2.

To maintain the initial position of the tibia, a pre-load of 0.2 N was applied before the dynamic compression. The compression waveform was composed of square like cycles at 2Hz of frequency, and amplitude from 1N minimum force during 0.25s followed by maximal force during 0.25s. The maximal force increased from 1N to 10N by steps of 1N every 20 cycles (Figure 4). Because of the natural curvature of the tibia, this simple axial loading induced combined compressive and bending strains.

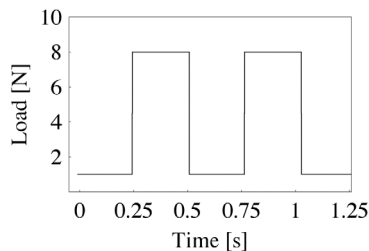


Figure 4 - Loading signal waveform with a frequency of 2Hz and maximum intensity at 8N for two consecutive loading cycles

Numerical model

Geometry

The geometry of a fresh specimen of mouse tibia was reconstructed from μ CT scan data (μ CT40, Scanco Medical AG, Switzerland) at a 9 μ m resolution. The axial reconstructed images were then imported in AMIRA (Mercury Computer Systems, MA, USA) for the segmentation of the tibial bone volume. Finally, a geometric model based on parametric surfaces was built from the Amira data using Geomagic (Geomagic, Inc., NC, USA).

Three-dimensional FE model

The geometric model of the tibia was then imported into Abaqus (Simulia, RI, USA). A total number of 26,000 three-dimensional (20-node quadratic brick, reduced integration) elements were used to mesh the tibia.

Material properties

The density of the cancellous and cortical bone can vary greatly in the tibia. To incorporate this parameter, the Hounsfield number was correlated to the bone density. The Young's modulus was then estimated using the equation derived by J.Y. Rho for a longitudinal compressed human tibia bone (RHO et al. 1995).

Boundary Conditions

Each of the articular end surfaces of the tibia were rigidly connected to a point placed at the center of the surface. The distal point was completely fixed while the proximal point was free to translate in the axial direction. An axial compressive force of 8N was applied on the proximal point.

Measurements

Strains were calculated in the direction of the experimental strain gauge, within the three locations (surface of bone) of the strain gauges. An average and standard deviation of the calculated strain was then obtained for each location.

Results

Experimental strain

At loading application, the strain has a peak of $\sim 10\%$ of the total strain and then drops to its plateau value until load is retrieved (Figure 5.a). The following measurements were recorded at plateau values.

The force-strain relationship was established by successively increasing loading cycles between 1N and 10N for each zone. The force-strain relationships are linear with $R^2 > 0.95$ for each zone (Figure 5.b).

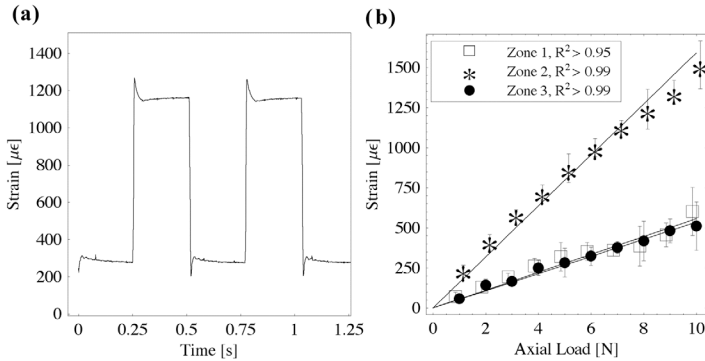


Figure 5: (a) Strain records at Zone 2 for a dynamic load of 8N for two consecutive loading cycles. (b) Force - strain experimental relations measured at three zones with the respective linear regressions and R^2 values.

For the 8N loading, the experimental values of the strain were $440 \pm 31 \mu\epsilon$ at zone 1, $1337 \pm 100 \mu\epsilon$ at zone 2 and $444 \pm 81 \mu\epsilon$ at zone 3. The strain values were significantly higher in zone 2 compared to zone 1 and zone 3.

Numerical model validation

For 8N loading, the numerical values of the strain were $472\pm225\mu\epsilon$ at zone 1, $1320\pm372\mu\epsilon$ at zone 2 and $420\pm127\mu\epsilon$ at zone 3. These results correspond to experimental measurements with an error smaller than 10% (Figure 6).

Extrapolation to the entire tibia, highest strain location

The octaedral shear strain distribution was calculated numerically for five different locations: proximal tibia, proximal-diaphysis, tibial-crest diaphysis, midshaft and distal tibia (Figure 7). Mean octaedral shear strain was calculated for each zone on the antero and the postero side (Table 1). The maximal octaedral shear strain was found at the postero-tibial crest ($1800\pm40\mu\epsilon$) and the antero-distal tibia ($1940\pm30\mu\epsilon$).

Orientation	Proximal tibia	Proximal diaphysis	Tibial crest	Midshaft Tibia	Distal Tibia
Antero	250±5	280±6	380±10	670±20	1940±30
Postero	330±7	1050±20	1800±40	1400±15	640±20

Table 1: Mean±SEM octaedral shear strain [$\mu\epsilon$] for each orientation of each of the five zones

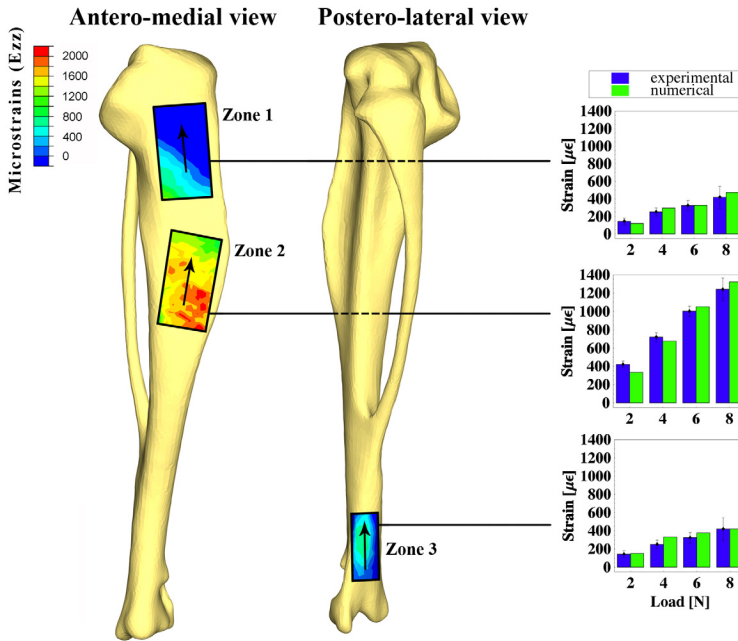


Figure 6: Distribution of the microstrains E_{zz} within each of the three measurement zones, relative to a locally defined coordinate system where the z -axis (arrows) is oriented along of the measurement axis and the y -axis is parallel to the measurement plate. Comparisons with experimental data are shown in the right column for each zone at different loading intensities. The relative differences are smaller than 10%.

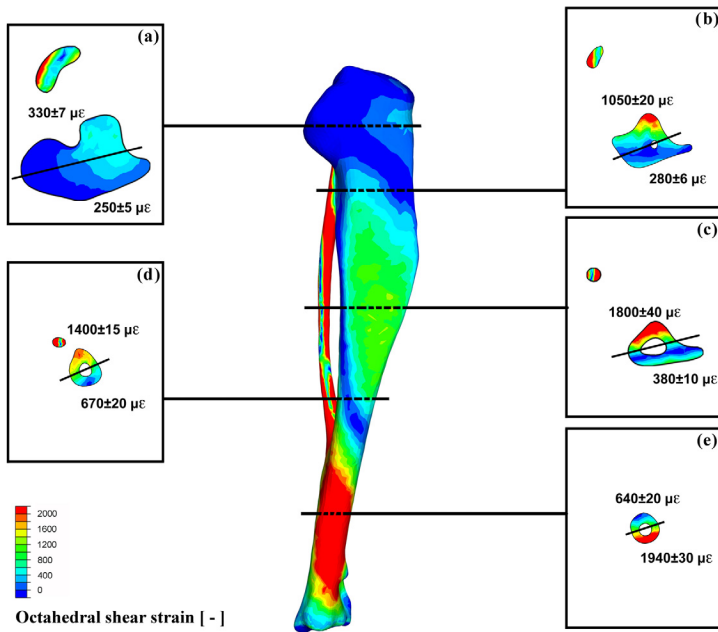


Figure 7: Octahedral shear strain distribution calculated numerically for five different locations: proximal tibia (a), proximal-diaphysis (b), tibial-crest diaphysis (c), midshaft (d) and distal tibia (e). Lines represent antero/postero separation and values represent the mean octahedral shear strain in the respective zone.

Discussion

Although bone adaptation to mechanical environment has been observed for decades, the mechanisms underlying the perception of the mechanical stimulus by the cell and the biological pathways of the cell response are still far from being completely understood.

The *in vivo* mechanical stimulation of mice tibias combined with histology and histomorphometry (μ CT) is certainly one of the most promising techniques to gain further understanding in the bone remodeling answer to mechanical stimulation. However, histology and μ CT are both very time-consuming techniques, and therefore these techniques are generally used only at few locations of the tibia (generally the midshaft, proximal and distal sections), regardless of the loading state.

The goal of this study was to estimate the 3D map of the octahedral shear strain distribution within the tibia of a mouse under specific axial loading that corresponds to our experimental setup. Octahedral shear strain intensity is a good approximation of the mechanical stimulus that cells can sense (Terrier et al. 1997). Thus, the 3D strain map will serve as a reference for our future histology and μ CT planning, and it might as well be useful to any similar axial stimulation experiments.

To determine the 3D map of the octahedral shear strain distribution within the loaded tibia, a finite-element model of a mouse tibia was built from μ CT images. The model was first validated with ex-vivo experimental measurements of strain at three different locations on loaded tibias. Then the model was used to extrapolate these values to the entire tibial volume. The maximal octahedral shear strain, calculated on the volumic model, was found at the postero-tibial crest ($1800 \pm 40 \mu\epsilon$) and the antero-distal tibia ($1940 \pm 30 \mu\epsilon$). These results indicate that bone remodeling should be quantified in these areas, either for histological or histomorphological measurements, as a maximal mechanical stimulus will generate a maximal response of the tissue. It should be noted however, that even in the maximal strain

zone, differences in strain values exist inside the tibial section. A precise correlation between applied external mechanical stimulus and biological response can then be obtained only by using the combined approach (experimental/numerical) followed in this study.

The loading force-local strain relationship was shown to be linear in the three experimental zones until at least 1500 $\mu\epsilon$ strain. Using a comparable loading system, the experimental strain values are in accordance (max 6% difference) with De Souza et al. (De Souza, Matsuura, Eckstein, Rawlinson, Lanyon and Pitsillides 2005). Our experimental set-up can then be considered as validated.

When experimental and numerical strain values were compared, a maximum difference of 10% was found for the three different zones. These differences can certainly be considered as acceptable, thus validating the numerical model. It should be mentioned that the results of the numerical model should be carefully considered for the very proximal and very distal part of the tibia as the joint surface and the underlying trabecular bone might affect the numerical results. However, as the maximal strain is not found in these two regions, this aspect does not invalidate the determination of the maximal strain zone.

A limitation for the correlation process between external load and biological response is related to the fact that loads were applied in the axis of the tibia, inducing combined axial compressive and bending strains due to the natural curvature of the bone. These different modes of strain were not accounted for in the presented analysis. Strictly from a biomechanical point of view, it is interesting to note that the numerical model indicated that the maximum bending was observed on the fibula. However, this information is of limited practical use as this bone is too small to place a gage to confirm the numerical result. Moreover, this tissue is also too small for histology or histomorphometry analysis.

In this study, we assumed that the mechanical stimulus is directly related to strain. In the literature, different mechanical stimuli have been proposed to explain bone remodeling

(Huiskes et al. 2000, Parfitt 1996, Prendergast and Huiskes 1994, Turner and Pavalko 1998). However, from an experimental point of view, only the tissue elongation transformed to a strain value is accessible. Other mechanical stimuli are mathematically related to the strain through constitutive laws. The calculated zone of highest strain obtained in this study can also be of general use for models using different descriptions of the mechanical stimulus.

To conclude, an experimental/numerical approach has been developed to identify the 3D octahedral shear strain map in an axial loading mode for a mouse tibia. It is proposed that quantification of bone remodeling should be performed at the tibial crest and at the distal diaphysis as the maximum biological response should correspond to the maximal applied strain. The numerical model could also be used to furnish a more subtle analysis as a precise correlation between local strain and local biological response can be obtained.

Acknowledgments

Project no. 04-P2 was supported by the AO Research Fund of the AO Foundation, Davos, Switzerland. We greatly acknowledge Marc Jeanneret for his technical support in designing and building the compression machine, Dr. Kossi Agbeviade and André Badertscher for their support with micro strain-gages manipulation. We also thank Tyler Thacher for English editing.

References

- Akhter MP, Cullen DM, Pedersen EA, Kimmel DB and Recker RR. 1998. Bone response to in vivo mechanical loading in two breeds of mice. *Calcif Tissue Int.* 63(5):442-449.
- Carter DR. 1987. Mechanical loading history and skeletal biology. *J Biomech.* 20(11-12):1095-1109.

Chambers TJ, Evans M, Gardner TN, Turnersmith A and Chow JWM. 1993. Induction of Bone-Formation in Rat Tail Vertebrae by Mechanical Loading. *Bone and Mineral*. 20(2):167-178.

Chow JW, Jagger CJ and Chambers TJ. 1993. Characterization of osteogenic response to mechanical stimulation in cancellous bone of rat caudal vertebrae. *Am J Physiol*. 265(2 Pt 1):E340-347.

De Souza RL, Matsuura M, Eckstein F, Rawlinson SC, Lanyon LE and Pitsillides AA. 2005. Non-invasive axial loading of mouse tibiae increases cortical bone formation and modifies trabecular organization: a new model to study cortical and cancellous compartments in a single loaded element. *Bone*. 37(6):810-818.

Fritton JC, Myers ER, Wright TM and van der Meulen MCH. 2005. Loading induces site-specific increases in mineral content assessed by microcomputed tomography of the mouse tibia. *Bone*. 36(6):1030-1038.

Gardner MJ, van der Meulen MC, Demetrakopoulos D, Wright TM, Myers ER and Bostrom MP. 2006. In vivo cyclic axial compression affects bone healing in the mouse tibia. *J Orthop Res*. 24(8):1679-1686.

Huiskes R, Ruimerman R, van Lenthe GH and Janssen JD. 2000. Effects of mechanical forces on maintenance and adaptation of form in trabecular bone. *Nature*. 405(6787):704-706.

Huiskes R, Weinans H, Grootenboer HJ, Dalstra M, Fudala B and Slooff TJ. 1987. Adaptive bone-remodeling theory applied to prosthetic-design analysis. *J Biomech*. 20(11-12):1135-1150.

Parfitt AM. 1996. Skeletal Heterogeneity and the purposes of Bone Remodeling. In: *Osteoporosis*: Academic Press. p. 315--329.

Prendergast PJ and Huiskes R. Mathematical Modeling of Microdamage in Bone Remodeling and Adaptation. In. *Bone Structure and Remodeling*; Amsterdam.

RHO JY, Hobatho MC and Ashman RB. 1995. Relations of Mechanical-Properties to Density and Ct Numbers in Human Bone. *Medical Engineering & Physics*. 17(5):347-355.

Rubin C, Gross T, Qin YX, Fritton S, Guilak F and McLeod K. 1996. Differentiation of the bone-tissue remodeling response to axial and torsional loading in the turkey ulna. *J Bone Joint Surg Am.* 78(10):1523-1533.

Rubin CT and Lanyon LE. 1984. Regulation of bone formation by applied dynamic loads. *J Bone Joint Surg Am.* 66(3):397-402.

Terrier A, Rakotomanana RL, Ramaniraka AN and Leyvraz PF. 1997. Adaptation Models of Anisotropic Bone. *Comput Methods Biomech Biomed Engin.* 1(1):47-59.

Turner CH and Pavalko FM. 1998. Mechanotransduction and functional response of the skeleton to physical stress: the mechanisms and mechanics of bone adaptation. *J Orthop Sci.* 3(6):346-355.

8 Paper 5: Combined effects of zoledronate and mechanical stimulation on bone adaptation in an axially loaded mouse tibia: A Preliminary study

Vincent A. Stadelmann, Dominique P. Pioletti

Laboratory of Biomechanical Orthopedics EPFL-HOSR, Institute of Translational
Biomechanics, Ecole Polytechnique Fédérale de Lausanne, Switzerland

To be submitted to Bone

*Corresponding author:

Dominique P. Pioletti, Ph.D.

Laboratory of Biomechanical Orthopedics EPFL-HOSR

Bat AI – Station 15

EPFL

1015 Lausanne

Switzerland

Tel: +41 21 693 83 41

Fax: +41 21 693 86 60

Email: dominique.pioletti@epfl.ch

Abstract

Local bisphosphonate delivery may be a solution to prevent periprosthetic bone loss and improve orthopedic implants fixation. In load-bearing implants, periprosthetic bone is exposed to high mechanical demands, which in normal conditions induce an adaptation of bone. In this specific mechanical situation, the modulation of the bone response by bisphosphonate remains uncertain.

We assessed the combined effects of zoledronate and mechanical loading on bone adaptation using an *in vivo* axial compression model of the mouse tibia and injections of zoledronate. Bone structure was assessed with *in vivo* μ CT before and after the period of stimulation and the biomechanical properties of the tibias were assessed with 3point-bending tests after sacrifice. Axial loading induced a localized increase of cortical thickness and bone area. Zoledronate increased cortical thickness, bone perimeter, and bone area. At the most loaded site of the tibia, the combined effect of zoledronate and mechanical stimulation was significantly smaller than the effect of zoledronate plus the effect of mechanical loading. This suggested that an interaction between zoledronate and mechanical loading might exist at high levels of strains.

Keywords

Bone adaptation; *In vivo* mechanical loading; Bisphosphonate; Zoledronate; *In vivo* μ CT

Introduction

Periprosthetic bone loss facilitates the occurrence of aseptic loosening. Periprosthetic bone loss is initiated at the very early stage after an implant is set. Different authors have suggested the solution of local bisphosphonate release from the orthopedic implant to prevent the bone resorption at this early post-operative stage [1, 2]. It has been shown that local bisphosphonate preserves periprosthetic bone stock, in rats and sheep [3-5] and also increases the fixation strength, in rats [4, 6]. In these studies the implants were not specifically loaded mechanically, in contrary of the clinical situation of load-bearing implants, where the periprosthetic bone is exposed to high mechanical demands [7]. In this specific mechanical situation, the modulation of the bone response by bisphosphonate remains uncertain.

Bone can adapt to mechanical demands. This process involves osteocytes, cells that sense mechanical stimulations, osteoclasts that resorb bone, and osteoblasts that form new bone. Bone adaptation relies upon the communication between these cells, through cell-cell contacts and local cytokines [8-11].

Bisphosphonates inhibit osteoclasts differentiation and activity, consequently they slow down the bone turnover rate. Given the constant communication between the bone cells, the changes that affect one type of cells has indirect consequences on the other types of cells. In the specific case of periprosthetic bone this could lead to an unwanted pathological response.

The aim of the present study was to assess the effect of zoledronate, the newer member of the third generation bisphosphonates [12-14], on bone adaptation to mechanical loading in order to anticipate pathological outcomes when using it in highly loaded bone structures. For this purpose, we used an *in vivo* axial compression model of the mouse tibia [15, 16] and analyzed the effect of zoledronate on site-specific bone adaptation.

Materials and Methods

Animals

Eleven C57BL6 male mice, 17±1 weeks old, were acclimated to our facility for three weeks. Mice were caged in groups of three or four. They were maintained under standard no barrier conditions and had access to mouse chow and water *ad libidum*. The local ethics committee on animal care approved all animal procedures (Protocol#2006.1).

The mice were separated randomly into two groups: on day 0, the five animals of the zoledronate group received a single subcutaneous injection (80 µl) of 1 µg/kg zoledronate (Novartis Pharmaceuticals AG, Switzerland) while the six animals of the control group received an equivalent injection of saline.

Anesthesia

General anesthesia was induced with a ketamine (80 mg/kg) and xylazine (5 mg/kg) cocktail administered intraperitoneally unless specified.

µCT

We assessed trabecular and cortical bone architecture using *in vivo* micro-computed tomography (µCT1076 *in vivo*, SkyScan, Belgium), at day 0 and day 11.

Animals were anesthetized. The lower limbs were fixed in a custom polystyrene support and aligned with the axis of rotation of the scanner. The tibias were then scanned with 9-µm isotropic voxel size, 50kV beam, 0.8° step rotation. Reconstructions and analysis were performed with built-in routines of manufacturer's softwares NRecon and CTan, following the standard protocols. The reconstructed tibia contained about 1900 slices.

Trabecular thickness (Tb.Th) was evaluated at the proximal tibial metaphysis, whereas cortical thickness (Ct.Th), bone perimeter (B.Pm) and bone area (B.Ar) were evaluated at four

different locations of the diaphysis: zones 1 and 2: 150 slices of the proximal diaphysis at 1/5 and 2/5 of the tibial length respectively; zone 3: 150 slices at the midshaft; zone 4: 150 slices of the distal diaphysis at 4/5 of the tibial length (Figure 1a). Zone 1 was then divided in four sub-regions of interest, corresponding to the four facets, to assess orientation specific remodeling (Figure 1b).

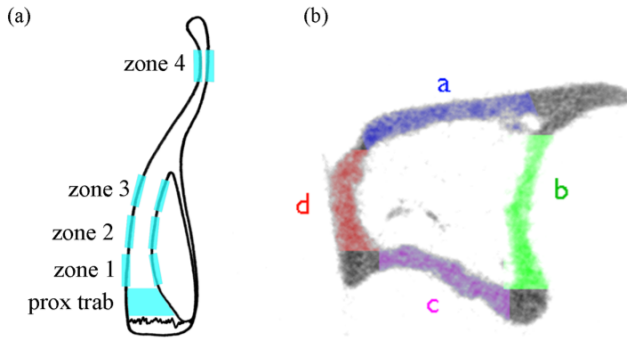


Figure 1 - Regions of interests. (a) Definition of the five ROIs: proximal for trabecular bone and zone 1 to 4 for cortical bone. (b) Definition of the 4 sub-regions of zone 1.

In vivo compression

A compression machine was developed to apply controlled compression cycles on the tibias, based on a previously published work [15, 16]. On day 1, 3, 5, 8 and 10 the left tibia of all animals were mechanically stimulated with dynamic axial compression sequences. Custom molded pads were designed on the axes ends to apply the compression on the leg.

Each animal was anesthetized and placed on a warm support with eye gel until completely unresponsive. The animal was then placed on the stimulation machine with the left leg between the moving pad on the knee and the fixed pad on the ankle (Figure 2a).

To maintain the initial position of the leg, a pre-load of 0.5 N was applied before the dynamic compression. The compression waveform was composed of square like cycles at 2Hz frequency, and amplitude from a force of 0.5 N during 0.25s followed by a force of 8N during 0.25s (Figure 2b).

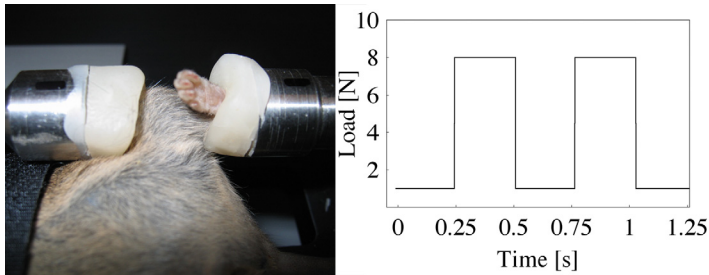


Figure 2 - (a) Animal's left tibia placed in the compression machine between the molded cups. (b) Compression waveform.

The sequence of compression was applied during 1 min. Then the animal was placed at rest on the warm support. After 15 min a second sequence of 1 min of dynamic compressions was applied. Then the animal was placed on the warm support until it moved.

Because of the natural curvature of the tibia, this simple axial loading induced combined compressive and bending strains. Axial compression of 8N induces maximum octahedral shear strain at the postero-tibial crest ($1800 \pm 40 \mu\epsilon$) and the antero-distal tibia ($1940 \pm 30 \mu\epsilon$) [17].

Sacrifice and tibias extraction

On day 11, while still under anesthesia for the μ CT, the animals were sacrificed with an overdose of ketamin. Both tibias were extracted surgically and placed in wet conditions at 4 °C.

Mechanical tests

Tibial biomechanical properties were assessed by 3-point bending [18, 19], using the Instron Microtester 5848, (Instron, MA, USA) equipped with a 100 N gauge and custom bone supports. The fibula was removed with a surgical blade before the tests. The lower supports distance was set to 12mm for all tibias, and the tibias always placed proximal end to the left and up, distal on the right. The crosshead speed was set to 0.02 mm/s and the force-displacement data sampling to 100 Hz.

The ultimate force, stiffness and postyield energy to failure were calculated from the collected data. The yield point was defined by using a 0.3 N offset from the stiffness line [20].

Analysis

Data is generally presented as Mean \pm SD and all statistical procedures were performed with Mathematica5® (Wolfram Research, USA). The number of tibias per group was accounted for as repetition of the measurement. Effects of mechanical loading and zoledronate were analyzed with two-way ANOVA and Tukey posthoc-tests. For independent data, Student-t test was used to determine the statistical power of the difference: $p < 0.05$ was considered significant and, given the small number of animals per group, $p < 0.1$ was considered as a strong trend.

Results

Twenty-two tibias were analyzed in this preliminary study (Table 1). In the control groups, two animals could not be scanned on day 0; they were excluded from follow-up data. Two tibias were damaged during extraction; they were excluded from biomechanical analyses.

	<i>force</i>	
<i>zoledronate</i>	0N (right)	8N (left)
no	6	6
yes (1µg/kg s.c.)	5	5

Table 1 - Number of tibias in each group

Effect of mechanical loading and zoledronate on biomechanical parameters

Mechanical loading significantly enhanced the tibial stiffness by 16% compared to control, but had no effects on ultimate force and postyield energy to failure. Zoledronate significantly increased the stiffness, ultimate force and postyield energy to failure by 31%, 24% and 60% respectively, compared to control group. The effect of zoledronate on all three biomechanical parameters was significantly higher than the effect of mechanical loading alone.

Mechanical loading combined with zoledronate significantly increased the biomechanical parameters, compared to control tibias. This effect was significantly higher than the effect of mechanical stimulation alone on ultimate force and postyield energy to failure. However, no significant difference was observed between the effect of zoledronate and the combined effect of mechanical loading and zoledronate (Figure 3).

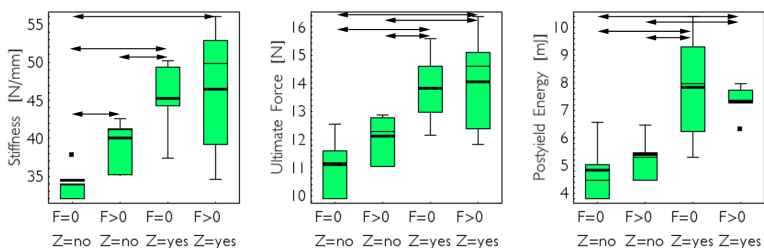


Figure 3 - Biomechanical parameters for each group. $F>0$ indicates mechanically stimulated groups. $Z=yes$ indicates zoledronate groups. Arrows indicate groups with significant differences ($p<0.05$).

Finally, for the three biomechanical parameters, the sum of the effect of mechanical loading and the effect of zoledronate was not significantly different than the effect of mechanical loading and zoledronate. Note that no effect was detected on paired comparison of the biomechanical parameters due to the loss of a tibia in the control group.

Effect of mechanical loading and zoledronate on histomorphometric parameters

When analyzing the evolution of individual tibias between day 0 and day 11 (Figure 4), we observed that mechanical loading alone induced a significant increase of Ct.Th in zone 1c compared to control tibias, and the increase of 9% and 12% in zones 1 and 2 respectively was a strong trend ($p<0.1$). Mechanical loading also induced a significant increase of B.Ar of 10% in zone 1. Mechanical loading had no significant effect on the evolution of B.Pm and Tb.Th in all zones.

Zoledronate treatment alone had no significant effect on the evolution of histomorphometric parameters. Zoledronate treatment combined with mechanical loading induced a significant increase of Ct.Th of 15% compared to control in zone 1d.

In zones 1 and 1b, mechanical loading had a significantly greater effect on Ct.Th than the zoledronate treatment.

Surprisingly, when analyzing pooled groups of tibias (Figure 5), we observed a different pattern of response: Ct.Th in zone 1c of mechanically loaded tibias was significantly greater by 10% compared to controls, but no differences in other zones were observed.

Ct.Th of tibias treated with zoledronate alone was significantly greater than controls by 10% in zone 4 ($p<0.05$), and we observed a trend of the same difference in zone 3 ($p<0.1$). In zone 1, 2, 3 and 4, B.Ar of tibias treated with zoledronate was significantly greater by 12%, 15%, 15% and 15% respectively compared to controls.

Tibias with zoledronate and mechanical loading had significantly higher B.Ar in all zones compared to controls and mechanically stimulated ones. However these tibias were not significantly different than zoledronate-treated tibias.

Finally in all zones except zone 1c, the effect of combined zoledronate and mechanical stimulation was equivalent to the sum of the effect of zoledronate and the effect of mechanical stimulation. In zone 1c, the effect of combined mechanical stimulation and zoledronate was significantly different than the sum of the effects.

Discussion

Local bisphosphonate release may be a solution to prevent periprosthetic bone loss and improve the implant fixation. However, in the case of load-bearing implants, periprosthetic bone is exposed to high mechanical demands, which in normal conditions induce an adaptation of bone. When zoledronate is present in bone, it alters its local metabolism. The aim of the study was to assess interactions between mechanical loading and zoledronate on bone adaptation in an *in vivo* stimulation experiment.

We observed that axial mechanical loading induced a localized increase of cortical thickness and cortical bone area. These site-specific changes are concordant with previous studies [15, 16]. Animals treated with zoledronate had site-specific increased of cortical thickness and cortical bone perimeter. The cortical bone area was increased in all zones, which is concordant with previous studies [21-23].

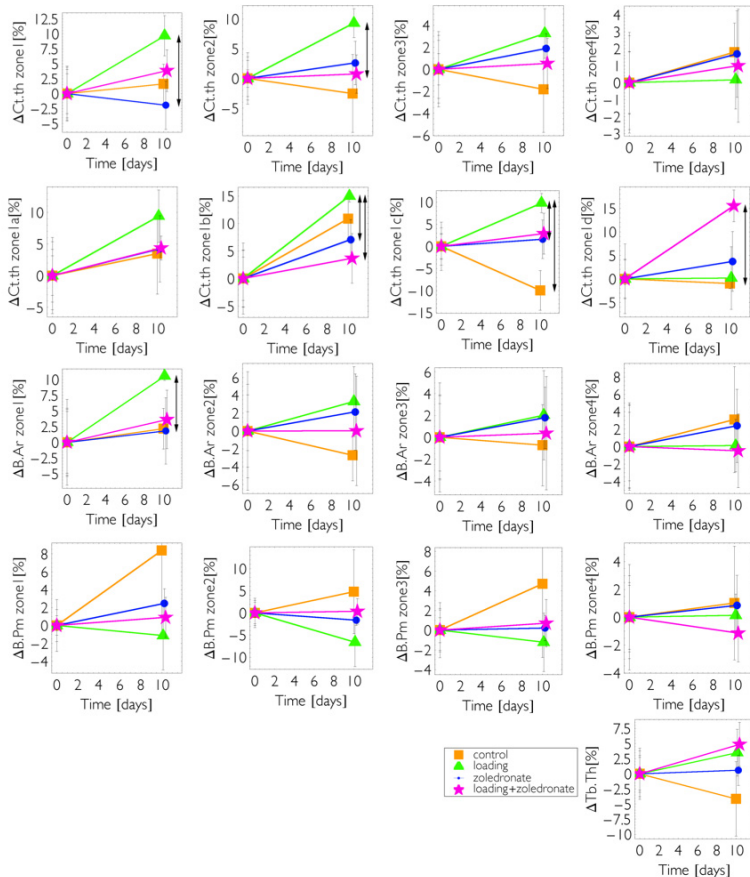


Figure 4 - Evolution of histomorphometric parameters of individual tibias from day 0 to day 11 in % change. Arrows indicate groups with significant difference ($p < 0.05$).

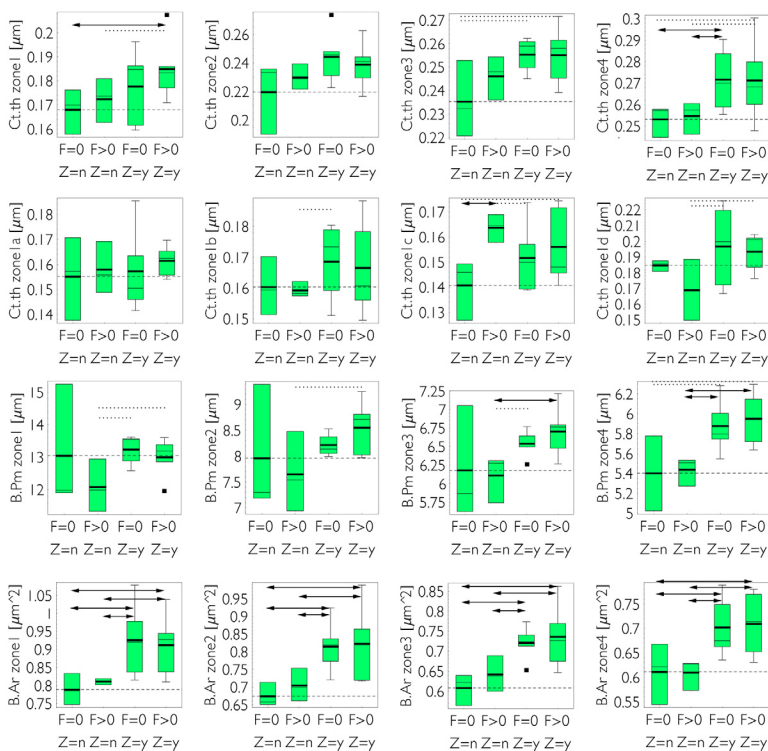


Figure 5 - Effect of mechanical loading ($F>0$) and zoledronate ($Z=y$) on histomorphometric parameters. Arrows indicate significant difference ($p<0.05$) between groups, while dotted lines indicate strong trends of difference ($p<0.1$).

In most cases, the effect of combined zoledronate and mechanical stimulation was equivalent to the sum of the effect of zoledronate and the effect of mechanical stimulation. However in zone 1c, the effect of combined zoledronate and mechanical stimulation was significantly smaller than the sum of the effects.

Using experimental measures and numerical simulations, we previously showed that during axial compression, bone in zone 1c undergoes the highest strain levels (about 1900 $\mu\epsilon$ for 8N load) while the rest of the tibia is less loaded. The specific results in zone 1c suggest that an interaction might exist between the bone response to mechanical stimulation and the effect of zoledronate at high levels of strains.

The decreased effect of combined mechanical stimulation and zoledronate compared to mechanical stimulation alone, might reflect an upper limit on bone adaptation rate induced by the zoledronate when mechanical stimulations reach a high intensity.

This result can seem to be contradicting previous studies that have assessed the impact of bisphosphonate on bone response to mechanical demands. As examples, Jagger *et al.* have shown that, in rats caudal vertebrae exposed to mechanical stimulus, the rate of bone apposition is not affected by bisphosphonate [24]. Braith *et al.* have shown that bone loss can be prevented by alendronate treatments and that alendronate combined with mechanical loading induced a gain of bone mass⁹. However, in these studies the strain levels were in the range of physiological loadings. In this range of strains (all zones except zone 1c), our data concord with the cited results. To our knowledge, no other data exists assessing the effect of bisphosphonate in over-physiological mechanical conditions.

This preliminary study intended to reveal possible interactions between zoledronate treatment and mechanical stimulations. It was therefore based on a reduced pool of mice. The hypothesis that the interaction appears in response to high strain condition cannot be verified with the present data. To verify this hypothesis, a regression study with different intensities of mechanical loading will be performed with a larger pool of mice.

⁹ this study was performed in the specific situation of bone loss associated to corticoid treatment following lungs transfer.

The possible limitation of the bone response to high mechanical stimulations by zoledronate would require a specific design of load-bearing implants, to prevent drug accumulation in high-loading areas of the periprosthetic bone.

Acknowledgements

Project no. 04-P2 was supported by the AO Research Fund of the AO Foundation, (Davos, Switzerland). We thank Novartis Pharma Research (Basel, Switzerland) for a generous gift of zoledronate. We thank Marc Jeanneret for his great technical assistance, Pierre Latin for his help with animal handling and Tyler Thacher because I copy-pasted the acknowledgements of the previous article.

References

- [1] Peter B, Pioletti DP, Terrier A, Rakotomanana LR. Orthopaedic Implant as Drug Delivery System: a Numerical Approach. *Computer Methods in Biomechanics and Biomedical Engineering* 12001;4: 505--513.

- [2] Horowitz SM, Gonzales JB. Inflammatory response to implant particulates in a macrophage/osteoblast coculture model. *Calcified Tissue International* 11996;59: 392-396.

- [3] Wermelin K, Tengvall P, Aspenberg P. Surface-bound bisphosphonates enhance screw fixation in rats - increasing effect up to 8 weeks after insertion. *Acta Orthopaedica* 12007;78: 385-392.

- [4] Peter B, Pioletti DP, Laib S, Bujoli B, Pilet P, Janvier P, Guicheux J, Zambelli PY, Bouler JM, Gauthier O. Calcium phosphate drug delivery system: influence of local zoledronate release on bone implant osteointegration. *Bone* 12005;36: 52-60.

- [5] Stadelmann VA, Terrier A, Gauthier O, Bouler JM, Pioletti DP. Implants delivering bisphosphonate locally increase periprosthetic bone density in an osteoporotic sheep model. Submitted to *European Cells Materials* 12008.

- [6] Peter B, Gauthier O, Laib S, Bujoli B, Guicheux J, Janvier P, van Lenthe GH, Muller R, Zambelli PY, Bouler JM, Pioletti DP. Local delivery of bisphosphonate from coated orthopedic implants increases implants mechanical stability in osteoporotic rats. *J Biomed Mater Res A* 12006;76: 133-43.

- [7] Huiskes R, Weinans H, Grootenboer HJ, Dalstra M, Fudala B, Slooff TJ. Adaptive bone-remodeling theory applied to prosthetic-design analysis. *J Biomech* 11987;20: 1135-50.

- [8] Puzas JE. The Osteoblast. In: *Primer on Metabolic Bone Diseases and Disorders of Mineral Metabolism*: American Society for Bone and Mineral Research; 1991.

- [9] Parfitt AM. Osteonal and hemi-osteonal remodeling: the spatial and temporal framework for signal traffic in adult human bone. *J Cell Biochem* 11994;55: 273-86.

- [10] Suda T, Udagawa N, Nakamura I, Miyaura C, Takahashi N. Modulation of Osteoclast Differentiation by Local Factors. *Bone* 11995;17: S87-S91.

- [11] Turner CH, Pavalko FM. Mechanotransduction and functional response of the skeleton to physical stress: the mechanisms and mechanics of bone adaptation. *J Orthop Sci* 1998;3: 346-55.
- [12] Green JR, Hornby SB, Evans GP, Muller K. Effect of 1-year treatment with zoledronate (CGP 42446) on bone mineral density, bone mechanical properties and biochemical markers in the ovariectomized rat. *Journal of Bone and Mineral Research* 1996;11: M631-M631.
- [13] Green J. Zoledronate: The preclinical pharmacology. *British Journal of Clinical Practice* 1996: 16-18.
- [14] Pataki A, Muller K, Green JR, Ma YF, Li QN, Jee WSS. Effects of short-term treatment with the bisphosphonates zoledronate and pamidronate on rat bone: A comparative histomorphometric study on the cancellous bone formed before, during, and after treatment. *Anatomical Record* 1997;249: 458-468.
- [15] De Souza RL, Matsuura M, Eckstein F, Rawlinson SC, Lanyon LE, Pitsillides AA. Non-invasive axial loading of mouse tibiae increases cortical bone formation and modifies trabecular organization: a new model to study cortical and cancellous compartments in a single loaded element. *Bone* 2005;37: 810-8.
- [16] Fritton JC, Myers ER, Wright TM, van der Meulen MCH. Loading induces site-specific increases in mineral content assessed by microcomputed tomography of the mouse tibia. *Bone* 2005;36: 1030-1038.

- [17] Stadelmann VA, Terrier A, Pioletti DP. Submitted to Computer Methods in Biomechanics and Biomedical Engineering l2008.
- [18] Jepsen KJ, Akkus O, Majeska RJ, Nadeau JH. Hierarchical relationship between bone traits and mechanical properties in inbred mice. *Mammalian Genome* l2003;14: 97-104.
- [19] Brodt MD, Ellis CB, Silva MJ. Growing C57B1/6 mice increase whole bone mechanical properties by increasing geometric and material properties. *Journal of Bone and Mineral Research* l1999;14: 2159-2166.
- [20] Schrieffer JL, Robling AG, Warden SJ, Fournier AJ, Mason JJ, Turner CH. A comparison of mechanical properties derived from multiple skeletal sites in mice. *J Biomech* l2005;38: 467-75.
- [21] Gasser JA, Ingold P, Grosios K, Laib A, Hammerle S, Kollr B. Noninvasive monitoring of changes in structural cancellous bone parameters with a novel prototype micro-CT. *Journal of Bone and Mineral Metabolism* l2005;23: 90-96.
- [22] Recker RR, Delmas PD, Halse J, Reid IR, Boonen S, Garcia-Hernandez PA, Supronik J, Lewiecki EM, Ochoa L, Miller P, Hu H, Mesenbrink P, Hartl F, Gasser J, Eriksen EF. Effects of intravenous zoledronic acid once yearly on bone remodeling and bone structure. *Journal of Bone and Mineral Research* l2008;23: 6-16.
- [23] Brouwers JEM, Lambers FM, Gasser JA, van Rietbergen B, Huiskes R. Bone degeneration and recovery after early and late bisphosphonate treatment of ovariectomized

wistar rats assessed by in vivo micro-computed tomography. *Calcified Tissue International* 12008;82: 202-211.

[24] Jagger CJ, Chambers TJ, Chow JWM. Stimulation of Bone-Formation by Dynamic-Mechanical Loading of Rat Caudal Vertebrae Is Not Suppressed by 3-Amino-1-Hydroxypropylidene-1-Bisphosphonate (Ahprbp). *Bone* 11995;16: 309-313.

Conclusion and perspectives

The long-term durability of total joint replacements depends critically on the preservation of periprosthetic bone stock. The bone stock can be compromised by micromotions and accumulation of debris wears, but the precise chronology of biological events that finally leads to a critical bone loss had not been determined yet. More insights of this chronology and of the biological role of micromotions would certainly provide valuable information toward the development of therapeutic solutions.

Early effects of micromotions

The first aim of this thesis project was therefore to assess the effect of micromotions on human bone at the cellular level. For this purpose, we applied micromotions on top of fresh human bone cores *ex-vivo*. We measured that one hour of micromotions increases the activation signal of osteoclasts (RANKL/OPG) by 24-fold [24]. This unique human data suggests that micromotions are the initiators of the early periprosthetic bone loss. In other words, early periprosthetic resorption is the rapid response of bone cells to a local stimulus, the micromotions. Thus, to prevent early bone loss, a local solution, such as local bisphosphonate release, seems more appropriate than a systemic approach!

Local release of bisphosphonate

The efficiency of the local bisphosphonate solution was already supported by a few *in vivo* studies [106, 111-113], however these studies had two major limitations: first, the design was mainly empirical, and second, they were only performed with rats.

To design future animal or clinical studies and to compare their outcomes, there was a need for a comprehensive model of bone adaptation in the specific conditions of local diffusion of

bisphosphonate. The second aim of this thesis was therefore to develop a mathematical model of periprosthetic bone adaptation around implants releasing bisphosphonate. The model that was developed updated a mechanically-driven bone adaptation model by adding an equation of drug-driven bone adaptation and a drug diffusion law. The identification of the model parameters was carried-out with existing data of zoledronate local release in rats. Based on the updated model, the dose of zoledronate that would maximize the periprosthetic bone density was predicted; this prediction was then confirmed *in vivo* with a good accuracy.

Complementary data in a big animal model was required to confirm the potential of the local bisphosphonate solution in human-like bone. Thus, the third aim of the thesis was to perform the necessary experiments to produce this complementary data. Using titanium implants releasing zoledronate in the trabecular bone of osteoporotic sheep, we measured that the periprosthetic bone was 50% denser with local zoledronate than without.

Comparison of rats and sheep data

Comparing the new sheep data to previous rats data provided interesting information about the possible extrapolation of the rat results to clinical perspectives. The sheep and rat data were compared within the developed theoretical framework. First, we tested the validity of the model in sheep: the bone density distribution, as calculated with the theoretical model¹⁰, fits the experimental bone density in sheep with a mean error smaller than 5% (Figure 17a). An interesting feature of the theoretical model is the “drug signature” that reflects the bone response to the drug in a specific animal model. This function is a measure of the local bone adaptation rate in response to the local drug concentration, in contrary to measurements of bone change in response to systemic administration, which strongly depend on the

¹⁰ In this calculation, we assumed that the diffusion coefficient of the drug and the boundary conditions were the same as in the rat model.

bioavailability, the drug distribution and the local bone metabolism. These remarks highlight the potential use of the theoretical model as a convenient framework to compare experimental outcomes, and even, as a rationale for the design of future experiments.

As an example, the signature function of zoledronate was calculated in sheep from the experimental data and compared to the signature function in rats obtained previously (Figure 17b).

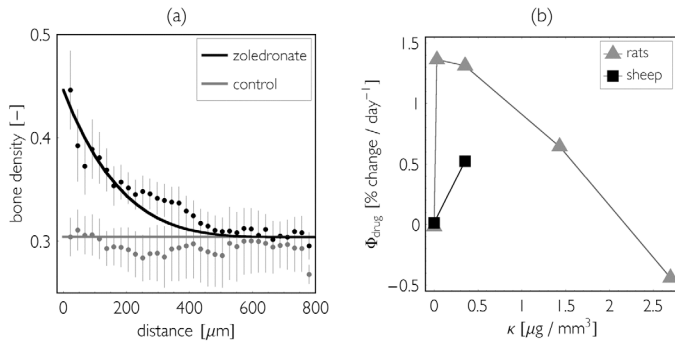


Figure 17 - (a) In sheep, the model prediction (lines) fits the experimental bone density (dots) with a mean error smaller than 5%. (b) Zoledronate signature in rats and sheep.

Although the signature in sheep is only available for two concentrations, it was striking to observe that the order of magnitude were comparable in the two species, at the same drug dose, despite the major differences in anatomy and metabolism.

Bone adaptation to mechanical stimulus and zoledronate

The fundamental assumption in the theoretical model was that the mechanical stimulus and the drug stimulus were independent, thus the effects of the two stimuli were simply summed up in the adaptation equation. However, as mentioned previously, the implants in rats and

sheep studies were not specifically loaded mechanically. Based on this experimental data, it was then not possible to formally confirm or reject the independence assumption.

The last aim of the thesis was then to investigate the potential interactions between mechanical loading and bisphosphonate on bone adaptation. Using a model of the mouse tibia adaptation to axial compression, combined with systemic injections of zoledronate, we observed that the effects of each stimulus can be added in general, however in locations with very high strains, about $2000\mu\epsilon$, zoledronate seemed to reduce the bone adaptation rate, but this result remains to be confirmed with more data.

If this effect was confirmed, the theoretical model would have to be update consequently with an interaction term. Nevertheless, as the effect was detected for very high strains, for most physiological values of strains, the model remains valid.

Clinical relevance

On a clinical perspective, the most meaningful results were, first, that a local and immediate mechanical process, micromotions, initiates periprosthetic bone resorption rapidly and thus favors aseptic loosening at long-term. This result provides a strong rationale for the local use of bisphosphonate rather than systemic. The second major result of the thesis was the demonstration that local bisphosphonate preserves periprosthetic bone stock in sheep. This result suggests that a preclinical study of total joint replacement with a bisphosphonate-coated implant can be performed in sheep, with good chances of success to demonstrate an increased fixation. Finally, although it is quite technical, the mathematical framework provides a useful tool to plan clinical studies and compare results. This framework could also be used to compare the performance of the different bisphosphonate in local applications.

References

1. Malchau, H., et al., *The Swedish total hip replacement register*. Journal of Bone and Joint Surgery-American Volume, 2002. **84A**: p. 2-20.
2. Witjes, S., et al., *[Complications within two years after revision of total hip prostheses]*. Ned Tijdschr Geneesk., 2007. **151**(35): p. 1928-34.
3. Chen, X.D., et al., Isolated acetabular revision after total hip arthroplasty: results at 5-9 years of follow-up. International Orthopaedics, 2005. **29**(5): p. 277-280.
4. Clarke, I.C., P. Campbell, and N. Kossovsky, Debris-mediated osteolysis-A cascade phenomenon involving motion, wear, particulates, macrophage induction, and bone lysis, in Particulate debris from medical implants: mechanisms of formation and biological consequences, ASTM STP 1144, K.R. St. John, Editor. 1992, American Society for testing and materials: Philadelphia. p. 7-26.
5. Horikoshi, M., et al., Comparison of interface membranes obtained from failed cemented and cementless hip and knee prostheses. Clin Orthop Relat Res, 1994(309): p. 69-87.
6. Korovessis, P. and M. Repanti, *Evolution of Aggressive Granulomatous Periprosthetic Lesions in Cemented Hip Arthroplasties*. Clinical Orthopaedics and Related Research, 1994(300): p. 155-161.
7. Aspenberg, P., et al., Intermittent micromotion inhibits bone ingrowth. Titanium implants in rabbits. Acta Orthop Scand, 1992. **63**(2): p. 141-5.
8. Schmalzried, T. and J. Callaghan, *Wear in total hip and knee replacements*. J Bone Joint Surg Am, 1999. **81**(1): p. 115-136.

9. Onsten, I., A.S. Carlsson, and J. Besjakov, *Wear in uncemented porous and cemented polyethylene sockets - A randomised, radiostereometric study*. Journal of Bone and Joint Surgery-British Volume, 1998. **80B**(2): p. 345-350.
10. Glant, T.T., et al., *Bone resorption activity of particulate-stimulated macrophages*. J Bone Miner Res, 1993. **8**(9): p. 1071-9.
11. Huiskes, R., et al., Adaptive bone-remodeling theory applied to prosthetic-design analysis. J Biomech, 1987. **20**(11-12): p. 1135-50.
12. Mandell, J.A., et al., A conical-collared intramedullary stem can improve stress transfer and limit micromotion. Clin Biomech (Bristol, Avon), 2004. **19**(7): p. 695-703.
13. Britton, J.R., C.G. Lyons, and P.J. Prendergast, *Measurement of the relative motion between an implant and bone under cyclic loading*. Strain, 2004. **40**(4): p. 193-202.
14. Jasty, M., et al., *In vivo skeletal responses to porous-surfaced implants subjected to small induced motions*. Journal of Bone and Joint Surgery-American Volume, 1997. **79A**(5): p. 707-714.
15. Engh, C.A., et al., Quantification of Implant Micromotion, Strain Shielding, and Bone-Resorption with Porous-Coated Anatomic Medullary Locking Femoral Prostheses. Clinical Orthopaedics and Related Research, 1992(285): p. 13-29.
16. Schmalzried, T.P., M. Jasty, and W.H. Harris, *Periprosthetic Bone Loss in Total Hip-Arthroplasty - Polyethylene Wear Debris and the Concept of the Effective Joint Space*. Journal of Bone and Joint Surgery-American Volume, 1992. **74A**(6): p. 849-863.
17. Karrholm, J., et al., Does early micromotion of femoral stem prostheses matter? 4-7-year stereoradiographic follow-up of 84 cemented prostheses. J Bone Joint Surg Br, 1994. **76**(6): p. 912-7.
18. Mjoberg, B., *The theory of early loosening of hip prostheses*. Orthopedics, 1997. **20**(12): p. 1169-75.

19. Petersen, M.M., et al., Preoperative bone mineral density of the proximal tibia and migration of the tibial component after uncemented total knee arthroplasty. *Journal of Arthroplasty*, 1999. **14**(1): p. 77-81.
20. Krismer, M., et al., *Early migration predicts late aseptic failure of hip sockets*. *Journal of Bone and Joint Surgery-British Volume*, 1996. **78B**(3): p. 422-426.
21. Dhert, W.J.A., et al., *Integration of press-fit implants in cortical bone: A study on interface kinetics*. *Journal of Biomedical Materials Research*, 1998. **41**(4): p. 574-583.
22. Stadelmann, V.A., In vivo assessment of enhanced hardware fixation with HydroSet™ bone cement: A comparative biomechanical short term evaluation in the femoral condyle of rabbits: Biomechanical testing. 2007, EPFL - Stryker - Biomatech. p. 42.
23. Venesmaa, P.K., et al., Monitoring of periprosthetic BMD after uncemented total hip arthroplasty with dual-energy X-ray absorptiometry - a 3-year follow-up study. *Journal of Bone and Mineral Research*, 2001. **16**(6): p. 1056-1061.
24. Stadelmann, V.A., A. Terrier, and D.P. Pioletti, Microstimulation at the bone-implant interface upregulates osteoclast activation pathways. *Bone*, 2008. **42**(2): p. 358-364.
25. Horowitz, S.M. and J.B. Gonzales, *Inflammatory response to implant particulates in a macrophage/osteoblast coculture model*. *Calcified Tissue International*, 1996. **59**(5): p. 392-396.
26. Jee, W.S.S., Integrated Bone Tissue Physiology: Anatomy and Physiology, in *Bone Mechanics Handbook*, S.C. Cowin, Editor. 2001, CRC Press.
27. Shea, J.E. and S.C. Miller, *Skeletal function and structure: Implications for tissue-targeted therapeutics*. *Advanced Drug Delivery Reviews*, 2005. **57**(7): p. 945-957.
28. Baron, R., Anatomy and Biology of Bone Matrix and Cellular Elements, in *Primer on the Metabolic Bone Diseases and Disorders of Mineral Metabolism*, M.J. Favus, Editor. 2003, ASBMR.

29. Baron, R., Anatomy and Ultrastructure of Bone, in Primer on Metabolic Bone Diseases and Disorders of Mineral Metabolism. 1991, American Society for Bone and Mineral Research.
30. Sutton-Smith, P., H. Beard, and N. Fazzalari, Quantitative backscattered electron imaging of bone in proximal femur fragility fracture and medical illness. Journal of Microscopy-Oxford, 2008. **229**(1): p. 60-66.
31. Roschger, P., et al., Validation of quantitative backscattered electron imaging for the measurement of mineral density distribution in human bone biopsies. Bone, 1998. **23**(4): p. 319-326.
32. Gasser, J.A., et al., Noninvasive monitoring of changes in structural cancellous bone parameters with a novel prototype micro-CT. Journal of Bone and Mineral Metabolism, 2005. **23**: p. 90-96.
33. Muller, R., et al., Morphometric analysis of human bone biopsies: a quantitative structural comparison of histological sections and micro-computed tomography. Bone, 1998. **23**(1): p. 59-66.
34. Müller, R. and W.C. Hayes. Biomechanical competence of microstructural bone in the progress of adaptive bone remodeling. in Developments in X-ray tomography. 1997. San-Diego: SPIE.
35. Prendergast, P.J. and M.C.H. Van der Meulen, *Mechanics of Bone Regeneration*, in *Bone Mechanics Handbook*, S.C. Cowin, Editor. 2001, CRC Press.
36. Boyle, W.J., W.S. Simonet, and D.L. Lacey, *Osteoclast differentiation and activation*. Nature, 2003. **423**(6937): p. 337-42.
37. Teitelbaum, S.L., *Bone resorption by osteoclasts*. Science, 2000. **289**(5484): p. 1504-1508.

38. Ducy, P., T. Schinke, and G. Karsenty, *The osteoblast: A sophisticated fibroblast under central surveillance*. Science, 2000. **289**(5484): p. 1501-1504.
39. Puzas, J.E., The Osteoblast, in Primer on Metabolic Bone Diseases and Disorders of Mineral Metabolism. 1991, American Society for Bone and Mineral Research.
40. Noble, B.S., et al., Identification of apoptotic changes in osteocytes in normal and pathological human bone. Bone, 1997. **20**(3): p. 273-82.
41. Robling, A.G. and C.H. Turner, Mechanotransduction in bone: genetic effects on mechanosensitivity in mice. Bone, 2002. **31**(5): p. 562-9.
42. Burger, E.H. and J. Klein-Nulend, *Mechanotransduction in bone--role of the lacuno-canalicular network*. Faseb J, 1999. **13 Suppl**: p. S101-12.
43. Mullender, M.G., et al., *Osteocyte density changes in aging and osteoporosis*. Bone, 1996. **18**(2): p. 109-113.
44. Prendergast, P.J. and R. Huiskes, Microdamage and osteocyte-lacuna strain in bone: a microstructural finite element analysis. J Biomech Eng, 1996. **118**(2): p. 240-6.
45. Everts, V., et al., The bone lining cell: its role in cleaning Howship's lacunae and initiating bone formation. J Bone Miner Res, 2002. **17**(1): p. 77-90.
46. Turner, C.H. and F.M. Pavalko, Mechanotransduction and functional response of the skeleton to physical stress: the mechanisms and mechanics of bone adaptation. J Orthop Sci, 1998. **3**(6): p. 346-55.
47. Vaananen, H.K., et al., *The cell biology of osteoclast function*. Journal of Cell Science, 2000. **113**(3): p. 377-381.
48. Parfitt, A.M., Osteonal and hemi-osteonal remodeling: the spatial and temporal framework for signal traffic in adult human bone. J Cell Biochem, 1994. **55**(3): p. 273-86.

49. Chow, J.W., C.J. Jagger, and T.J. Chambers, Characterization of osteogenic response to mechanical stimulation in cancellous bone of rat caudal vertebrae. *Am J Physiol*, 1993. **265**(2 Pt 1): p. E340-7.
50. Chow, J.W.M., et al., *Role for parathyroid hormone in mechanical responsiveness of rat bone*. *American Journal of Physiology-Endocrinology and Metabolism*, 1998. **37**(1): p. E146-E154.
51. Quinn, J.M.W. and M.T. Gillespie, *Modulation of osteoclast formation*. *Biochemical and Biophysical Research Communications*, 2005. **328**(3): p. 739-745.
52. Khosla, S., *Minireview: the OPG/RANKL/RANK system*. *Endocrinology*, 2001. **142**(12): p. 5050-5.
53. Anderson, D.M., et al., A homologue of the TNF receptor and its ligand enhance T-cell growth and dendritic-cell function. *Nature*, 1997. **390**(6656): p. 175-179.
54. Lacey, D.L., et al., Osteoprotegerin ligand is a cytokine that regulates osteoclast differentiation and activation. *Cell*, 1998. **93**(2): p. 165-176.
55. Simonet, W.S., et al., Osteoprotegerin: a novel secreted protein involved in the regulation of bone density. *Cell*, 1997. **89**(2): p. 309-19.
56. Fazzalari, N.L., et al., The ratio of messenger RNA levels of receptor activator of nuclear factor kappaB ligand to osteoprotegerin correlates with bone remodeling indices in normal human cancellous bone but not in osteoarthritis. *J Bone Miner Res*, 2001. **16**(6): p. 1015-27.
57. Komarova, S.V., et al., Mathematical model predicts a critical role for osteoclast autocrine regulation in the control of bone remodeling. *Bone*, 2003. **33**(2): p. 206-15.
58. de Pollak, C., et al., Age-related changes in bone formation, osteoblastic cell proliferation, and differentiation during postnatal osteogenesis in human calvaria. *J Cell Biochem*, 1997. **64**(1): p. 128-39.

59. Dempster, D.W., et al., *Anabolic Actions of Parathyroid-Hormone on Bone*. Endocrine Reviews, 1993. **14**(6): p. 690-709.
60. Gesty-Palmer, D., et al., Distinct beta-arrestin- and G protein-dependent pathways for parathyroid hormone receptor-stimulated ERK1/2 activation. J Biol Chem, 2006. **281**(16): p. 10856-64.
61. Karlsson, M.K., O. Johnell, and K.J. Obrant, *Bone-Mineral Density in Weight Lifters*. Calcified Tissue International, 1993. **52**(3): p. 212-215.
62. Kontulainen, S., et al., Effect of long-term impact-loading on mass, size, and estimated strength of humerus and radius of female racquet-sports players: a peripheral quantitative computed tomography study between young and old starters and controls. J Bone Miner Res, 2003. **18**(2): p. 352-9.
63. Zouch, M., et al., Long-term soccer practice increases bone mineral content gain in prepubescent boys. Joint Bone Spine, 2008. **75**(1): p. 41-49.
64. Sibonga, J.D., et al., Recovery of spaceflight-induced bone loss: Bone mineral density after long-duration missions as fitted with an exponential function. Bone, 2007. **41**(6): p. 973-978.
65. Frost, H.M., The Mechanostat - a Proposed Pathogenic Mechanism of Osteoporoses and the Bone Mass Effects of Mechanical and Nonmechanical Agents. Bone and Mineral, 1987. **2**(2): p. 73-85.
66. Frost, H.M., M. Klein, and A. Villanueva, *Osteodynamics - Its Application to Osteoporosis*. Journal of Bone and Joint Surgery-American Volume, 1964. **46**(5): p. 1142-1143.
67. Frost, H.M., *Bone Mass and the Mechanostat - a Proposal*. Anatomical Record, 1987. **219**(1): p. 1-9.

68. Frost, H.M., *Bone's mechanostat: A 2003 update*. Anatomical Record Part a- Discoveries in Molecular Cellular and Evolutionary Biology, 2003. **275A**(2): p. 1081-1101.
69. Huiskes, R., Validation of Adaptive Bone-emodeling Simulation Models, in Bone Research in Biomechanics, L. G. and e. al., Editors. 1997, IOS Press. p. 33--48.
70. Hart, R.T., Bone Modeling and Remodeling: Theories and Computation, in Bone Mechanics Handbook, S.C. Cowin, Editor. 2001, CRC Press.
71. Hernandez, C.J., G.S. Beaupre, and D.R. Carter, *A model of mechanobiologic and metabolic influences on bone adaptation*. J Rehabil Res Dev, 2000. **37**(2): p. 235-44.
72. Terrier, A., L.R. Rakotomanana, and P.F. Leyvraz, Effect of loading history on short-term bone adaptation after total hip arthroplasty, in Computer Methods in Biomechanics and Biomedical Engineering, J. Middleton, M.L. Jones, and G.N. Pande, Editors. 1997, Gordon and Breach Science Publishers. p. 115--122.
73. Terrier, A., et al., *Adaptation Models of Anisotropic Bone*. Comput Methods Biomech Biomed Engin, 1997. **1**(1): p. 47-59.
74. Turner, C.H. and D.B. Burr, *Experimental Techniques for Bone Mechanics*, in *Bone Mechanics Handbook*, S.C. Cowin, Editor. 2001, CRC Press.
75. Weinbaum, S., S.C. Cowin, and Y. Zeng, A Model for the Excitation of Osteocytes by Mechanical Loading-Induced Bone Fluid Shear Stresses. Journal of Biomechanics, 1994. **27**(3): p. 339-360.
76. You, J.D., et al., A model for strain amplification in the actin cytoskeleton of osteocytes due to fluid drag on pericellular matrix. Journal of Biomechanics, 2001. **34**(11): p. 1375-1386.
77. Skerry, T.M., et al., Early Strain-Related Changes in Enzyme-Activity in Osteocytes Following Bone Loading Invivo. Journal of Bone and Mineral Research, 1989. **4**(5): p. 783-788.

78. Bonewald, L.F., *Mechanosensation and transduction in osteocytes*. BoneKey-Osteovision, 2006. **3**(10): p. 7--15.
79. Stains, J.P. and R. Civitelli, *Cell-to-cell interactions in bone*. Biochemical and Biophysical Research Communications, 2005. **328**(3): p. 721-727.
80. Doty, S.B., *Morphological Evidence of Gap-Junctions between Bone-Cells*. Calcified Tissue International, 1981. **33**(5): p. 509-512.
81. Donahue, H.J., et al., Cell-to-Cell Communication in Osteoblastic Networks - Cell Line-Dependent Hormonal-Regulation of Gap Junction Function. Journal of Bone and Mineral Research, 1995. **10**(6): p. 881-889.
82. Martin, R.B., Is all cortical bone remodeling initiated by microdamage? Bone, 2002. **30**(1): p. 8-13.
83. Aspenberg, P. and H. Van der Vis, *Migration, particles, and fluid pressure - A discussion of causes of prosthetic loosening*. Clinical Orthopaedics and Related Research, 1998(352): p. 75-80.
84. Stadelmann, V.A., A. Terrier, and D.P. Pioletti, Microstimulation at the bone-implant interface upregulates osteoclast activation pathways. Bone, 2008: p. 358--364.
85. Fleisch, H., et al., Effect of Diphosphonates on Deposition and Dissolution of Calcium Phosphate in Vitro and in Vivo. Helvetica Physiologica Et Pharmacologica Acta, 1968. **26**(3): p. C345-&.
86. Fleisch, H., Bisphosphonates in bone disease: from the laboratory to the patient. 4th ed. 2000, San Diego: Academic Press. 212.
87. Hoffman, A., et al., Mode of administration-dependent pharmacokinetics of bisphosphonates and bioavailability determination. International Journal of Pharmaceutics, 2001. **220**(1-2): p. 1-11.

88. Villikka, K., et al., The absolute bioavailability of clodronate from two different oral doses. *Bone*, 2002. **31**(3): p. 418-421.
89. Dannemann, C., et al., Jaw osteonecrosis related to bisphosphonate therapy: a severe secondary disorder. *Bone*, 2007. **40**(4): p. 828-34.
90. Diel, I.J., R. Bergner, and K.A. Grotz, *Adverse effects of bisphosphonates: current issues*. *J Support Oncol*, 2007. **5**(10): p. 475-82.
91. Fleisch, H., *Development of bisphosphonates*. *Breast Cancer Research*, 2002. **4**(1): p. 30-34.
92. Sato, M., et al., Bisphosphonate Action - Alendronate Localization in Rat Bone and Effects on Osteoclast Ultrastructure. *Journal of Clinical Investigation*, 1991. **88**(6): p. 2095-2105.
93. Russell, R.G.G., et al., *The pharmacology of bisphosphonates and new insights into their mechanisms of action*. *Journal of Bone and Mineral Research*, 1999. **14**: p. 53-65.
94. Green, J.R., *Bisphosphonates: Preclinical review*. *Oncologist*, 2004. **9**: p. 3-13.
95. Xing, L.P. and B.F. Boyce, *Regulation of apoptosis in osteoclasts and osteoblastic cells*. *Biochemical and Biophysical Research Communications*, 2005. **328**(3): p. 709-720.
96. Im, G.I., et al., *Osteoblast proliferation and maturation by bisphosphonates*. *Biomaterials*, 2004. **25**(18): p. 4105-15.
97. Reinholz, G.G., et al., Distinct mechanisms of bisphosphonate action between osteoblasts and breast cancer cells: identity of a potent new bisphosphonate analogue. *Breast Cancer Research and Treatment*, 2002. **71**(3): p. 257-268.
98. Harris, S.T., N.B. Watts, and Z. Li, Two-year efficacy and tolerability of risedronate once a week for the treatment of women with post-menopausal osteoporosis (vol 20, pg 757, 2004). *Current Medical Research and Opinion*, 2004. **20**(10): p. 1690-1690.

99. Bone, H.G., et al., Ten years' experience with alendronate for osteoporosis in postmenopausal women. *N Engl J Med*, 2004. **350**(12): p. 1189-99.
100. Liberman, U.A., et al., Effect of oral alendronate on bone mineral density and the incidence of fractures in postmenopausal osteoporosis. The Alendronate Phase III Osteoporosis Treatment Study Group. *N Engl J Med*, 1995. **333**(22): p. 1437-43.
101. Harris, S.T., et al., Effects of risedronate treatment on vertebral and nonvertebral fractures in women with postmenopausal osteoporosis - A randomized controlled trial. *Jama-Journal of the American Medical Association*, 1999. **282**(14): p. 1344-1352.
102. Kanis, J.A., et al., *The components of excess mortality after hip fracture*. *Bone*, 2003. **32**(5): p. 468-473.
103. Salkeld, G., et al., Quality of life related to fear of falling and hip fracture in older women: a time trade off study. *Bmj*, 2000. **320**(7231): p. 341-6.
104. Jensen, T.B., et al., Systemic alendronate treatment improves fixation of press-fit implants: A canine study using nonloaded implants. *Journal of Orthopaedic Research*, 2007. **25**(6): p. 772-778.
105. Eberhardt, C., et al., The bisphosphonate ibandronate accelerates osseointegration of hydroxyapatite-coated cementless implants in an animal model. *J Orthop Sci*, 2007. **12**(1): p. 61-6.
106. Hilding, M. and P. Aspenberg, Local peroperative treatment with a bisphosphonate improves the fixation of total knee prostheses: A randomized, double-blind radiostereometric study of 50 patients. *Acta Orthop*, 2007. **78**(6): p. 795-9.
107. Hilding, M., et al., Clodronate prevents prosthetic migration: a randomized radiostereometric study of 50 total knee patients. *Acta Orthop Scand*, 2000. **71**(6): p. 553-7.

108. Jakobsen, T., et al., *Effect of topical alendronate treatment on fixation of implants inserted with bone compaction*. Clinical Orthopaedics and Related Research, 2006(444): p. 229-234.
109. Jakobsen, T., et al., Local alendronate increases fixation of implants inserted with bone compaction: 12-week canine study. Journal of Orthopaedic Research, 2007. **25**(4): p. 432-441.
110. Roussiere, H., et al., Hybrid materials applied to biotechnologies: coating of calcium phosphates for the design of implants active against bone resorption disorders. Journal of Materials Chemistry, 2005. **15**(35-36): p. 3869-3875.
111. Wermelin, K., P. Tengvall, and P. Aspenberg, Surface-bound bisphosphonates enhance screw fixation in rats - increasing effect up to 8 weeks after insertion. Acta Orthopaedica, 2007. **78**(3): p. 385-392.
112. Peter, B., et al., Calcium phosphate drug delivery system: influence of local zoledronate release on bone implant osteointegration. Bone, 2005. **36**(1): p. 52-60.
113. Peter, B., et al., Local delivery of bisphosphonate from coated orthopedic implants increases implants mechanical stability in osteoporotic rats. J Biomed Mater Res A, 2006. **76**(1): p. 133-43.
114. Peter, B., et al., The effect of bisphosphonates and titanium particles on osteoblasts: an in vitro study. J Bone Joint Surg Br, 2005. **87**(8): p. 1157-63.
115. Fuchs, R.K., et al., Synergistic effects of exercise plus alendronate on bone mass and structural properties in ovariectomized rats. Journal of Bone and Mineral Research, 2002. **17**: p. S192-S192.
116. Chilibeck, P.D., et al., The effect of strength training combined with bisphosphonate (etidronate) therapy on bone mineral, lean tissue, and fat mass in postmenopausal women. Canadian Journal of Physiology and Pharmacology, 2002. **80**(10): p. 941-950.

117. Lespessailles, E. and S. Prouteau, *Is there a synergy between physical exercise and drug therapies for osteoporosis?* CLINICAL AND EXPERIMENTAL RHEUMATOLOGY, 2006. **24**(2): p. 191--195.

Curriculum Vitae

Vincent Stadelmann

Ch. Des Cottages 8

1007 Lausanne

Switzerland

vincent.stadelmann@a3.epfl.ch

EDUCATION

2004 - 2008 PhD at the Swiss Federal Institute of Technology, Lausanne (EPFL).

Thesis entitled: 'Prevention of micromotion-related periprosthetic bone loss using local release of bisphosphonate: Theoretical developments and experimental validations.'

2004 Management of Biotech, Medtech and Pharma Ventures, organized jointly by EPFL MoT and the University of Lausanne, School of Business.

2003 Master project, Laboratory of Cell and Computational Biology, University of California, Davis under supervision of Prof. J.M. Scholey

Project entitled: 'The Gradient of Defects in anti-KLP3A Injected Drosophila Embryos Reflects the Gradient of Concentration of the Injected Antibody.'

2003 Biomedical Engineering graduate course, organized jointly by Geneva University, the Neuchatel University, CHUV and EPFL.

2001 - 2002 MSc in Engineering Physics at the Swiss Institute of Technology (EPFL)

1996 - 2001 BSc in Engineering Physics at the Swiss Institute of Technology (EPFL)

WORK HISTORY

2007 - 2008 Scientific consultant, Stryker Osteosynthesis.

In charge of biomechanical testing for a FDA approval protocol of a new device

2003 - 2004 Physics and Computer Science teacher, Lausanne high school

2002 - 2003 Research assistant at the Autonomous Systems Laboratory (EPFL)

In charge of the project "Hands-On Mechatronics" of the Swiss project "New Learning Technologies - Swiss Virtual University".

2000 Internship at Ecole des Mines de Albi, France

SCIENTIFIC PUBLICATIONS

V. A. Stadelmann *et al.*, "Implants delivering bisphosphonate locally increase periprosthetic bone density in an osteoporotic sheep model", Submitted to European Cells & Materials Journal

V. A. Stadelmann *et al*, “A model to predict the optimal bone density around implant as bisphosphonate delivery system: theoretical developments and experimental validation”, *Submitted to The Journal of Orthopedic Research*

V. A. Stadelmann *et al*, “Spatial strain distribution in an axially loaded mouse tibia”, *Accepted in Computer Methods in Biomechanics and Biomedical Engineering*

V. A. Stadelmann *et al*, “Microstimulations at the bone implant interface upregulate osteoclast activation pathway”, *Bone*, vol. 42, 2008, p. 358-364

D.P. Pioletti, *et al*, “Orthopedic implant used as drug delivery system: clinical situation and state of the research”, *Current Drug Delivery*, vol. 5, 2008, p. 59-63

L.S. Nissen-Meyer *et al*, “Osteopenia, decreased bone formation and impaired osteoblast development in Sox4 heterozygous mice”, *Journal of Cell Science* 120, 2785-2795 (2007)

ORAL COMMUNICATIONS

V. A. Stadelmann *et al*, “Development of a theoretical model for the design of orthopedic implants as drug-delivery systems”, CORS 2007, Hawaii, USA

V. A. Stadelmann *et al*, “Increased response of *Barrestin2*-ko mice after tibial compressions in vivo”, BMES 2007, Los Angeles CA, USA

V. A. Stadelmann *et al*, “Micromotions at the bone implant interface up-regulate osteoblasts-mediated activation of osteoclasts in ex vivo human samples”, Keystone CO, USA

V. A. Stadelmann *et al*, “Differential response of mice lacking Barrestin2 after tibial compressions in vivo”, SBMS 2007, Zurich, Switzerland

V. A. Stadelmann *et al*, “Using orthopedic implants for local bisphosphonate delivery in osteoporotic animals: a theoretical model”, World Congress of Biomechanics 2006, Munich, Germany

V. A. Stadelmann *et al*, “Orthopedic implants as drug-delivery systems: a theoretical study”, ASME - Summer Bioengineering Conference 2005, Vail CO, USA

V. A. Stadelmann and D. P. Pioletti, “Bone-implant interface: effect of microstimulations on bone cells gene expression”, EORS 2005, Lisbon, Portugal